QUARTERLY PROGRESS REPORT

April 1 to June 30, 2017

Florida International University's Continued Research Support for the Department of Energy's Office of Environmental Management

Principal Investigator:

Leonel E. Lagos, Ph.D., PMP®

Prepared for:

U.S. Department of Energy
Office of Environmental Management
Under Cooperative Agreement No. DE-EM0000598

Applied Research Center
Florida International University

Introduction

The Applied Research Center (ARC) at Florida International University (FIU) executed work on four major projects that represent FIU-ARC's continued support to the Department of Energy's Office of Environmental Management (DOE-EM). The projects are important to EM's mission of accelerated risk reduction and cleanup of the environmental legacy of the nation's nuclear weapons program.

The period of performance for FIU Performance Year 7 under the DOE Cooperative Agreement (Contract # DE-EM0000598) is August 29, 2016 to August 28, 2017. The information in this document provides a summary of the FIU-ARC's activities under the Cooperative Agreement for the period of April 1 to June 30, 2017. Executive highlights during this reporting period include:

***Program-Wide:* DOE-FIU Cooperative Agreement**

1. FIU completed the development of the Continuation Application for FIU Performance Year 8 of the DOE-FIU Cooperative Agreement that will begin on August 29, 2017 at the conclusion of the current FIU Performance Year 7 on August 28, 2017. The three-volume continuation application package was submitted to DOE three months prior to the end of the current performance year, on May 25, 2017.
2. ARC researchers and DOE Fellows participated in the first ever TechNeeds seminar which brought together robotic experts from federal agencies, national research laboratories, industry and academia to address the integration of robotic systems into hazardous work environments. Robots, Sensors & Humans – Benefits & Challenges of the Implementation of Robotic Systems in Hazardous Environments was held at the Modesto A. Maidique campus of Florida International University (FIU) in Miami, FL, on May 3 and 4, 2017.

***Project 1*: High level waste (HLW)/waste processing**

FIU is assisting DOE EM in evaluating the double-shell tank (DST) structural integrity and to ensure that the stringent operating conditions of the DSTs are being met through technology evaluations and the use of sensors. To support this need, FIU has been developing inspection tools and investigating the use of a number of sensors to aid in understanding tank integrity issues and tank operating conditions. In addition, FIU has been developing a full-scale sectional mockup that includes the inner and outer liners, the annulus and the refractory slots and drain lines of the DSTs. The mockup will be used to evaluate inspection systems and instrumentation and provide challenges similar to those in the Hanford DSTs.

1. FIU hosted Kayte Denslow and Dr. Vicky Freedman from PNNL in April. Project 1 presented summaries of the progress on the current tasks and proposed scope for the next fiscal year (FIU Performance Year 8), including the initiation of a new task related to developing an experimental test loop to investigate critical velocity and resuspension studies.
2. FIU completed the evaluation of the sensors to be integrated into the inspection tools and developed the conceptual design modifications needed to both the miniature rover and pneumatic crawler. Sensors that will be integrated include temperature, humidity, and

radiation sensors. FIU is investigating the integration of UT sensors for non-destructive evaluation.

3. FIU completed the bottom structure of the mock up that represents the concrete foundation and contains the drain lines for the DSTs. The structure is 40 ft long and 8 ft wide. The foundation was constructed using wood and overlayed with a protective film. The surface/film of the foundation was then covered with a metal mesh and a thin layer of concrete. Carbon steel sheets representing the outer liner will be placed on top of the foundation and the refractory structure will be placed on top of the outer liner. Finally, carbon steel plates representing the inner liner will be placed on the refractory structure to complete the mockup.

***Project 2:* Environmental remediation (ER)**

FIU is assisting DOE EM to meet the challenges of managing the environmental restoration of subsurface contamination in soil and groundwater.

1. FIU hosted a visit from Dr. Vicky Freedman (Research Scientist, Hydrology) and Dr. Kayte Denslow (Scientist, Applied Physics and Material Characterization) from PNNL, as well as Dr. Elizabeth Hoffman (Manager, Engineering Process Development) from SRNL, to discuss progress on current tasks and proposed scope for the next fiscal year (FIU Performance Year 8).
2. DOE Fellow Claudia Cardona completed her dissertation defense and graduated with a Ph.D. degree in environmental engineering. Claudia's research was conducted in close collaboration with PNNL researchers to support remediation efforts to control uranium mobility in the subsurface at the Hanford Site.
3. FIU completed batch experiments designed to investigate how the natural subsurface microbial community influences autunite stability and affects the release of uranium back to the aqueous phase. This would allow for a more thorough understanding of the phenomena influencing uranium mobility in the complex natural environment.
4. FIU visited SRS in June to conduct follow-up field work, with assistance from Dr. John Seaman and his research team at the Savannah River Ecology Lab (SREL). The aim was to measure cross-section profiles along the main Tims Branch stream and to collect *in situ* water quality and flow data to use for calibration of the hydrological models. Water and biofilm samples were also collected for analysis of radiological and other contaminants of concern, and to monitor the by-product of the tin-based DOE EM remediation technology.
5. A video teleconference (VTC) was held between FIU ARC's Environmental Remediation Science & Technology group and SRNL personnel to discuss potential future areas of research to meet the site needs related to technetium (Tc) management. Tc is a major contaminant of concern at SRS and other DOE sites. The ARC team was led by Dr. Leonel Lagos, the Center's Director of Research, while the SRNL team was led by Program Manager, Dr. Elizabeth Hoffman.

***Project 3:* Deactivation and decommissioning (D&D)**

FIU is assisting DOE EM to meet high priority D&D needs and technical challenges across the DOE complex through technology development, demonstration and evaluation. As part of this effort, FIU is investigating the use of intumescent coatings to mitigate the release of radioisotopes during fire and/or extreme heat conditions that can potentially occur at a DOE contaminated facility/building. Standardizing and implementing proven processes to refine and better synchronize DOE-EM technology needs, requirements, testing, evaluation, and acquisition by development of uniformly accepted testing protocols and performance metrics is an essential component of these efforts. In addition, leveraging the research being performed on intumescent coatings, FIU is conducting a cold demonstration / test and evaluation of applying intumescent coatings in a full scale SRS 235-F hot cell mock-up at the FIU Hot Cell Test Bed.

1. FIU has completed construction of the Hot Cell Test Bed in support of the final test plan (*Adapting Intumescent Coatings as Fire Resilient Fixatives in Support of SRS 235-F D&D Activities Phase II: Construction of SRS 235-F Hot Cell Test Bed and Application Demonstration*). This to-scale SRS 235-F Hot Cell Test Bed was developed on site at ARC to mirror the operating environment encountered in an adjoining corner and middle hot cell configuration at the SRS 235-F facility. FIU is evaluating the mechanics and processes associated with applying the selected intumescent coatings in the hot cell configuration. This evaluation is expected to be completed by the end of June.
2. During the ASTM International Conference (June 19-22, 2017), the E10 Committee on Nuclear Technology and Applications approved the two (2) standard specifications on fixative technologies developed by the E10.03 Subcommittee. A DOE EM news release highlighted this effort in EM Update, Vol. 9, Issue 12, on 28 June 2017. These 2 standards were formally approved by ASTM International and will be promulgated in July 2017.

Project 4: STEM workforce development

FIU created the DOE Fellows Program in 2007 to assist DOE EM to address the problem of an aging federal workforce. The program provides training, mentorship, and professional development opportunities to FIU STEM students. The DOE Fellows provide critical support to the DOE EM research being conducted on high impact/high priority research being conducted at FIU.

1. DOE Fellows have been participating in numerous opportunities for sharing the research that they have performed in support of DOE EM at FIU-ARC and during their past summer internships at DOE sites, DOE Headquarters, and national research laboratories. In addition to the Waste Management Symposia in early March in Phoenix, AZ, DOE Fellows have presented at recent events including the 253rd American Chemical Society National Meeting & Exposition in San Francisco, CA, on April 2-6, 2017; the 5th Annual Life Sciences South Florida Undergraduate Research Symposium at Palm Beach State College, FL on April 1, 2017; the 2nd Annual FIU Undergraduate Research Conference on March 31, 2017; the 2017 Society of Toxicology Expo in Baltimore, MD, on March 12-17, 2017; the FIU Undergraduate Research Presentation event for FIU's Foundation Board of Directors on January 27, 2017; the 2017 National Conference on Undergraduate Research on April 6-8, 2017, in Memphis, TN; and FIU's Panther Alumni Week (PAW) first-year Honors College interdisciplinary course.
2. This summer, twelve (12) DOE Fellows are participating in 10-week internships across the DOE Complex and at two universities. The DOE Fellows are engaging in research projects at DOE Headquarters in Maryland, DOE national laboratories (Savannah River

Nat. Lab and Sandia Nat. Lab), Savannah River Ecology Lab, the Waste Isolation Pilot Plant, University of Texas-Austin Nuclear and Applied Robotics Group, and San Jose State University. Each DOE Fellow will develop a summer internship technical report once they return to ARC based on the research they performed over the summer.

Milestones and Deliverables

Project 1: Milestone 2016-P1-M18.3.1 was completed on March 31, 2017 and a summary document was submitted on April 14, 2017, summarizing the results from the bench-scale tests using an infrared sensor. Milestone 2016-P1-M19.1.1 was completed on May 12, 2017 and a summary document was submitted on May 26, 2017, summarizing the results from the bench-scale tests using the Permasense UT sensors. Milestone 2016-P1-M18.2.2 was completed on May 26, 2017 and a summary email was sent to DOE, highlighting aspects of the sensors incorporated into the design of the inspection tools. Due to funding issues, milestone 2016-P1-M18.2.1 and 2016-P1-M17.1.2 will be reforecast. The expected delay has been communicated to the site points-of-contact as well as the DOE HQ Project Lead, Gary Peterson, during regular project teleconferences. A reforecast date of completion will be set once future funding amounts and dates are known.

Project 2: Milestone 2016-P2-M5, under subtask 1.4, was completed with trial-and-error experiments for separations and determination of Tc(IV) and Tc(VII). Milestone 2016-P2-M4, investigation of acidified sediment and contaminant mobility for SRS, was completed and notification sent via email on May 9, 2017 to all project points of contact. Milestone 2016-P2-M9, complete batch experiments on the biodissolution of Na-autunite (subtask 1.2), was also completed with a notification email being sent out on May 8. In addition, FIU submitted the technical report deliverable on the effect of ionic strength on the sorption of neodymium to dolomite (Task 5) on May 15. Milestone 2016-P2-M7, column experiments using modified humic acid for subtask 2.3, was completed and notification sent via email on June 29, 2017 to all project points of contact.

The following changes have been communicated to both the site collaborators, who have agreed to the revised dates and/or format, and DOE HQ via email as well as during regular project teleconferences. The results for the research under subtask 2.3, originally planned to be included in a technical report (investigation of the removal of uranium by Huma-K sorbed on SRS sediments via batch experiments) will be included in the Year End Report. In addition, FIU is reforecasting, the completion of the coupling of the MIKE SHE and MIKE 11 models (milestone 2016-P2-M10 for subtask 3.1) to the next performance year. In addition, a deliverable on the surface water modeling of Tims Branch (Task 3) has been reforecast from June 15, 2017 to August 17, 2017.

Project 3: FIU completed milestone 2016-P3-M3.3 by deploying two pilot technology videos from D&D KM-IT onto the YouTube platform on April 24, 2017. FIU also briefed DOE HQ officials visiting FIU during the week of May 1 on the current project accomplishments and planned scope of work for FIU Performance Year 8, which included the recommended D&D technologies to test using the 3-phased model, completing a deliverable under Task 2. FIU completed milestone 2016-P3-M1.1 on April 27, 2017 by importing the WIMS 2017 data set for waste forecast and transportation data; the new data set went live on the WIMS website on May 10, 2017. In addition, the security audit reports for D&D KM-IT were submitted to DOE on May

30, 2017.Milestone 2016-P3-M2.3, participation in the ASTM E10 committee meeting to coordinate developing standardized testing protocols and performance metrics for D&D technologies (subtask 2.2.1), was completed during the ASTM International Conference on June 19-21, 2017. In addition, milestone 2016-P3-M3.2, the integration of D&D knowledge/information into four Wikipedia edits/articles, was completed and a summary report was submitted to DOE on June 28, 2017.

Project 4: No milestones or deliverables for this project were due in April, May, or June 2017.

The program-wide milestones and deliverables that apply to all projects (Projects 1 through 4) for FIU Performance Year 7 are shown on the following table. The FIU Research Review presentations to DOE HQ and site points-of-contact is scheduled for July 18-19, 2017. These presentations will include the progress and accomplishments of the current performance year (FIU Performance Year 7) as well as the planned scope of work for the next performance year (FIU Performance Year 8).

Task	Milestone/ Deliverable	Description	Due Date	Status	OSTI
Program-wide (All Projects)	Deliverable	Draft Project Technical Plan	9/30/16	Complete	
	Deliverable	Monthly Progress Reports	Monthly	On Target	
	Deliverable	Quarterly Progress Reports	Quarterly	On Target	
	Deliverable	Draft Year End Report	10/13/17	On Target	OSTI
	Deliverable	Presentation overview to DOE HQ/Site POCs of the project progress and accomplishments (Mid-Year Review)	4/7/17* Reforecasted	Reforecasted to 7/18/17	
	Deliverable	Presentation overview to DOE HQ/Site POCs of the project progress and accomplishments (Year End Review)	9/29/17*	On Target	

**Completion of this deliverable depends on availability of DOE-HQ official(s).*

Project 1
Chemical Process Alternatives for Radioactive Waste

Project Manager: Dr. Dwayne McDaniel

Project Description

Florida International University has been conducting research on several promising alternative processes and technologies that can be applied to address several technology gaps in the current high-level waste processing retrieval and conditioning strategy. The implementation of advanced technologies to address challenges faced with baseline methods is of great interest to the Hanford Site and can be applied to other sites with similar challenges, such as the Savannah River Site. Specifically, FIU has been involved in: modeling and analysis of multiphase flows pertaining to waste feed mixing processes, evaluation of alternative HLW instrumentation for in-tank applications and the development of technologies to assist in the inspection of tank bottoms at Hanford. The use of field or *in situ* technologies, as well as advanced computational methods, can improve several facets of the retrieval and transport processes of HLW. FIU has worked with site personnel to identify technology and process improvement needs that can benefit from FIU's core expertise in HLW. The following tasks are included in FIU Performance Year 7:

Task No	Task
Task 17: Advanced Topics for Mixing Processes	
Subtask 17.1	Computational Fluid Dynamics Modeling of HLW Processes in Waste Tanks
Task 18: Technology Development and Instrumentation Evaluation	
Subtask 18.2	Development of Inspection Tools for DST Primary Tanks
Subtask 18.3	Investigation Using an Infrared Temperature Sensor to Determine the Inside Wall Temperature of DSTs
Task 19: Pipeline Integrity and Analysis	
Subtask 19.1	Pipeline Corrosion and Erosion Evaluation
Subtask 19.2	Evaluation of Nonmetallic Components in the Waste Transfer System

Task 17: Advanced Topics for HLW Mixing and Processing

Task 17 Quarterly Progress

Subtask 17.1: Computational Fluid Dynamics Modeling of HLW Processes in Waste Tanks

FIU hosted a number of visitors from PNNL LANL, SRNL and DOE HQ. After discussions with the visitors, it was suggested that FIU utilize its current 300-ft test loop for pipeline unplugging issues to address technical gaps related to particle re-suspension and flushing. FIU currently has the capability to expand the loop to 2000-ft.

Figure 1-1. Pipe test loop being considered for expansion for critical velocity and flushing tests at FIU.

In this period, FIU reviewed the literature about transfer and flushing practices of Newtonian and non-Newtonian slurries. The emphasis was on previous works conducted in national labs and reports generated for non-Newtonian high-level waste (HLW) at Hanford and Savannah River sites. The goal was to recognize the existing technologies and gaps and develop test mythologies and loops to bridge those gaps. This report explains some theoretical analysis and mythologies that were considered for future steps.

Evaluation of shortlisted critical velocity correlations for Hanford waste transport was conducted and the effect of particle diameter on critical velocity was investigated. Some correlations that estimate the excess velocity of non-Newtonian slurry flow based on Newtonian slurry flow were examined. Application of suspension velocity correlations for mixer jet pumps to pipeline flushing was also investigated. In addition, FIU investigated previous work in the area of flushing related to high level waste (HLW) at Hanford. This review is being conducted to develop a plan for constructing a test loop that will allow for engineering-scale testing.

Technical Gaps

Results reported for flushing tests of 15 simulants in the WTP-RPT-175 Rev. 0 document [2] indicated that a minimum flush-to-line volume ratio of two would likely leave behind only small traces of particles in the pipeline. Increasing this ratio to three was suggested without guaranteeing that it would clean the pipeline completely. In addition, use of a system with automatic valve control based on different feedbacks was strongly suggested. The reported results for several tests indicated that velocity in the pipeline could reach values close to 20 ft/s before and after the overshoot in density profile. This overshoot indicated a maximum in solid concentration in the system. In several cases, high velocities were obtained even in steady conditions (flat sections of the density and velocity profiles) where traces of particles were probably flowing in the system. Flow of this solid-liquid mixture with these reported velocities which were higher than the upper limit set by the design guide (24590-WTP-GPG-M-0058, Rev. 0 [5]) can cause some level of erosion in the pipeline. This excessive velocity could be due to the nature of the system as the pneumatic system used for flushing provided flow rates on the order of 500 gpm to 1000 gpm for a 100-gallon loop. Erosion levels can be magnified by increased flush duration which could be the scenario in a cross-site pipeline at Hanford. A flush duration with a flush velocity of 20 ft/s is approximately 13 minutes in a 3-mile pipeline. To control the flow rate while maintaining pressure, an electric pump or other method can replace the pneumatic flush system.

Critical Velocity Correlations

Shortlisted correlations of critical velocity for Hanford waste are the Oroskar and Turian (1980) and Gillies and Shook (1991) models [1]. The correlation of Oroskar and Turian (1980) was used in the study of waste transport at Hanford [2-4]. FIU evaluated these correlations with some inputs available fall Hall [5]. FIU's simulation results were very similar to those by Poloski et al. [2] with the Oroskar and Turian (1980) model. The results show conservatism once compared to the experimental values. However, use of the Gillies and Shook (1991) model resulted in a significant underestimation of critical velocity since this correlation works well for mass mean particle diameter of 180 µm according to Poloski et al. [6]. For this reason, this correlation was not applicable to the first and second cases because of small particle mean sizes. The numbers in parenthesis are results of applying this correlation. Excellent agreement was obtained for the third case as d_{50} would be closer to 180 µm.

Table 1-1. Calculation of Critical Velocity Using Shortlisted Correlations

Case	Experiment Hall 2006	Poloski et al. 2009 Model [1]	This Report Model [1]	This Report Model [2]
1	3	4	4.03	N/A (0.09)
2	4	4.1	4.09	N/A (1.48)
3	8	8.1	8.19	8.04
[1] Oroskar and Turian (1980) [2] Gillies and Shook (1991)				

In another effort, the effect of particle size reduction on critical velocity was assessed. The d_{95} parameter of the second case was reduced from 182 µm to 91 µm, and it was assumed that the majority of particles (85% volume fraction) were less than 74 µm. The properties of the carrier fluid such as viscosity and density were updated using ρ_f = ρl * C_l + ρ_sf * C_sf and an equation from Thomas (1965), µ_f = µ_l* (1 +2.5 C_sf + 10.05*C_sf2+0.00273*exp(16.6* C_sf)). It was observed that critical velocity was reduced by a factor of 1.52. A similar analysis from Poloski et al. [2] shows a significant change of critical velocity with a change of particle size.

Other efforts included evaluation of correlations that provide excess velocity based on the critical velocity of Newtonian fluids. This analysis could be useful to provide an estimate for the flow increase requirement when a Newtonian slurry is replaced by a non-Newtonian slurry. Correlations of Wilson-Thomas (1985, 1987) for the power-law (n=0.376, α = 7.4, ρ = 1000 kg/m3), Bingham plastic (τy_B=4.4 pa, η_p=0.0066 Pa.s, ρ= 1159 kg/m3), and Casson type (τy_c=20 pa, η_c=0.0017 Pa.s, ρ = 1159 kg/m^3) fluids (these values were extracted from [7,8]). Calculations with a wall stress value of 30 Pa revealed excess velocities as large as 1.63 ft/s, 1.14 ft/s, and 3.66 ft/s, respectively. Therefore, if 4.6 ft/sec was assumed to be sufficient for a Newtonian slurry to prevent solid deposition, 6.23 ft/sec is the velocity needed for a non-Newtonian velocity based on an excess velocity of 1.63 ft/s.

Further, application of the suspension velocity correlation of Kale and Patwardhan [9] [10], which was originally developed for pulse jet mixer (PJM) applications, to pipeline flushing was examined. Erosion of a sediment bed sitting in a pipe invert with a bed height equal to the fraction of pipe inside diameter was considered. It was assumed that a high-velocity flow entering a partially plugged pipe acts like a jet which impacts on the surface of the sediments. Determining the velocity of this jet, which is sufficient to erode this sediment layer with a length equal to multiple pipe diameters, is desired. The nozzle diameter was assumed to be the hydraulic diameter of the unplugged portion of the pipe's cross-sectional area, defined as dj = 4* $A_{unplugged}$/ $P_{unplugged}$). Results of this preliminary application were compared to the critical velocity calculated from correlation of Oroskar and Turian (1980). Since the suspension velocity is usually higher than the critical velocity, this comparison could be used as a primitive check on the analysis. Table 1-2 shows the results obtained for solid loading of 20%, solid and liquid densities of 2500 and 999 kg/m3, respectively, liquid viscosity of 1 cP, and length of the sediment layer of 1 meter or 13.2 times the pipe diameter (pipe diameter was selected as 3 inches or 0.078 m).

Table 1-2. Calculation of Suspension Velocity for Particles in a 3" pipe

D_pipe/z	V_susp	d_nozzle* (m)
2	10.43114	0.0046
3	7.780723	0.054
4	6.592275	0.059
5	5.954697	0.062
6	5.562316	0.064
7	5.297831	0.066
8	5.107917	0.067
*This value is 0.04 m in the analysis of Wells et al. (2011)		

Testing Methodology

To provide the necessary pressure head and flow rates in flushing tests, three systems are being considered: (1) use of an elevated water tank with a fixed water level, (2) use of a variable-speed electric water pump, and (3) use of compressed air to pressurize water in a flush vessel. The third configuration is meant to advance the flushing system that was used in previous testing [2]. The systems in the first and third configuration would be equipped with a motor-operated valve for flow rate adjustment. Results in WTP-RPT-175 Rev. 0 showed that adequate flushing was obtained with pressure reaching values of 80 to 100 psi during flushing of simulants. To construct the second system, an electric water pump capable of delivering 100 gpm of water at 80 psi could be a candidate to avoid high velocities in the system. A review of existing manufacturer products has indicated that a variable frequency drive (VFD) may be needed to meet these requirements. Examples of candidate pumps can be found in one of the listed references [12].

FIU's flushing test loop will have some differences from the existing loops used for the Hanford waste testing. A controller module would be used to control the opening and closing of a motor-operated valve in the first and third system configuration, or to ramp up/down and shut off the electric pump in the second system configuration. All systems could be excited with a regulated signal from a controller module to provide variable pressure in the pipeline if such a practice could result in better flushing performance. This controller can analyze the signals received from a tank level transmitter and two Coriolis meters placed upstream (right after the water pump, elevated tank, or the flush vessel) and downstream (close to the capture tank) of the loop to correctly adjust the flow rate and duration of the flush. Signals from the upstream and downstream meters will indicate flow velocity and traces of particles (density), respectively. If density signals from the upstream and downstream meters are very close, then almost pure water is being discharged to the capture tank and the controller shuts off the water pump to end the flushing operation. As per FIU’s communications with manufacturers, Micro-Motion F series-2700 and 5700 models provide 4 to 20 mA signal outputs of mass and density that could be input into a LabView program for flow rate and velocity calculations and further used by the controller module.

A slightly more complicated but more accurate system can incorporate a sampling port with a valve just before the capture tank. Visual inspections or analysis through a particle size analyzer can then help to qualitatively and quantitatively evaluate the flush performance. Complexity can be increased by operating based on signals received from other instruments, such as a PulseEcho sensor, a Lasentec sensor, or from an optical probe in a clear section of the system [13]. The system could be designated empty if no results come from the PulseEcho and Lasentec sensors. Use of PulseEcho and Lasentec sensors in the loop can be an extension of the sensor utilization from particle velocity and size measurements in documents WTP-RPT-175 Rev. 0 [2] and WTP-RPT-189 Rev. 0 [11] to provide real-time monitoring of the particle presence and concentration during flushing operations.

Presently, FIU is assessing the availability of equipment that is necessary for simulant preparation as well as flow rate and pressure measurements. A pipeline made of approximately 270 feet of 3-inch-diameter carbon steel schedule 40 pipeline is currently ready to be connected to tanks, pumps, and other instrumentation to form a test loop. FIU has the capacity to make this pipeline shorter or longer for down scaling and up-scaling purposes.

An integrated system with automatically-controlled valves which is suitable for both critical velocity and flushing tests is illustrated in Figure 1-2. This figure shows existing, up-scaled, and down-scaled versions of FIU’s candidate loop. In ideal configuration, system includes instrumentations for measurements of mass flow rate, density, particle size, particle chord length, pressure gradient, particle speed, and sediment bed height. Table 1-3 lists the instrumentation and equipment needed for an ideal system. The shortest pipeline in Figure 1-2 could potentially be constructed with transparent sections and be equipped with most of the instrumentation included in Table 1-3. This system would allow for better visibility of sediment beds or plug formation, in addition to providing better characterization of the system before and after flushing operations.

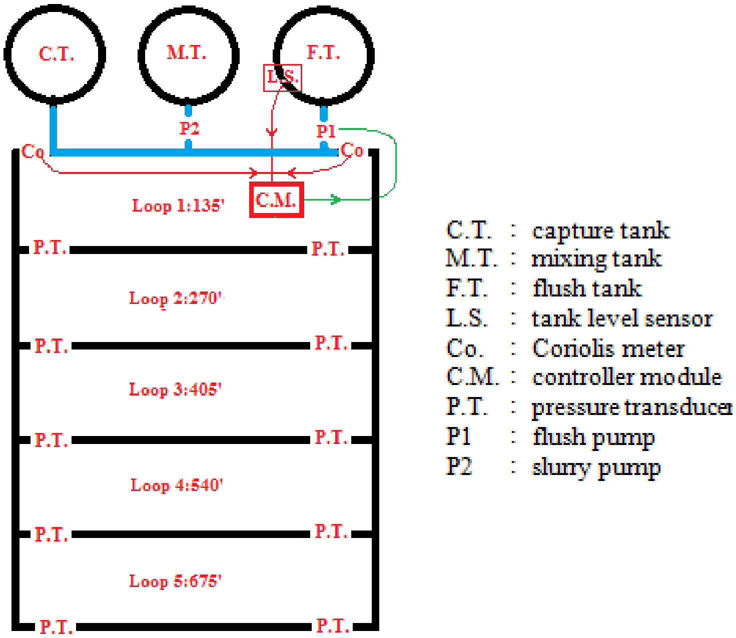

Figure 1-2. Five versions of FIU's candidate loop.

Table 1-3. Potential Data/Instrumentation and Equipment

No.	variable	Instrument type	#
F & C	Mass flow rate	Coriolis meter model 2700/5700	2
F & C	Density		
F & C	Pressure	Differential pressure transducer	2
C	Mixing tanks with agitator	400 gallons	1
F	Water tank	900 gallons	1
F & C	Capture tank	900 gallons	2
F	Electric water pump	15 HP	1
F & C	Ultrasonic sensor for bed detection	PulseEcho	2
F	Particle trace measurement	Mettler Toledo Lasentec	1
F	Control module	TBD	1
F	Motor-operated valves	TBD	1
F	Tank level transmitter	TBD	1
C	Rheometer	TBD	1
C	Slurry pump	TBD	1
C	Particle size analyzer	TBD	1
	Data acquisition (DAQ)	TBD	1
F: flushing C:critical velocity TBD: To be determined			

References

[1] Liell K.C. and Burnett D.F., 2000, Critical Transport Velocity: A Review of Correlations and Models. RPP-7185, Rev-0, CH2M Hill Hanford Group, Richland, Washington

[2] Poloski A.P., Bonebrake M.L, Casella A.M., Johnson M.D., MacFarlan P.J., Toth J.J., Adkins H.E., Chun J., Denslow K.M., Luna M.L., Tingey J.M., 2009, Deposition

Velocities of Newtonian and Non-Newtonian Slurries in Pipelines, PNNL-17639 WTP-RPT-175 Rev. 0

[3] Welch T.D., 2001, Tank Waste Transport, Pipeline Plugging, and the Prospects for Reducing the Risk of Waste Transfers, ID: ORNL/TM-2001/157

[4] Julyk, L. J., Oten J. C., Willis W. L.. 2000, Waste Feed Delivery Transfer System Analysis, RPP-5346, CH2MHILL Hanford Group, Inc., Richland, Washington (May).

[5] Hall MN. 2006. Minimum Flow Velocity for Slurry Lines. WTP Project Doc. No. 24590-WTP-GPGM-0058, Rev 0, Bechtel National, Inc., Richland, Washington.

[6] Poloski A.P., Etchells A.W., Chun J., Adkins H.E., Casella A.M., Minette M.J., Yokuda S.T., A A Pipeline Transport Correlation for Slurries with Small But Dense Particles, The Canadian Journal Of Chemical Engineering, Volume 88, April 2010

[7] Escudier M.P., Poole R.J., Presti F., Dales C., Nouar C., Desaubry C., Graham L., Pullum L., 2005, Observations of symmetrical flow behaviour in transitional pipe flow of yield-stress and other shear-thinning liquids, J. Non-Newtonian Fluid Mech. 127, p.p.143–155

[8] Heywood N., 2008, Slurry retrieval, pipeline transport and plugging and mixing workshop, January 14-18, 2008, Tampa, Florida

[9] Kale R.N, and Patwardhan A.W., 2005, Solid Suspension in Jet Mixers, The Canadian Journal of Chemical Engineering 83(5):816-828.

[10] Wells B.E., Gauglitz P.A., Rector D.R., 2011, Comparison of Waste Feed Delivery Small Scale Mixing Demonstration Simulant to Hanford Waste, PNNL-20637 Rev. 0

[11] Poloski A.P., Adkins H.E., Abrefah J., Casella A.M., Hohimer R.E., Nigl F., Minette M.J., Toth J.J., Tingey J.M., Yokuda S.T., 2009, Deposition Velocities of Newtonian and Non-Newtonian Slurries in Pipelines: Complex Simulant Testing, PNNL-18316 WTP-RPT-189 Rev. 0.

[12] http://apps.taco-hvac.com/wizard_pumps.html.

[13] Goosen, P., H. Ilgner and S. Dumbu, 2011, Settlement in backfill pipelines: its causes and a novel online detection method, International Conference on Mining with Backfill.

Subtask 17.1.2: Computational Fluid Dynamics Modeling of a Non-Newtonian Fluid Undergoing Sparging for Estimating PJM Mixing Times

FIU conducted additional simulations in order to establish a simulation foundation. This included simulating the work of Chen et al. (2016). Decent agreement between simulation and experiments were observed, as shown below:

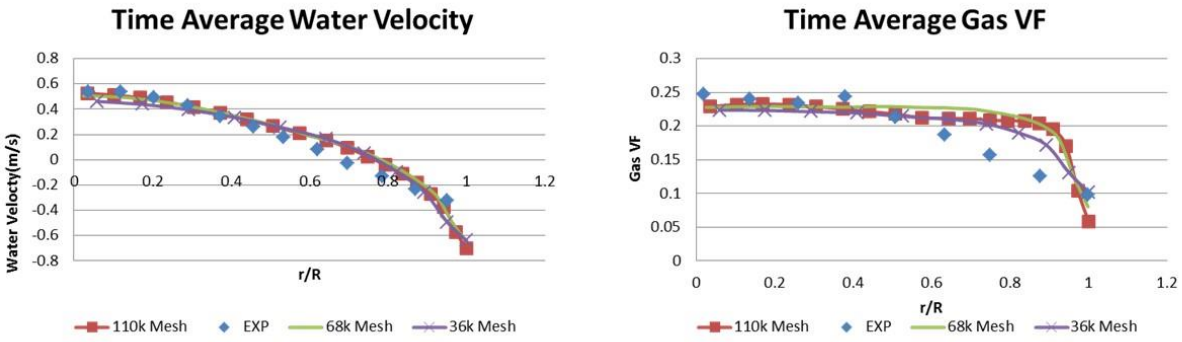

Figure 1-3. Mesh sensitivity analysis and comparison between simulation and Chen et al. (2016) experimental data.

For this task, a mesh grid sensitivity analysis for a bubble column with a Newtonian fluid was also completed. It was concluded that the mesh was stable enough to provide consistent results in Newtonian bubble columns.

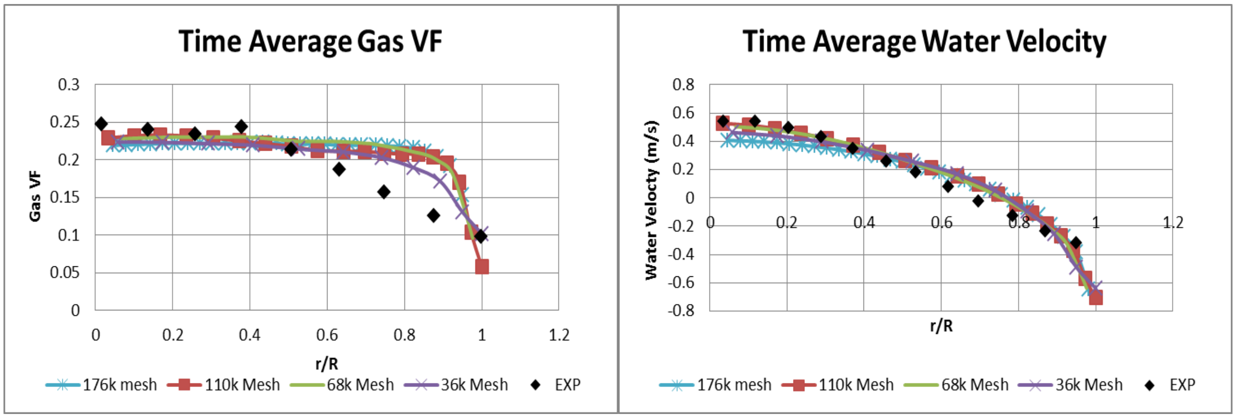

Figure 1-4. Mesh sensitivity analysis with Newtonian fluids.

Furthermore, it was observed that a standard k-epsilon model improves the discrepancy observed in the volume fraction profile, as shown below.

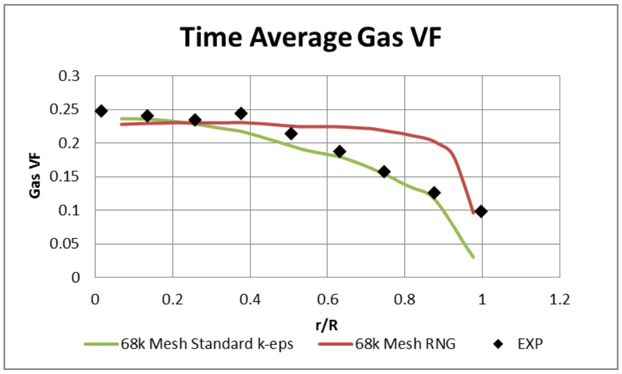

Figure 1-5. Turbulence model comparison.

As can be observed in the previous two figures, a relatively accurate bubble column simulation with Newtonian fluid has been established. A simulation using non-Newtonian fluid was developed. The literature has limited published works on non-Newtonian fluids and, specifically, no experimental data on bubble columns with a Bingham plastic. One experimental paper on flow characteristics of shear thinning fluids in bubble columns by Esmaeili et al. (2015) was found. The Newtonian simulation model was re-used with exception of the addition of the power law viscosity model, different geometric conditions, and inlet conditions. Below are the simulation results after 30 seconds of time-averaged results.

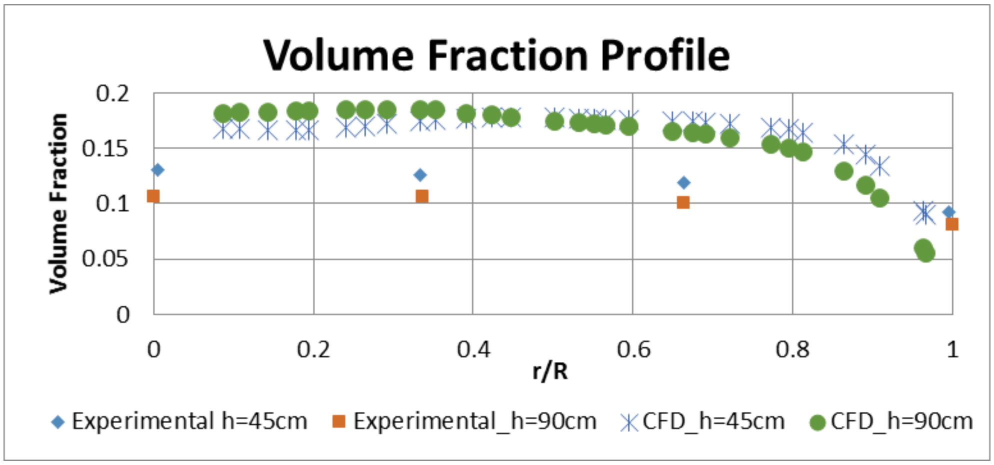

Figure 1-6. Comparison between Esmaeili et al. (2015) and simulation at two different bubble column heights.

For this first attempt, the simulation over predicts the volume fraction profile by a factor of about 2 as can be seen in the previous figure. It was observed through a contour plot of viscosity that the viscosity was held largely constant throughout this simulation, explaining why the results resemble those of a Newtonian bubble column at similar inlet conditions.

Upon additional simulations replicating the works of Esmaeili et al. (2015) to investigate sparging non-Newtonian fluid, the discrepancies of the volume fraction previously observed were improved as shown in the following figure.

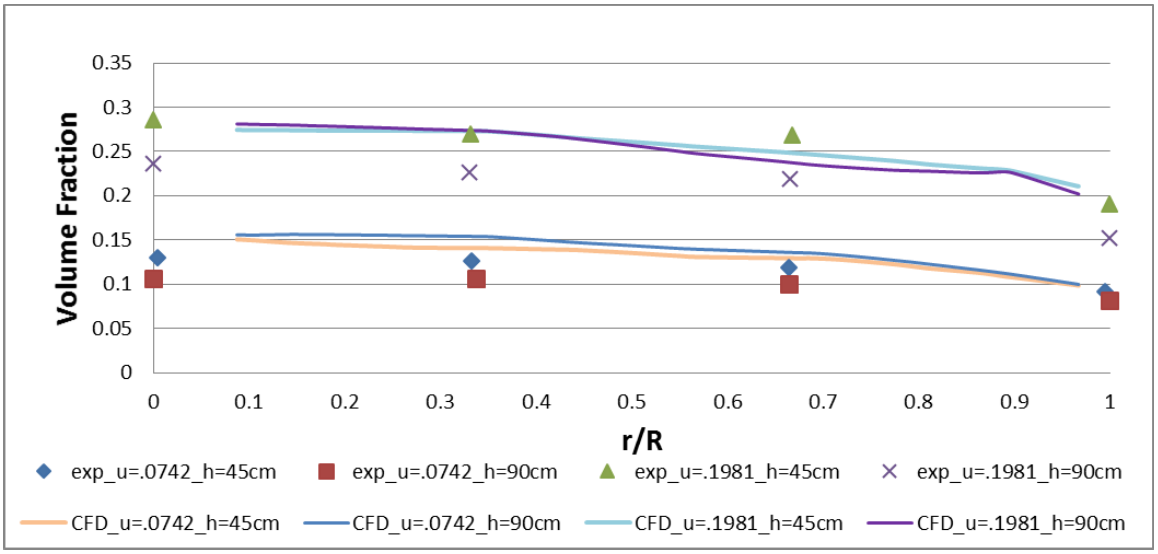

Figure 1-7. Volume fraction comparison of Ismaeli (2015) experimental and CFD predictions.

Esmaeili conducted two experiments with different sparging flow rates and measured volume fraction at two distinct heights of his experimental bubble column. An investigation on the effects of the simulated bubble diameter was conducted and it was observed that the higher the bubble diameter, the lower the volume fraction value that was recorded. In the Esmaeili experiments, he recorded a slight increase in bubble diameter as the bubble traveled upwards. In the current simulations, a constant bubble diameter was used and is, therefore, considered to be the main contributor to the slight discrepancies between the simulations and the experimental data. Lastly, the velocity profile between the current simulations and Esmaeili's experiments were also compared.

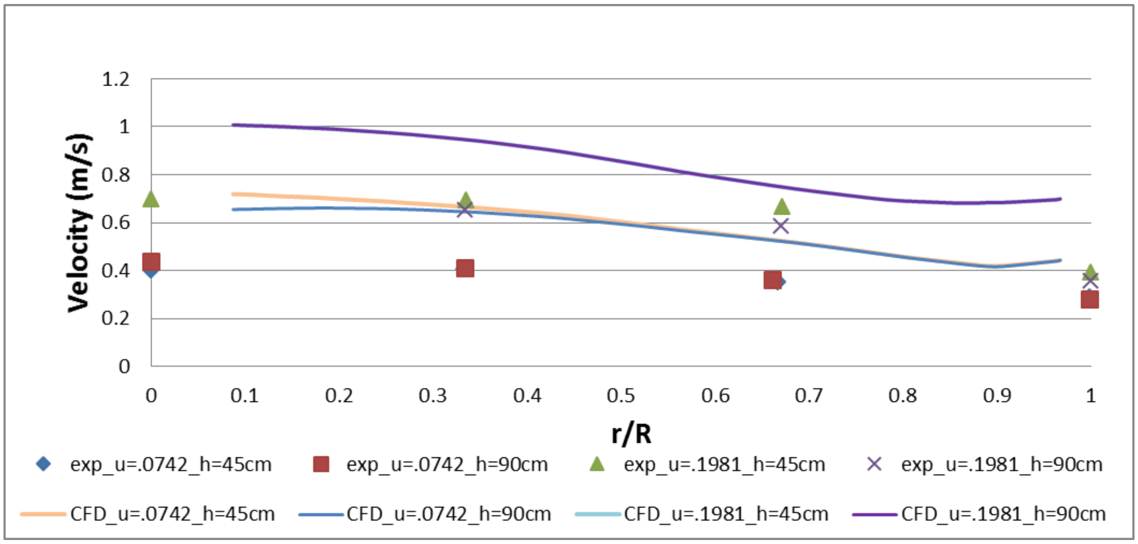

Figure 1-8. Time averaged Z velocity comparison of Ismaeli (2015) experimental and CFD predictions.

In the previous figure, it is clear that the current CFD simulations over-predict the velocity profile at the two different heights and sparging flow rates. It is shown that there is a consistent over-prediction in maximum velocity of 0.3 m/s. As a path forward, different drag models and turbulence models will be used in order to better match the velocity profile. Benchmark problems of a Bingham plastic will be simulated with the Eulerian model to finish laying a foundation which will enable the project to conduct mixing time simulations.

Task 18: Technology Development and Instrumentation Evaluation

Task 18 Overview

The objective of this task is to assist site engineers in developing tools and evaluating existing technologies that can solve challenges associated with the high level waste tanks and transfer systems. Specifically, the Hanford Site has identified a need for developing inspection tools that provide feedback on the integrity of the primary tank bottom in DSTs. Under this task, FIU is developing inspection tools that can provide visual feedback of DST bottoms from within the insulation refractory pads and other pipelines leading to the tank floor.

As part of the Hanford DST integrity program, engineers at Hanford are also interested in understanding the temperatures inside the primary tanks and to safeguard against exceeding specified limits. These limits are set to ensure that the tanks are not exposed to conditions that could lead to corrosion of the tank walls. Previously, analysis was conducted to determine the viability of using an infrared (IR) temperature sensor within the annulus space to estimate the temperature of the inside wall of the tank. The analysis suggested that variations due to heat loss would be minimal and reasonable estimates using the sensor within the annulus is viable. Under this task, FIU is also evaluating the ability of IR sensors to detect inner tank wall temperatures via bench scale testing.

Task 18 Quarterly Progress

Subtask 18.2: Development of Inspection Tools for DST Primary Tanks

Miniature Rover Inspection Tool

Redesigns of the inspection tool were developed in order to improve visual quality, increase the pull force, improve the overall functionality of the inspection tool, and facilitate integration of various environmental and radiation sensors.

Patch LEDs were used to replace the standard bulb LEDs and tests were conducted to investigate the number of patch LEDs needed to provide an adequate amount of illumination. Instead of 2 bulb-LED lights that were used for the previous design, 4 patch-LED are being used for the new design (Figure 1-9). The new design not only increases the amount of light, which is essential for better image quality, but also re-positions both the camera and LED light locations to make room for sensor integration on the hood of the inspection tool.

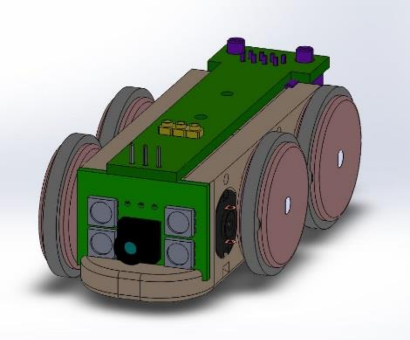

Figure 1-9. The redesigned inspection tool without the hood. Both the camera and the LED lights are connected perpendicularly to the base-PCB. Three extra connector-pins (yellow) are added on the base-PCB to provide connections to the sensors.

A space for an extra magnet was also added at the front of the unit. This was done in order to increase the unit's magnetic pull-force with the metallic surface. The increase in the magnetic pull-force between the unit and the surface also results in an increase of the overall traction of the inspection tool. This is important to ensure that the inspection tool is able to overcome the friction of the tether.

Work also began on the conceptual design to integrate sensors into the inspection tool. The sensors considered include temperature, infrared, and ultra-sonic (UT) sensors. The first conceptual design integrated a one-wire temperature sensor (Maxim DS18B20), as shown in the following figure. The hood, which was previously used just for covering the base PCB board, will now house the actual sensors. The conceptual design promotes interchangeability where hoods with different sensors can be fabricated and exchanged onto the inspection tool for different inspection objectives.

Three sensors for the inspection tool were received, including the temperature sensor (Maxim DS18B20), the temperature and humidity sensor (Maxim DS1923) and the radiation sensor (Teviso RD2014). FIU conducted testing to ensure the sensors are functioning correctly. These tests included the wiring (with necessary supporting electronic components like resistors and capacitors) as well as powering and sensor driver programming. For the radiation sensor, a Cs-137 source was used to make sure it correctly registers the radiation count. All of the sensors are functioning as expected and the sensor drivers are ready to be integrated to the final system. The outcomes from the sensor testing helped in designing the sensor printed circuit boards (Sensor PCBs) that will be attached on top the mini inspection tool.

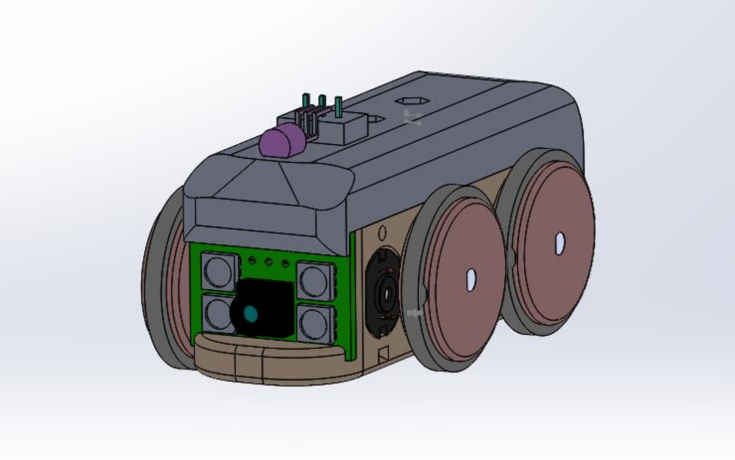

Figure 1-10. Initial conceptual design with a temperature sensor attached (purple) to the top of the inspection tool. The design also includes a patch-LED inserted on the front PCB, replacing the bulb LED.

The individual PCBs' location within the mini inspection tool is shown in Figure 1-11. The base PCB carries the power for the motor control, as well as providing communication for both the sensor and camera PCBs. The base PCB provides a common three-pin connector for different sensor PCBs to be attached. This design allows for different sensor PCBs to be designed and fabricated for different sensors, without any modification to the base PCB, thus, providing a generic interface for different sensor integration and expansion. The camera PCB houses both the camera and the LED light source. Details of the sensors that are currently being considered are shown in the table below.

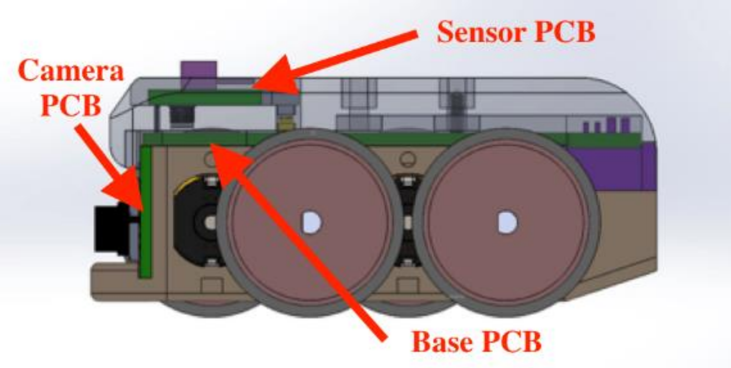

Figure 1-11. CAD drawing showing various PCBs for the electronic components.

Table 1-4. Sensors Considered for Integration into the Miniature Rover

Sensors Types	Sensors	Communication	Descriptions
Temperature (Maxim DS18B20)		One-Wire	Ambient temperature sensor
Temperature and humidity (Maxim DS1923)		One-Wire	Ambient temperature and humidity sensor
Radiation (Teviso RD2014)		TTL	Beta, gamma, x-rays sensor
Infra-red non-contact temperature sensor (CMCIEL mTS017)		One-Wire	Non-contact Infra-red temperature sensor

The finalized conceptual designs for the integration of sensors described in the previous table are shown below.

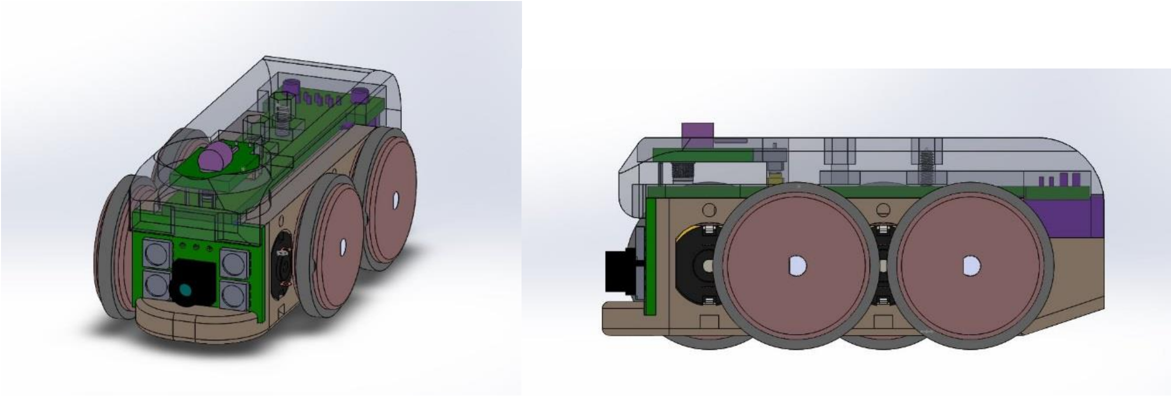

Figure 1-12. Conceptual design of temperature sensor integration for measuring the ambient temperature.

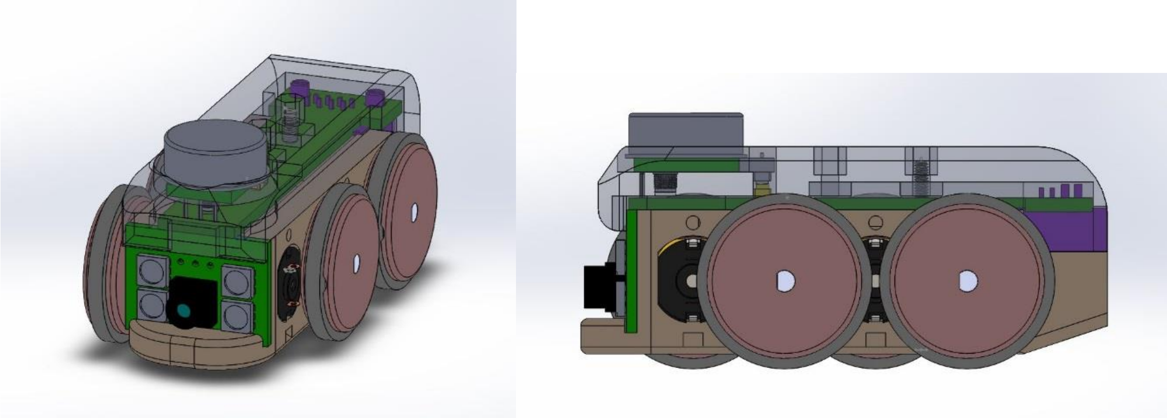

Figure 1-13. Conceptual design of iButton integration for measuring both the ambient temperature and humidity.

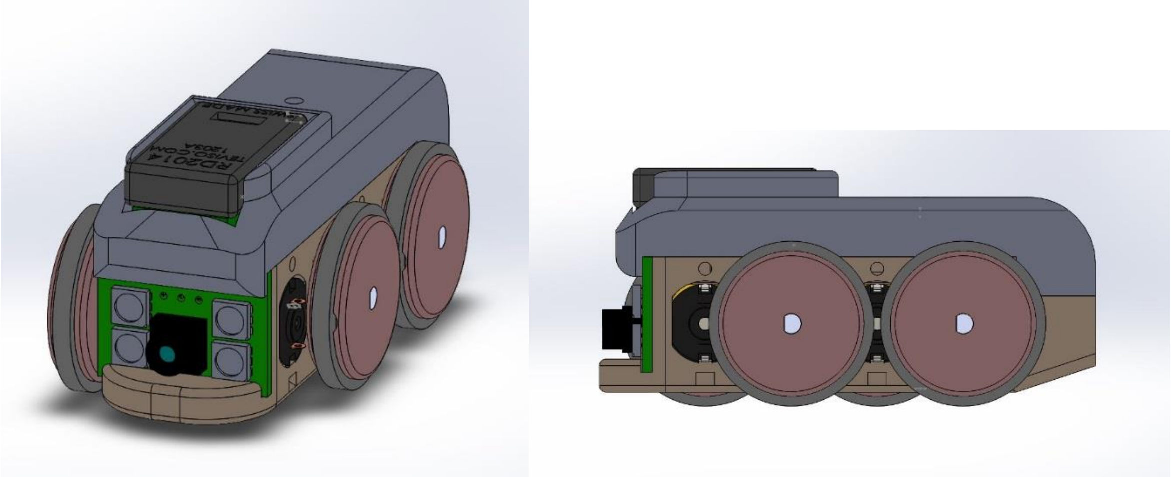

Figure 1-14. Conceptual design of radiation sensor integration for measuring beta, gamma and x-rays.

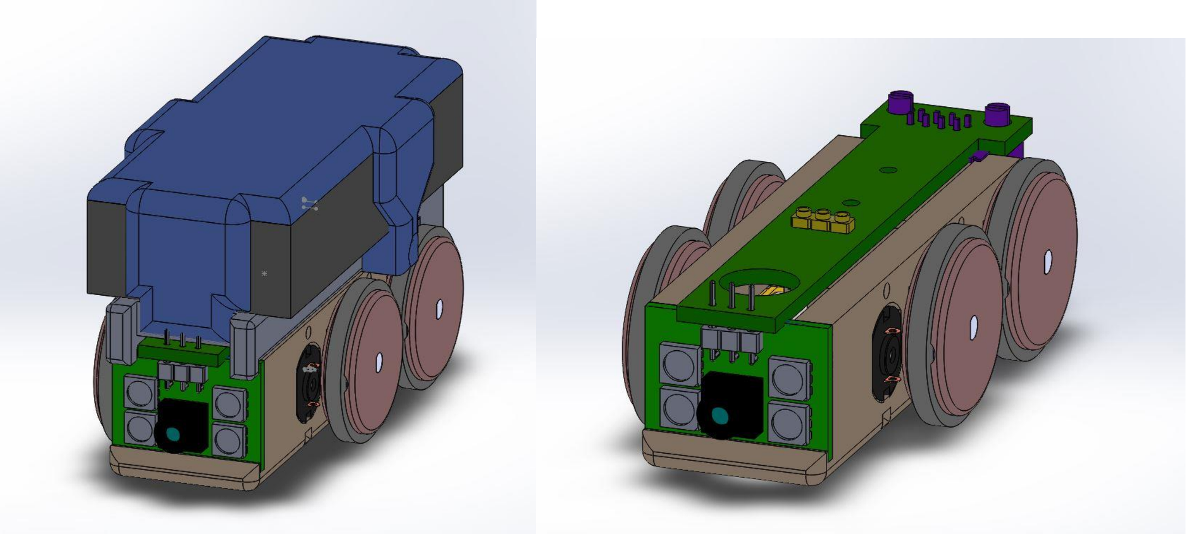

Figure 1-15. Conceptual design of non-contact infrared temperature sensor for measuring the surface temperature of the tank bottom. The circular cutout (on right) through the inspection tool's body allows the IR sensing element to be fitted to measure the surface temperature of the tank.

Additional efforts concentrated on fine-tuning the camera image processing and proportional–integral–derivative (PID) control of the semi-autonomous control for the mini inspection tool. In addition, sensor testing and software integration were conducted. The outcome from the sensor testing also assisted in designing the sensor printed circuit boards (PCBs) that will be attached to the mini inspection tool.

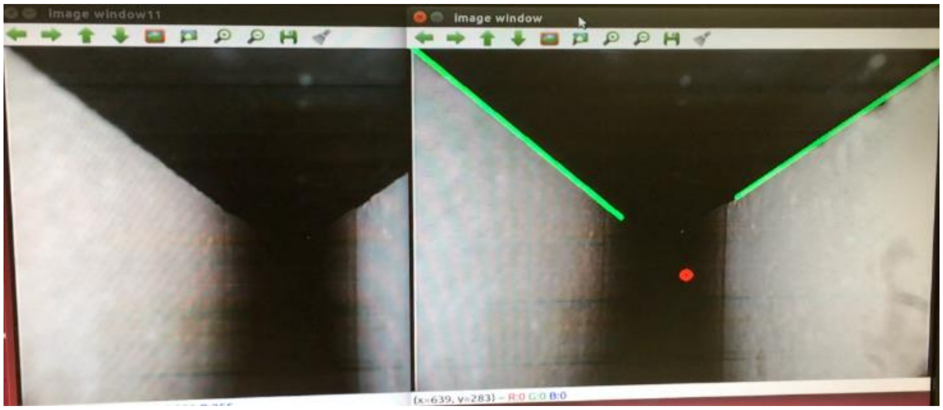

Figure 1-16. (Raw image from the camera (left) and processed image with the detected channel boundaries overlaid in green (right).

Additional efforts concentrated on fine-tuning the camera image processing and proportional–integral–derivative (PID) control of the semi-autonomous control for the mini inspection tool is currently underway. Some of the parameters for edge and line detection, as well as color segmentation, were fine-tuned. This results in clearer and more stable detection of the lane (Figure 1-16) for the semi-autonomous control of the inspection tool. A preliminary PID control has been designed and implemented to navigate the mini inspection tool along the central location of the detected lane, while the operator controls the tool's forward and backward motion. The semi-autonomous operation frees the operator from having to keep the inspection tool away from the narrow refractory wall. Figure 1-17 shows the PID's performance in controlling the inspection tool along the reference (Ref) signal. Although the results are preliminary, the controller was able to navigate the inspection tool within tolerable errors.

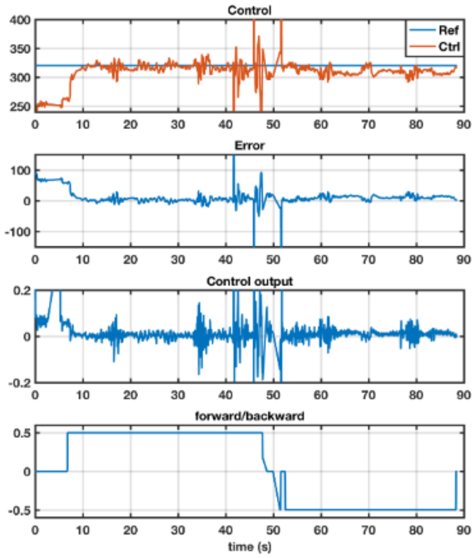

Figure 1-17. The PID's control outputs.

<u>Pneumatic Crawler Inspection Tool</u>

The main activity for the pipe crawler task was focused on enhancing the inspection tool capabilities by adding sensors integration. In addition, the pneumatic crawler design has been enhanced to integrate several sensors, with the objective of improving the inspection tool capabilities, robustness and operational feedback.

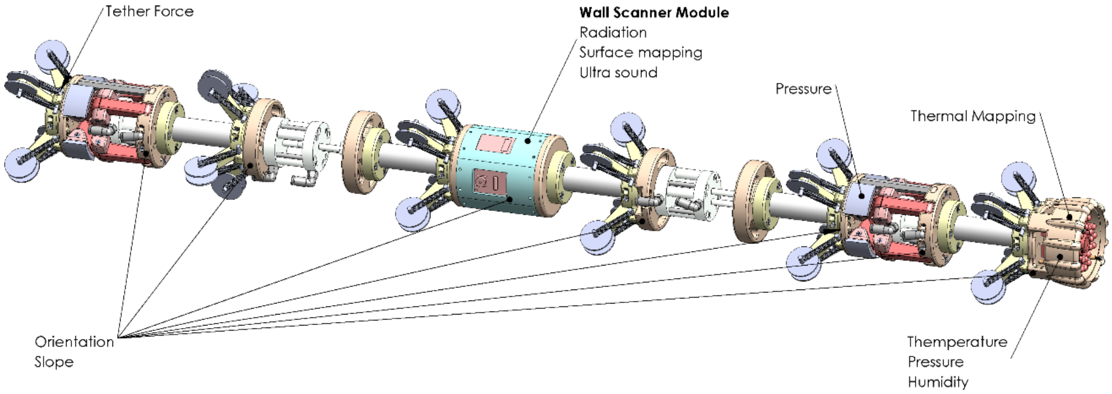

Figure 1-18. Sensor integration.

As illustrated in the previous figure, FIU completed the evaluation of the following sensors to be integrated into the inspection tool, improving capabilities and robustness:

a) additional thermal infrared camera to the camera module, providing thermal imaging mapping, hot spot detection and temperature gradient analysis;
b) ambient temperature, pressure and humidity, providing environmental conditions;
c) additional wall scanner module, providing radiation, ultrasound, and visual surface mapping;
d) tether force to the last module, providing drag estimation;
e) contact pressure sensors to the grippers, providing grip condition;
f) inclinometer, providing slope and orientation for each module.

An embedded computer will be utilized to control the modules and manage and communicate with the sensors. The controller area network (CAN bus) protocol will be used to provide communication between the on-board computer and the portable control box thru the tether. Listed below are the sensors that are currently being considered for prototyping. The initial sensors selected are affordable and high precision versions may be considered for deployment.

Table 1-5. Sensors Considered for Integration into the Pneumatic Crawler

Description	Sensor
Thermal infrared camera	FLIR LEPTON® Long Wave Infrared (LWIR)
Ambient temperature, pressure and humidity	Adafruit BMP280 I2C or SPI Barometric Pressure & Altitude Sensor
Radiation	Teviso RD2014
Ultrasound	Ultran Group WD25-2
Visual surface mapping	PTC06 Serial Camera Specification
Tether force	Phidgets Micro Load Cell CZL635 (0-20kg) SparkFun Load Cell Amplifier - HX71
Pressure sensors	Sparkfun Force Sensitive Resistor 0.5"
Inclinometer	AltIMU-10 Gyro, Accelerometer, Compass, and Altimeter

The additional module evaluated will be a carrousel type scanner that rotates and maps the surface along the pipe inspection. As illustrated in Figure 1-19, the module uses six (6) modular panels that can be customized for different sensors.

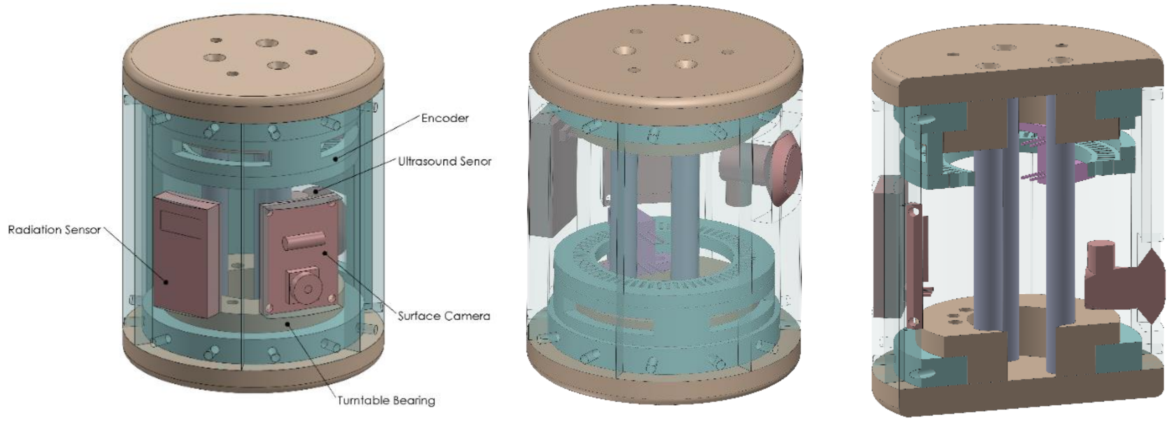

Figure 1-19. Wall scanner module.

Full-Scale Sectional Mockup

Construction of the full-scale sectional mockup testbed of a double-shell tank (DST) also continued during the last quarter. The testbed will include modular sections of the refractory air slots underneath the primary liner and the drain slots underneath the secondary liner. The following figure shows the concrete foundation design which includes a wooden structure coated with concrete.

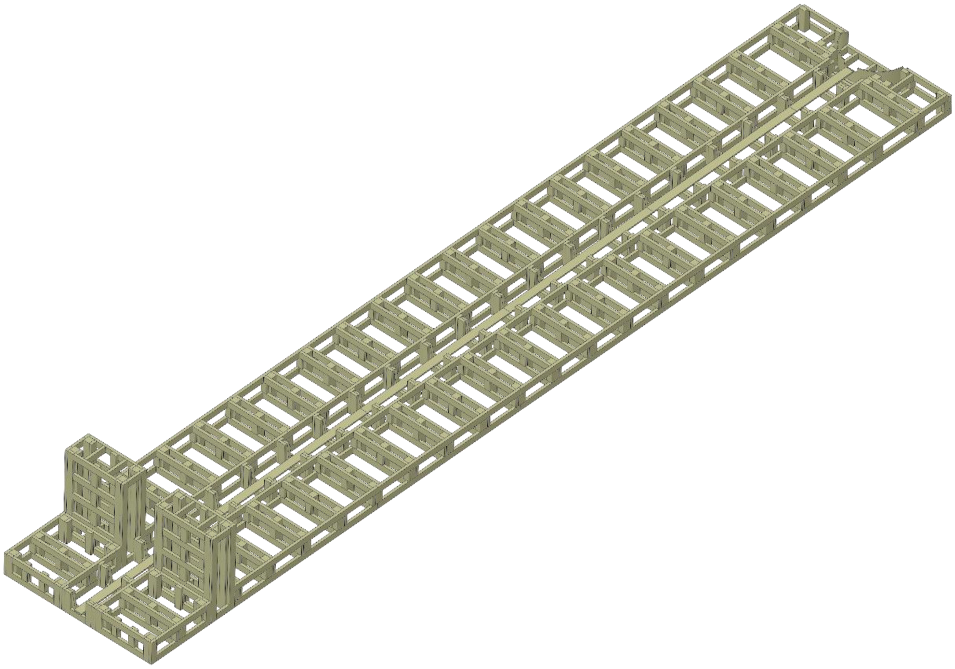

Figure 1-20. Concrete foundation structure with draw slots.

The construction progress is captured in a number of pictures shown below.

Figure 1-21. Testbed foundation construction.

As shown in the photographs, the foundation frame has been completed and was covered in wood paneling. The wood structure was then covered with a protective film and a mesh has been overlayed in preparation for the concrete coating.

The team's efforts will continue to focus on the construction of the full-scale sectional mockup. A timeline for completion is shown below. The grayed columns in the construction schedule shows the elapsed weeks. The next major effort will be manufacturing the air refractory structure. Efforts will be made to manufacture the system to be modular and easy to modify if different configurations are needed.

Table 1-6. Timeline for Construction of the Full-Scale HLW Tank Mockup

		Weeks							
Module	**Construction**	**1st**	**2nd**	**3th**	**4th**	**5th**	**6th**	**7th**	**8th**
Concrete Foundation	Metal lathing	x	x	x	x				
	Concrete coating				x	x			
Refractory Pad	Frame designing				x	x			
	Frame construction					x	x	x	
	Frame Paneling					x	x	x	
	Concrete Coating					x	x	x	
Mockup	Assembly								x

Subtask 18.3: Investigation Using an Infrared Temperature Sensor to Determine the Inside Wall Temperature of DSTs

A milestone summary document (2016-P1-M18.3.1) for this activity was drafted and submitted. In addition, the integration of an IR sensor with the mini rover was investigated. The milestone summary document included the results obtained from the engineering-scale experiments conducted using the IR sensor to obtain the temperature profile on the inner shells of the DSTs. Experiments were also conducted to investigate the sensitivity of the Raytek IR sensor to different emissivity values and materials. A method was established to accurately calibrate and test the Raytek mini IR sensor. The tests were conducted with hot water as the liquid medium. It was concluded that the Raytek sensor was capable of taking temperature measurements in the DSTs within specified limits.

In addition, integration aspects of the IR sensor with inspection devices for deployment into the tanks and other pipelines have been investigated. Previously, the sensor was temporarily attached to the mini rover to check for its dimensional and design feasibility. Basic testing was later conducted to observe the effect of the magnets (in the mini-rover) on the IR sensor performance. The mini rover has 4 mini magnets and the sensor head consists of a lens to capture the IR rays. The sensor head attached to the mini rover was used to measure surface temperature of a test piece at room temperature and at elevated temperatures. To validate the temperature, a thermocouple was permanently attached to the test piece and the readings were recorded. The set-up was as shown in the following figure. It was concluded that the IR sensor was not affected by the magnetic field produced by the mini magnets in the rover for the time that it was exposed.

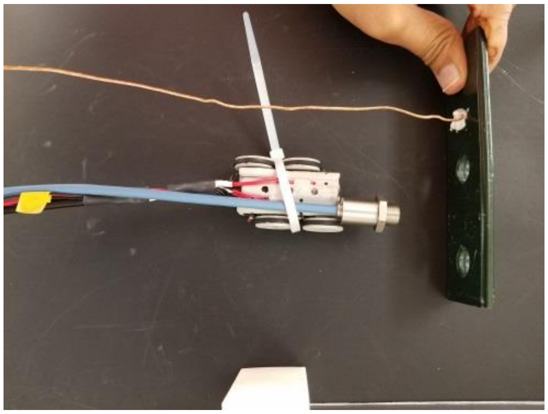

Figure 1-22. IR sensor head on the mini rover measuring temperature of the test piece.

This task has been completed. FIU will discuss with Hanford engineers whether additional testing is needed. Currently, FIU is researching options for permanently integrating the IR sensor with the mini rover and testing it on the full-scale mockup testbed being constructed at FIU ARC.

Task 19: Pipeline Integrity and Analysis

Task 19 Overview

The objective of this task is to support the DOE and site contractors at Hanford in their effort to evaluate the integrity of waste transfer system components. The objective of this task is to evaluate potential sensors for obtaining thickness measurements of HLW pipeline components. Specific applications include straight sections, elbows and other fittings used in jumper pits, evaporators, and valve boxes. FIU will assess the accuracy and use of down selected UT systems for pipe wall thickness measurements. FIU will also demonstrate the use of the sensors on the full-scale sectional mock-up test bed of the DSTs. An additional objective of this task is to provide the Hanford Site with data obtained from experimental testing of the hose-in-hose transfer lines, Teflon® gaskets, EPDM O-rings, and other nonmetallic components used in their tank farm waste transfer system under simultaneous stressor exposures.

Task 19 Quarterly Progress

Subtask 19.1: Pipeline Corrosion and Erosion Evaluation

The pipeline erosion system with the Permasense sensors was transferred to the high-bay lab facility at FIU ARC. The initial bench scale validation tests for the Permasense sensor system and a summary document for milestone 2016-P1-M19.1.1 was completed.

A pipe loop has been designed that can be used to erode the pipes and demonstrate the use of the sensors in realistic time frames. For space and safety reasons, the loop will need to be constructed in the high-bay testing facility at ARC. Thus, the current setup was transferred to the new location and the wireless gateway, computer and data acquisition were reconnected. The network was established and data recording was confirmed. The new set-up is shown in the following figure.

Figure 1-23. Permasense pipe system in ARC's high-bay laboratory.

The sensors collected data for over 4 months. A typical output of the excel spreadsheet generated by the software is shown in Table 1-7. From the table, it is evident that the thickness readings are stable throughout up to two decimal places of accuracy. Temperature compensation adds to the measurement accuracy.

Table 1-7. Sample UT Sensor Measurements for 3in Straight Section

ID	Name	Sent Time	UT measurement (mm)	Temperature (Â°C)	Temp. compensation Flag
#00001	3 inch straight	10/25/2016 18:09	5.487	19.93	1
#00001	3 inch straight	10/25/2016 18:13	5.483	19.87	1
#00001	3 inch straight	10/26/2016 9:54	5.489	18.9	1
#00001	3 inch straight	10/26/2016 9:57	5.483	19.49	1
#00001	3 inch straight	10/26/2016 11:04	5.484	19.84	1
#00001	3 inch straight	10/26/2016 11:17	5.483	19.93	1
#00001	3 inch straight	10/26/2016 17:20	5.487	19.55	1
#00001	3 inch straight	10/26/2016 23:24	5.488	19.22	1
#00001	3 inch straight	10/27/2016 5:27	5.49	19.61	1
#00001	3 inch straight	10/27/2016 11:31	5.489	19.17	1
#00001	3 inch straight	10/27/2016 17:34	5.489	19.61	1
#00001	3 inch straight	10/27/2016 23:37	5.488	19.25	1
#00001	3 inch straight	10/28/2016 5:41	5.488	18.87	1
#00001	3 inch straight	10/28/2016 11:44	5.489	18.9	1
#00001	3 inch straight	10/28/2016 17:47	5.488	19.61	1
#00001	3 inch straight	10/28/2016 23:50	5.489	19.55	1
#00001	3 inch straight	10/29/2016 5:54	5.489	19.93	1
#00001	3 inch straight	10/29/2016 11:58	5.485	19.93	1
#00001	3 inch straight	10/29/2016 18:00	5.487	19.55	1
#00001	3 inch straight	10/30/2016 0:03	5.488	19.61	1
#00001	3 inch straight	10/30/2016 6:06	5.488	18.63	1
#00001	3 inch straight	10/30/2016 12:09	5.489	19.61	1

In addition, sample 2-inch elbow measurements from October 2016 through January 2017 are provided in Figure 1-24. The maximum thickness measured was 4.346 mm and the minimum value was 4.336 mm. The average for the sample data was 4.340 mm and the standard deviation of the data was 0.0015.

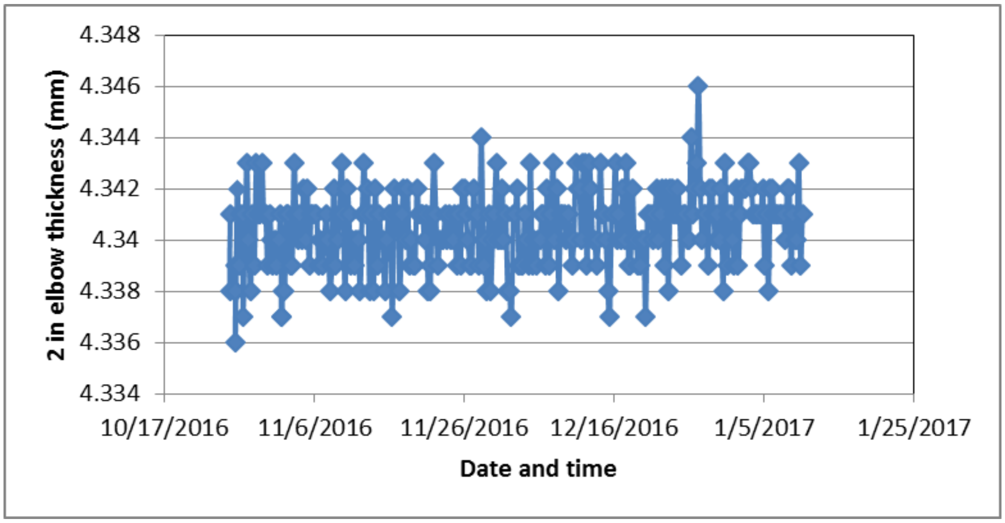

Figure 1-24. Sample thickness measurements for 2-in elbow section from Oct 2016 to Jan 2017.

During the testing period, there was no significant change in the average readings, which is as expected since the thickness remained the same. In addition, the thickness readings matched the manufacturer's specified thickness.

Options being considered to investigate erosion, corrosion effects include circulating a caustic fluid such as NaCl solution, Na_2SO_4 solution, NaOH solution or, alternatively, an abrasive fluid, through a closed loop pipe section to record the thinning of the pipe using UT sensors.

FIU finalized the pump requirements needed for caustic fluid circulation through the pipe loop to investigate real-time erosion/corrosion effects. A specific pump has been selected based on the proposed caustic solution (NaOH). Pump details are as below and the pump is shown in Figure 1-25:

- Model: 2P043 (Little Giant)
- Maximum Temperature: 200° F
- Maximum NaOH Concentration: 50%
- 1/8 HP PPS 115/230V Magnetic Drive Pump, 29.3 ft. Max. Head, Full Load Amps 3.00/1.50
- Length 11-1/4 in., Width 5-1/4 in., Height 7-1/2 in.

Figure 1-25. Pump to handle caustic solutions (Little Giant - 2P043).

As an alternative to a caustic solution, the typical erosion corrosion pilot pipe loop can also use sand as the abrasive solid media within the test loop since it is by far the easiest media to manage, from the initial procurement all the way to the final disposal. This media has been used in several areas including the oil and gas industry. For example, the characterization of erosion of gas pipelines by dry sand was studied by Naz et al. [1]. The study investigated the factors affecting the erosion of carbon steel in a dry sand stream on a laboratory-scale test rig. The study revealed that the normal incidence sand stream of larger particles and higher impact velocities causes more erosion of the carbon steel. The size of the sand particles varied from 200 µm to 600 µm; the incident angles varied between 30º and 90º; and the sand particle velocities considered were 10 m/s and 20 m/s.

Similar to sand, the effect of ocean, lake and de-ionized water on corrosion of carbon steel was researched by Morris [2]. Six samples of carbon steel coupons were immersed for 49 days in Lake Erie water, ocean water, and de-ionized water. The results obtained are shown in Figure 1-26. It is evident that the de-ionized water is most corrosive and Lake Erie water the least. These results provide a basis for the experiments to be conducted by FIU.

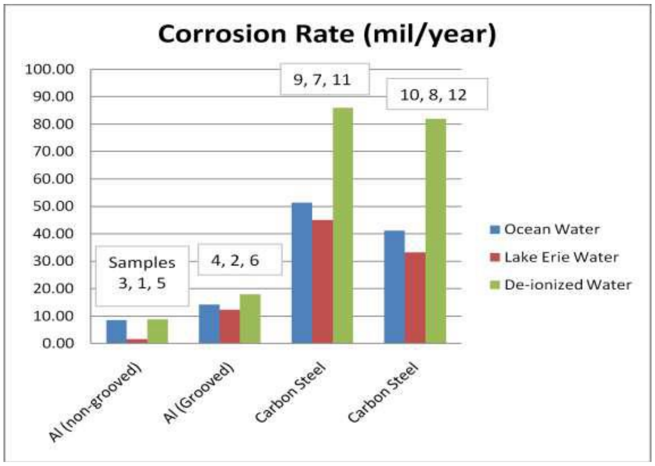

Figure 1-26. Corrosion in carbon steel and aluminum.

The effect of erosion/corrosion in oil and gas production was explored by Lu [3]. Modelling of synergistic effects on erosion is summarized in the work. The erosion-corrosion mechanisms, the methods to evaluate the erosion-corrosion resistance of materials and the approaches to mitigate the damage caused by erosion-corrosion are discussed in this reference [3].

The corrosion rate of steel in caustic solutions has been summarized in another one of the references [4]. It is generalized that the corrosion by caustic solutions (sodium or potassium hydroxide) at all concentrations is easily handled at room temperature with a variety of metals and alloys, including carbon steel. It becomes increasingly more corrosive with increasing temperature and concentration. The useful safe limit for carbon steel is approximately 150ºF/65ºC, both with regard to caustic stress corrosion cracking (CSCC) and corrosion. Stainless steel is more resistant to general corrosion compared to carbon steel; however, stainless steel can suffer CSCC at approximately 250ºF/121ºC. Corrosion rates using caustic solutions are shown in Table 1-8.

Table 1-8. Corrosion Rates of Steel in Caustic Solutions

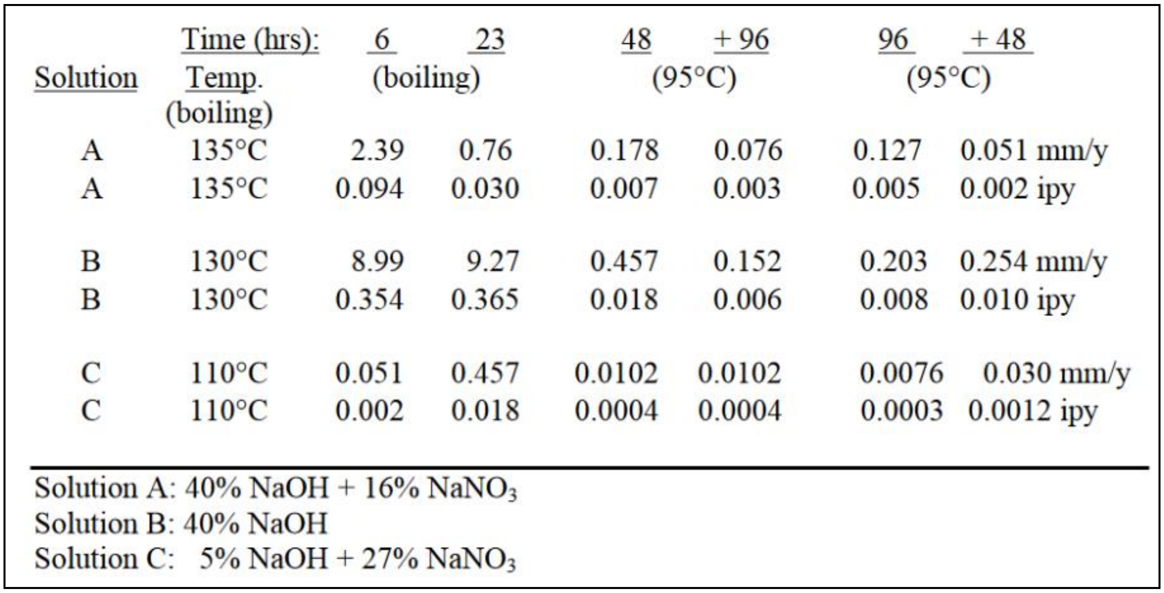

	Time (hrs):	6	23	48	+ 96	96	+ 48
Solution	Temp. (boiling)	(boiling)		(95°C)		(95°C)	
A	135°C	2.39	0.76	0.178	0.076	0.127	0.051 mm/y
A	135°C	0.094	0.030	0.007	0.003	0.005	0.002 ipy
B	130°C	8.99	9.27	0.457	0.152	0.203	0.254 mm/y
B	130°C	0.354	0.365	0.018	0.006	0.008	0.010 ipy
C	110°C	0.051	0.457	0.0102	0.0102	0.0076	0.030 mm/y
C	110°C	0.002	0.018	0.0004	0.0004	0.0003	0.0012 ipy

Solution A: 40% NaOH + 16% $NaNO_3$
Solution B: 40% NaOH
Solution C: 5% NaOH + 27% $NaNO_3$

References

1. Naz., M. Y., Ismail, N. I., Sulaiman, S. A., Shukrullah, S., "Characterization of erosion of gas pipelines by dry sand", Instrumentation Science and Technology, 2017, VOL. 45, NO. 1, 62–72 http://dx.doi.org/10.1080/10739149.2016.1194295.

2. Morris, K., "Investigation of Various Water Sources on the Corrosion of Carbon Steel and Aluminum", 2017, Honors Research Project, Dept. of Chemical Engineering, University of Akron, OH, USA.

3. Lu, B., " Erosion-Corrosion in Oil and Gas Production", Research and Reviews in Materials Science and Chemistry, Vol. 2, Issue 1, 2013, Pages 19-60, ISSN 2319-6920.

4. http://hghouston.com/resources/technical-newsletters/corrosion-in-caustic-solutions

Subtask 19.2: Evaluation of Nonmetallic Components in the Waste Transfer System

During this period of performance, the one-year aging of the remaining specimens continued. Completion of the aging is expected by mid-August. FIU performed troubleshooting and repairs to leaks that developed. Pumps 1 and 3 both developed leaks as a result of a motor barrier failing, a continuing issue with the Finish Thompson pumps. Even with the new impeller design in pump 1, the motor barrier failed. Additional leaks developed on pump 1 as a result of a crack in the impeller housing (Figure 1-27). Epoxy was used to repair the crack and the loop was returned back into service. An additional leak on pump 3 was a result of a crack in the PVC pipe coupling on the discharge side of the pump. The coupling was replaced and the loop was returned back into service. When the pump on loop 1 once again began to leak, it was from the impeller housing, thus the entire impeller housing was replaced.

Figure 1-27. Cracked impeller housing (left) and cracked PVC coupling discharge pipe (right).

FIU also took sample coupons from the hoses used during the 6-month burst pressure tests as well as the non-aged hoses (Figure 1-28). As can be seen in Figure 1-29, the aged coupon (on bottom) from loop 1 (170°F) has a discoloration on its inner surface when compared to the un-aged coupon sample. The discoloration appears to be only on the surface of the material and does not appear to have penetrated into the material.

Figure 1-28. Hose sample coupons.

Figure 1-29. Aged (bottom) vs. un-aged (top) coupons.

The samples will be further trimmed for evaluation in the scanning electron microscope with energy dispersive X-ray spectroscopy (SEM-EDX). This analysis will determine if there was any change in the surface microstructure and measure how far the NaOH penetrated into the EPDM material.

Milestones and Deliverables

The milestones and deliverables for Project 1 for FIU Performance Year 7 are shown on the following table. Milestone 2016-P1-M18.3.1 was completed on March 31, 2017 and a summary document was submitted on April 14, 2017, summarizing the results from the bench-scale tests using an infrared sensor. Milestone 2016-P1-M19.1.1 was completed on May 12, 2017 and a summary document was submitted on May 26, 2017, summarizing the results from the bench-scale tests using the Permasense UT sensors. Milestone 2016-P1-M18.2.2 was completed on May 26, 2017 and a summary email was sent to DOE, highlighting aspects of the sensors incorporated into the design of the inspection tools. Due to funding issues, milestone 2016-P1-M18.2.1 and 2016-P1-M17.1.2 will be reforecast. The expected delay has been communicated to the site points-of-contact as well as the DOE HQ Project Lead, Gary Peterson, during regular project teleconferences. A reforecast date of completion will be set once future funding amounts and dates are known.

FIU Performance Year 7 Milestones and Deliverables for Project 1

Task	Milestone/ Deliverable	Description	Due Date	Status	OSTI
Task 17: Advanced Topics for Mixing Processes	2016-P1-M17.1.1	Complete literature review and selection of baseline experimental cases	2/3/17	Complete	
	Deliverable	Draft Summary Report for Subtask 17.1.1	2/17/17	Complete	OSTI
	2016-P1-M17.1.2	Complete CFD simulations of air sparging experiments	4/21/17 Reforecasted to 8/25/17	Reforecast	
	Deliverable	Draft Summary Report for Subtask 17.1.2	5/5/16	Reforecast - to be included in YER	OSTI
Task 18: Technology	2016-P1-M18.2.1	Complete assembly of full-scale sectional mock-up test bed	12/16/16	Reforecast Date TBD	

Development and Instrumentation Evaluation	Deliverable	Draft Summary Report for Subtask 18.3.1	4/14/17	Complete	OSTI
	2016-P1-M18.2.2	Complete evaluation of sensor integration into inspection tools	5/26/17	Complete	
	Deliverable	Draft Summary Report for Subtask 18.2.3	6/30/17	Reforecast - to be included in YER	OSTI
	2016-P1-M18.2.4	Complete conceptual design of miniature rover platform	8/25/17	On Target	
	2016-P1-M18.2.5	Complete conceptual design of 6 inch peristaltic crawler	8/25/17	On Target	
	2016-P1-M18.3.1	Complete bench-scale testing for temperature measurements using IR sensors	3/31/17	Complete	
Task 19: Pipeline Integrity and Analysis	2016-P1-M19.1.1	Assess the accuracy of the down selected UT system via bench-scale testing	5/12/17	Complete	
	2016-P1-M19.1.2	Develop test loop for evaluating UT sensors	8/25/17	On Target	
	2016-P1-M19.2.1	Complete experimental testing of 6 month aged materials	3/17/17	Complete	
	Deliverable	Draft Summary Report for Subtask 19.2.2	3/31/17	Complete	OSTI
	Deliverable	Draft Summary document on UT assessment for Subtask 19.1.1	5/26/17	Complete	OSTI

Work Plan for Next Quarter

Project-wide:

- Draft the Year End Report (YER) for FIU Performance Year 7.
- Draft the Project Technical Plan (PTP) for FIU Performance Year 8.

Task 17: Advanced Topics for Mixing Processes

- During the next quarter, FIU will finalize a test plan to address a variety of technical gaps associated with critical velocities and flushing techniques. This plan will include objectives, a test matrix consisting of the most important variables given reasonable priorities, methodologies and instrumentations suitable for obtaining the target information, and an estimate of costs for candidate loops. FIU will engage in discussions with field experts from the sites and national labs for suggestions and move forward with selection and purchasing of necessary components.

Task 18: Technology Development and Instrumentation Evaluation

- FIU will continue to develop the sectional full scale mock-up of the DSTs that will allow for the demonstration of robotics/sensor systems from FIU as well as other collaborators. In the up-coming quarter, the refractory channels will be completed and the pipes and tank liners will be installed. Initial testing of the pneumatic crawler will commence.

- For the mini rover, FIU will focus on fabricating the PCBs and populating the electronic components shown in the finalized conceptual designs. This work will be carried out in parallel with integrating the sensors and drivers onto the final system. Once the system integration is completed, experimental and field testing will be carried out at the sectional full-scale DST mock-up, along with any necessary system enhancements and adjustments that are deemed important to continue to improve the reliability, functionality and robustness of the inspection tool.
- For the IR sensor task, FIU will continue to investigate the integration of the sensor into both the pneumatic crawler and miniature rover. After integration, both systems will be validated on the sectional full-scale DST mock-up.

Task 19: Pipeline Integrity and Analysis

- For the UT sensor task, the pipe loop will be completely assembled to test the real time erosion/corrosion effects using abrasive and caustic materials. Upon completion of the assembly, tests will be conducted based on the developed test matrices.
- For the non-metallic materials task, FIU will continue to age the specimens. It is anticipated that the aging for one year will be completed at the end of August. After completing the one year aging, burst pressure testing will be conducted on the hose specimens. In addition, FIU will also complete the surface characterization of the 6-month as well as the 1-year specimens and investigate the feasibility of irradiating the coupon samples.

Project 2
Environmental Remediation Science and Technology

Project Description

This project will be conducted in close collaboration between FIU and national laboratory scientists and engineers at SRNL, SREL, PNNL and LANL in order to plan and execute research that supports the resolution of critical science and engineering needs, leading to a better understanding of the long-term behavior of contaminants in the subsurface. Research involves novel analytical methods and microscopy techniques for characterization of various mineral and microbial samples. Tasks include studies which predict the behavior and fate of radionuclides that can potentially contaminate the groundwater system in the Hanford Site 200 Area; laboratory batch and column experiments, which provide relevant data for modeling of the migration and distribution of natural organic matter injected into subsurface systems in the SRS F/H Area; laboratory experiments investigating the behavior of the actinide elements in high ionic strength systems relevant to the Waste Isolation Pilot Plant; surface water modeling of Tims Branch at SRS supported by the application of GIS technology for storage and geoprocessing of spatial and temporal data.

The following tasks are included in FIU Performance Year 7:

Task No	Task
Task 1: Remediation Research and Technical Support for the Hanford Site	
Subtask 1.1	Remediation Research with Ammonia Gas for Uranium
Subtask 1.2	Investigation on Microbial-Meta-Autunite Interactions - Effect of Bicarbonate and Calcium Ions
Subtask 1.3	Investigation of Electrical Geophysical Response to Microbial Activity in the Saturated and Unsaturated Environments
Subtask 1.4	Contaminant Fate and Transport Under Reducing Conditions
Task 2: Remediation Research and Technical Support for Savannah River Site	
Subtask 2.1	Investigation on the Properties of Acid-Contaminated Sediment and its Effect on Contaminant Mobility
Subtask 2.2	The Synergistic Effect of Humic Acid and Colloidal Silica on the Removal of Uranium (VI)
Subtask 2.3	Humic Acid Batch Sorption and Column Experiments with SRS Soil
Task 3: Surface Water Modeling of Tims Branch	
Subtask.3.1	Modeling of Surface Water and Sediment Transport in the Tims Branch Ecosystem
Subtask 3.2	Application of GIS Technologies for Hydrological Modeling Support
Subtask 3.3	Biota, Biofilm, Water and Sediment Sampling in Tims Branch Watershed
Task 5: Research and Technical Support for WIPP	

Task 1: Remediation Research and Technical Support for the Hanford Site

Task 1 Overview

Radioactive contamination at the Hanford Site has created plumes that threaten groundwater quality due to downward migration through the unsaturated vadose zone. FIU is supporting basic research into the fate and remediation of radionuclides such as uranium in the vadose zone as a cost effective alternative to groundwater pump and treat technologies. One technology under consideration to control U(VI) mobility in the Hanford vadose zone is a manipulation of sediment pH via ammonia gas injection to create alkaline conditions in the uranium-contaminated sediment. This project also investigates the biodissolution of autunite solids created in sediments after injections of polyphosphate amendments and studies the potential detection of biofilms via the spectral induced polarization method (SIP). Another focus of this project is to investigate the properties of Tc and its compounds under Hanford Site conditions to better understand and predict Tc fate and transport in the subsurface and for designing remedial strategies for this contaminant.

Task 1 Quarterly Progress

Subtask 1.1. Remediation Research with Ammonia Gas for Uranium

During the months of April - June, DOE Fellow Silvina Di Pietro presented a professional oral presentation at the American Chemical Society 253rd meeting in San Francisco and for eMerge Americas Conference + Life Sciences of South Florida in Miami Beach, Florida. Mineral dissolution results are presented below for all minerals for each of the targeted conditions in synthetic groundwater and NaCl. Uranium partitioning data will be presented in the June monthly report. Furthermore, both the summer 2016 internship data and FIU batch experiments are being organized for peer-reviewed publications.

Batch Experiments with Pure Minerals and U

Greater removal of uranium (U) is observed with base treatment in the presence of synthetic groundwater (SGW) as compared to 3.2 mM NaCl for all conditions for illite and Hanford sediment (Figure 2-1). However, removal in the presence of SGW is less than with NaCl for the NaOH treatment and NH_4OH treatment for Hanford sediments, and overall greater removal occurs for the NH_3 gas treatment. This is likely due to co-precipitation processes in the synthetic groundwater as has been presented in previous monthly reports and our recent publication (Emerson et al., 2017).

Although previous work investigating sorption of U to minerals and sediments at near neutral pH has observed a relatively fast attainment of equilibrium with respect to sorption, these systems are much more complex as sorption, dissolution, and co-precipitation processes are likely occurring for U and mineral phases. Tables 2-1 and 2-2 show that dissolution is incongruent for both SGW and NaCl background electrolytes, respectively. This indicates that there are likely secondary precipitates forming because Al and Si are not present in stoichiometric ratios. Moreover, it is apparent that dissolution is more incongruent in the SGW background electrolyte likely because of the presence of Ca and Mg increasing co-precipitation processes. Figure 2-3 is an example of mineral dissolution based on the measurement of aqueous Si after three days of equilibration with the minerals at pH ~ 11.5. Statistical analysis is ongoing to confirm whether or not the dissolution was different depending on treatments. Due to these complex processes, greater removal of U has occurred after three weeks than after three days (Figure 2-4), highlighting that steady-state was likely not reached after three days.

Furthermore, a comparison of the treatment with NH_3 gas shows that greater removal was observed for this treatment than the other treatments. The working hypothesis is that greater removal of U will occur for this treatment because much of the carbonate and oxygen will be stripped from the aqueous phase during gas injection which may lead to reduction and precipitation of U. Although FIU cannot measure carbonate concentrations in the samples, the oxidation-reduction potential (ORP) is significantly decreased for both NH_4OH and NH_3 treatments with the lowest values measured for the NH_3 gas treatment (Table 2-3). Another indication that U reduction is occurring is shown upon comparison of U partitioning coefficients (mL/g) versus ORP (mV) for all of the background electrolytes and treatments as shown in Figure 2-2. Although this depiction does not take into account the pH of the samples, which is extremely significant, it shows that below 200 mV, removal of U increases dramatically. This is consistent with previous work predicting that a reduction of uranium will occur below 250 mV (Eh with respect to a SHE) (Zachara, et al., 2007).

The significantly greater removal for the three base treatments for illite, muscovite, and Hanford sediment is highlighted in Figure 2-4 for synthetic groundwater, although similar results were observed for the NaCl background electrolyte (not shown). It should be noted that the other minerals investigated did not show such significant differences. For illite, muscovite, and Hanford sediments, the removal appears to increase significantly in the order $NaOH < NH_4OH < NH_3$ gas. Although FIU is currently conducting a literature review to explain these results, FIU suspects that the illite and muscovite minerals may be capable of heterogeneous reduction of uranium on the surface which would be expected to increase removal. Although comparable results for illite and Hanford sediments have not yet been located in literature, Moyes et al. previously observed surface precipitation of U on muscovite, likely as a mixed U(IV/VI) oxide (Moyes et al., 2000). Based on these results, further efforts for this task in FIU's next performance year will focus on understanding the behavior of muscovite and illite minerals. Because muscovite and illite follow a similar trend to the Hanford sediments, FIU hypothesizes that they may ultimately control the behavior of U during ammonia gas injection. Therefore, it is necessary to understand the mechanisms leading to U removal in the presence of these minerals.

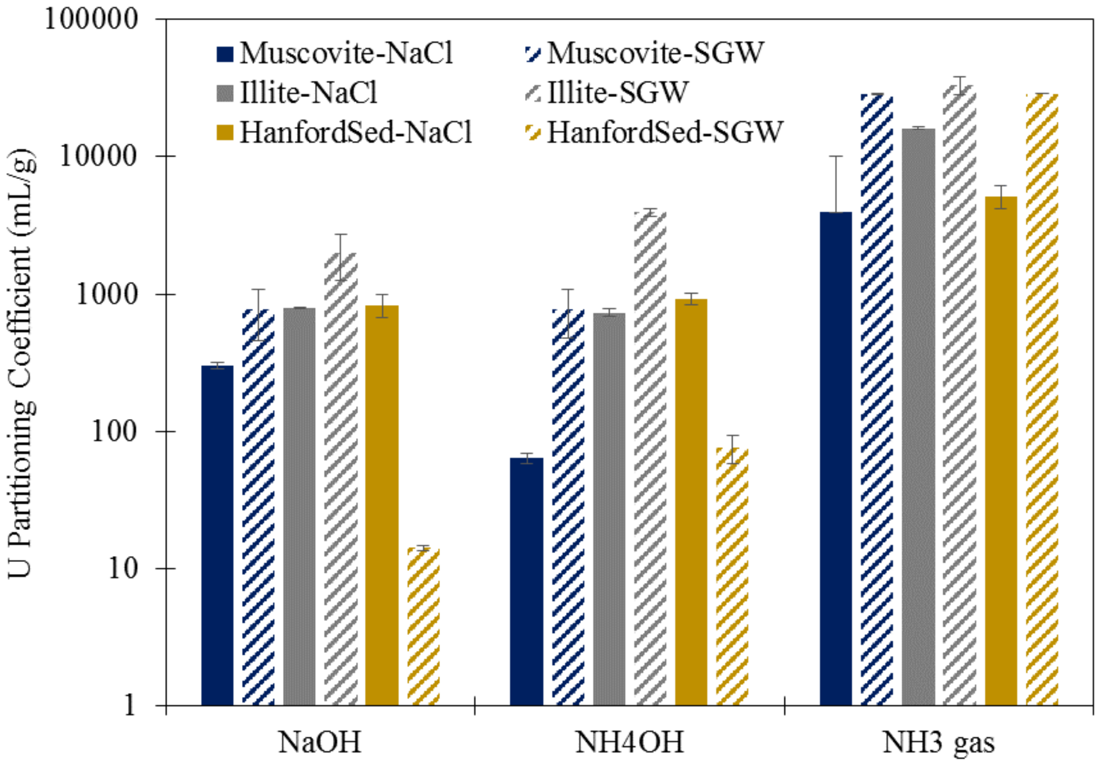

Figure 2-1. U partitioning in the presence of pure minerals [muscovite (blue) and illite (gray)] or Hanford sediments (yellow) with a background electrolyte of 3.2 mM NaCl (solid) or synthetic groundwater (striped) with base treatment to pH ~ 11.5 via NaOH, NH_4OH, or NH_3 (gas). Note: error bars are based on measurement of triplicate samples.

Table 2-1. Comparison of Al:Si Ratios in the Aqueous Phase in Synthetic Groundwater (SGW) Following Mineral Dissolution with Base Treatment by NH_3 Gas, NH_4OH or NaOH to pH ~ 11.5

Mineral	NH_3 gas	NH_4OH	NaOH	Theoretical
Kaolinite	*	**	0.10	1
Illite	0.03	**	0.05	0.5
Montmorillonite	*	0.09	0.02	0.5
Muscovite	0.44	0.53	0.65	1
Hanford Sediment	0.08	0.96	0.11	-

*Note: *indicates samples were not measured or **were below detection limits*

Table 2-2. Comparison of Al:Si Ratios in the Aqueous Phase in 3.2 mM NaCl Following Mineral Dissolution with Treatment by NH3 Gas, NH4OH or NaOH to pH ~ 11.5

Mineral	NH_3 gas	NH_4OH	NaOH	Theoretical
Kaolinite	*	0.90	0.93	1
Illite	0.07	0.50	0.20	0.5
Montmorillonite	*	0.24	0.004	0.5
Muscovite	0.81	0.82	0.86	1
Hanford Sediment	0.02	0.04	0.08	-

*Note: *indicates samples were not measured or **were below detection limits*

Table 2-3. Summary of ORP (mV) Measurements with Respect to Treatments

Condition	Average	StDev
Initial	527	48
NaOH	296	15
NH_4OH	187	28
NH_3	165	8

Note: not all samples measured and SGW and NaCl samples were combined

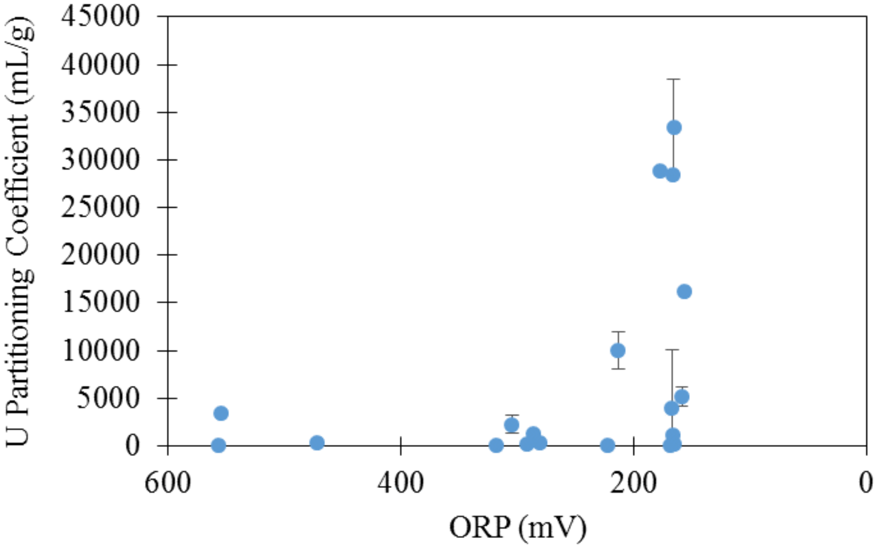

Figure 2-2. Comparison of U partitioning coefficients (mL/g) versus ORP (mV) for all minerals, initial electrolyte solutions, and treatments.

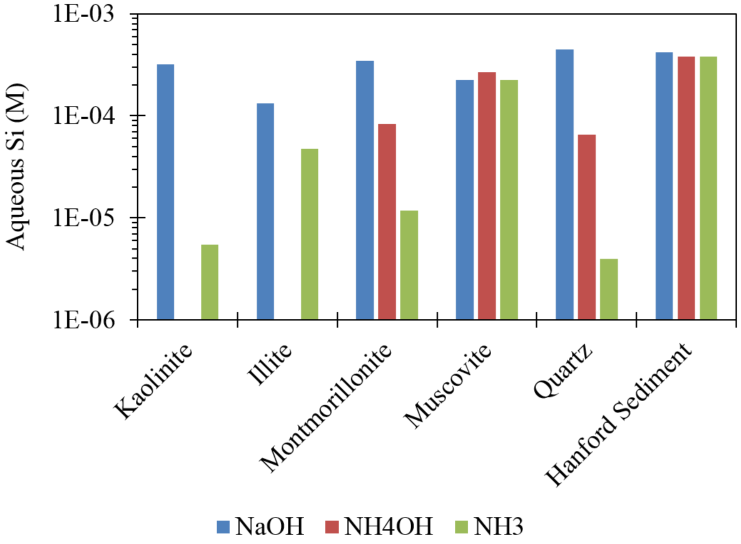

Figure 2-3. Aqueous Si concentrations (mol/L) after three days of equilibration at pH ~ 11.5 in synthetic groundwater (SGW) in the presence of various minerals and sediments.

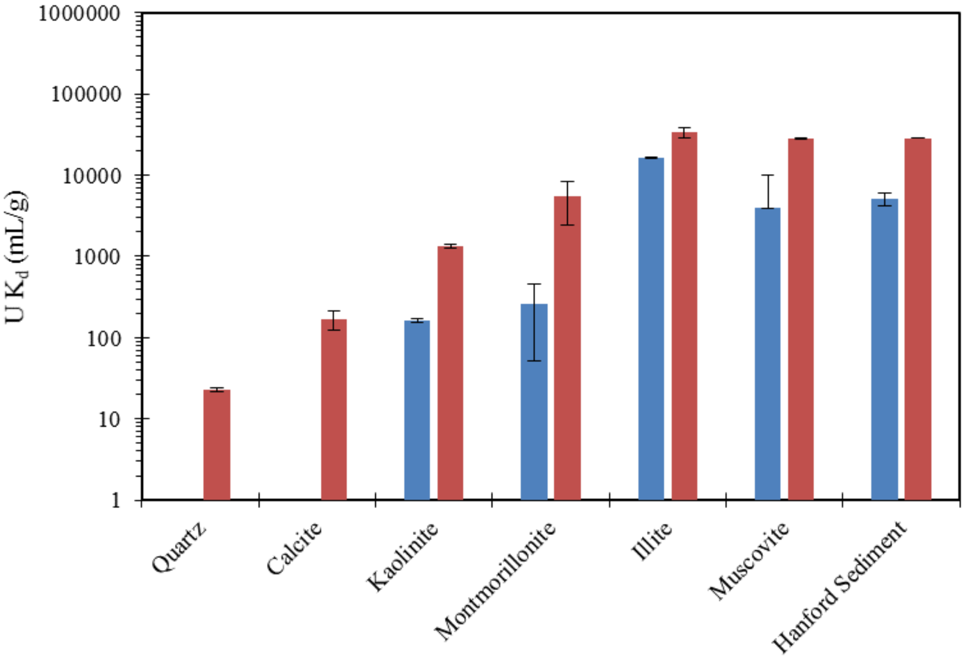

Figure 2-4. 3-day (blue) versus 3-week (red) partitioning coefficients (K_d) in mL/g for initially 500 ppb U sorption to various minerals in 7.2 mM NaCl with treatment with NH_3 gas to pH ~ 11.5. Note: error bars are based on triplicate measurements.

PNNL 2016 Internship – Additional analysis

Ms. Di Pietro continued analysis of mineral dissolution data from her summer 2016 internship experience at PNNL. Figures 2-5 and 2-6 represent the aqueous Si leached per gram of mineral for six sampling time periods (1 hour, 1 day, 3 days, 10 days, 30 days, and ~ 60 days) under two different conditions: anaerobic with 3.1 M NH_4OH in DIW (Figure 2-5) and anaerobic with 0.01 M NaOH in DIW (Figure 2-6). Although Figure 2-5 shows no clear trend for the minerals, a divergence is noticeable after sampling day 3 (approximately 87 hours). Initially, leaching is similar; however, after 10 days, different minerals display different trends. While epidosite and illite remain constant, muscovite and montmorillonite show increasing leaching rates. Montmorillonite may increase in dissolution due to its mid-expanding layer exposing a greater surface area. Moyes *et al*. make a distinction between the two phyllosilicates. While muscovite does not have an interlayer, montmorillonite's can expand to ~8.0 Å. Thus, greater dissolution of montmorillonite may be occurring due to the above mechanisms. Further investigation is needed to understand the dominant mechanisms especially with respect to epidosite.

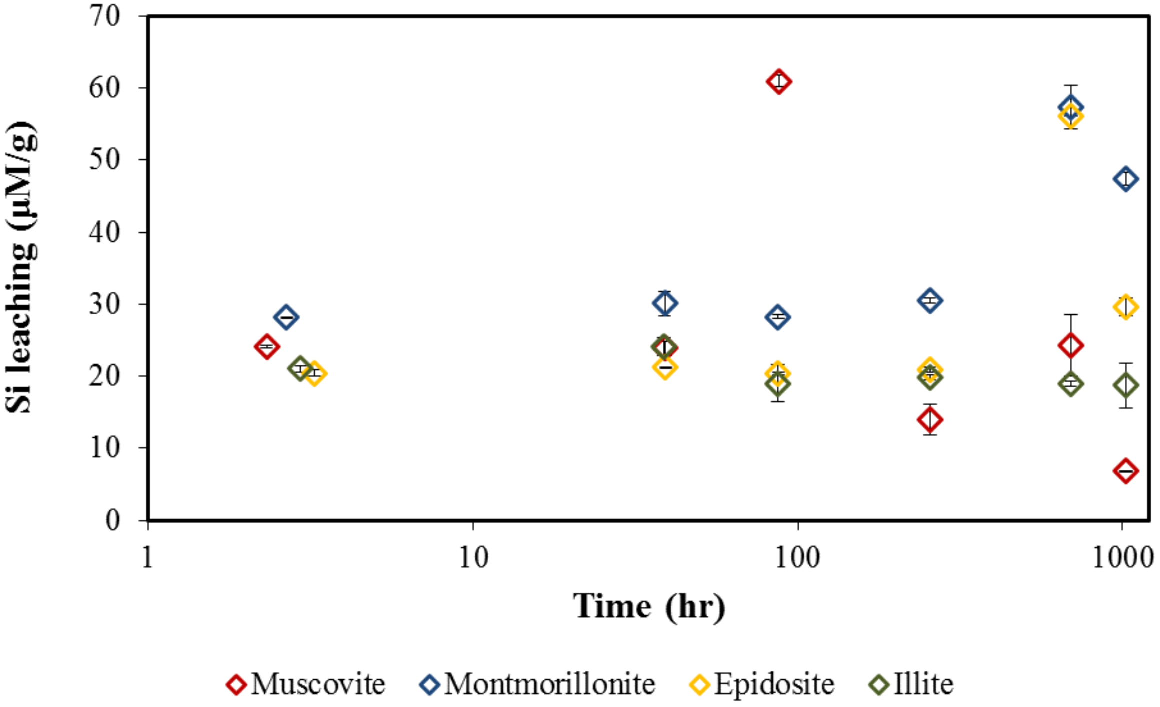

Figure 2-5. Silicon leaching [µM/g] (muscovite, montmorillonite, epidosite, and illite) for anaerobic condition with 3.1 M NH_4OH in DIW as a function of time.

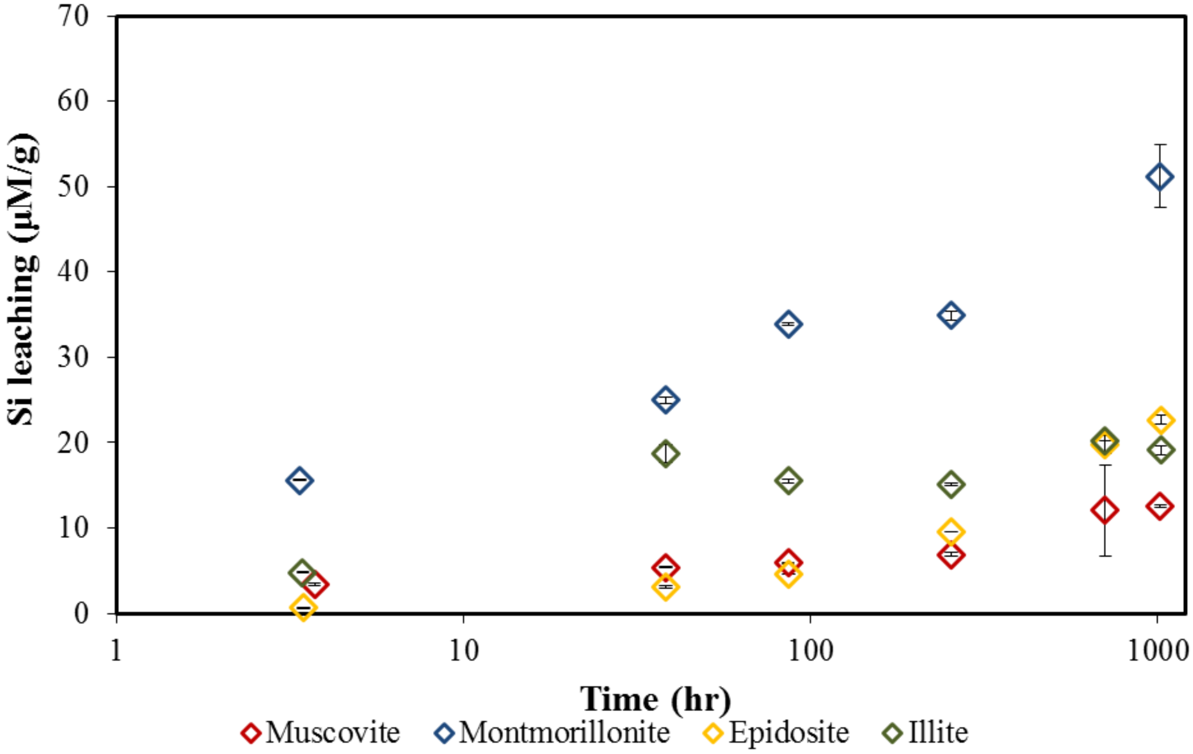

Figure 2-6. Silicon leaching [µM/g] (muscovite, montmorillonite, epidosite, and illite) for anaerobic condition with 0.01 M NaOH in DIW as a function of time.

Figures 2-7 and 2-8 represent the aqueous Ca leached per gram of mineral for anaerobic with 3.1 M NH_4OH and anaerobic with 0.01 M NaOH in DIW, respectively. To begin, both figures show a decrease in leaching concentration as a function of time. This may be due to a precipitation mechanism occurring following saturation of the aqueous phase with respect to Ca. Upon analysis, epidosite and montmorillonite were above the level of detection (LOD) with 3.4 ppm for Ca and 2.7 ppm for Si, corrected for dilutions, for anaerobic condition with NaOH while all other minerals were below detection. Calcite, epidosite, and montmorillonite minerals were above detection limits for anaerobic condition with NH_4OH. Although the minerals represented contain less Ca percent abundance than Si in their molecular formula, Ca leaching is approximately 8.0-25% compared to <1% Si leached for the same minerals (<5 Ca versus ~55 Si µg/g). These data are in accordance to PNNL's 2010 report in which the authors suggest that secondary phases such as cancrinite were formed as a result of mineral dissolution (Szecsody et al., 2010). However, these authors also indicated the formation of sodium silicates and zeolites. FIU's data is inconclusive for formation of Si or Al precipitates, but additional solids characterization and data analysis from dissolution experiments is ongoing.

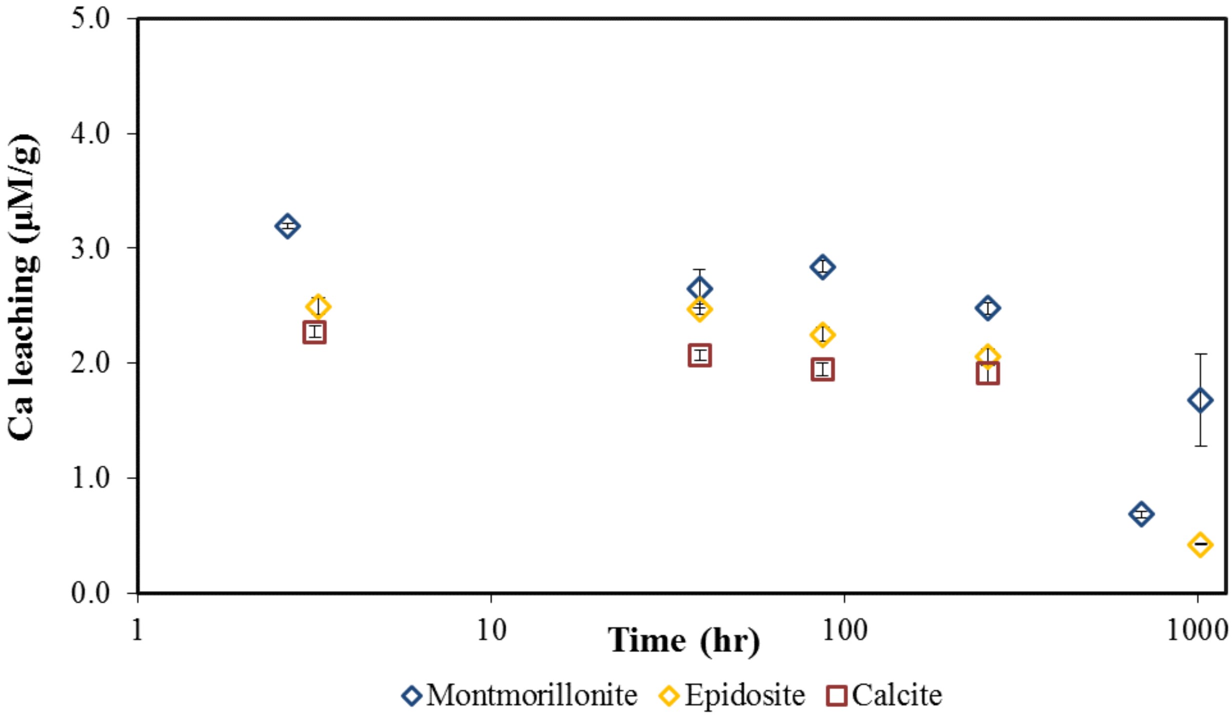

Figure 2-7. Calcium leaching [µM/g] (montmorillonite, epidosite, and calcite) for anaerobic condition with 3.1 M NH_4OH in DIW as a function of time.

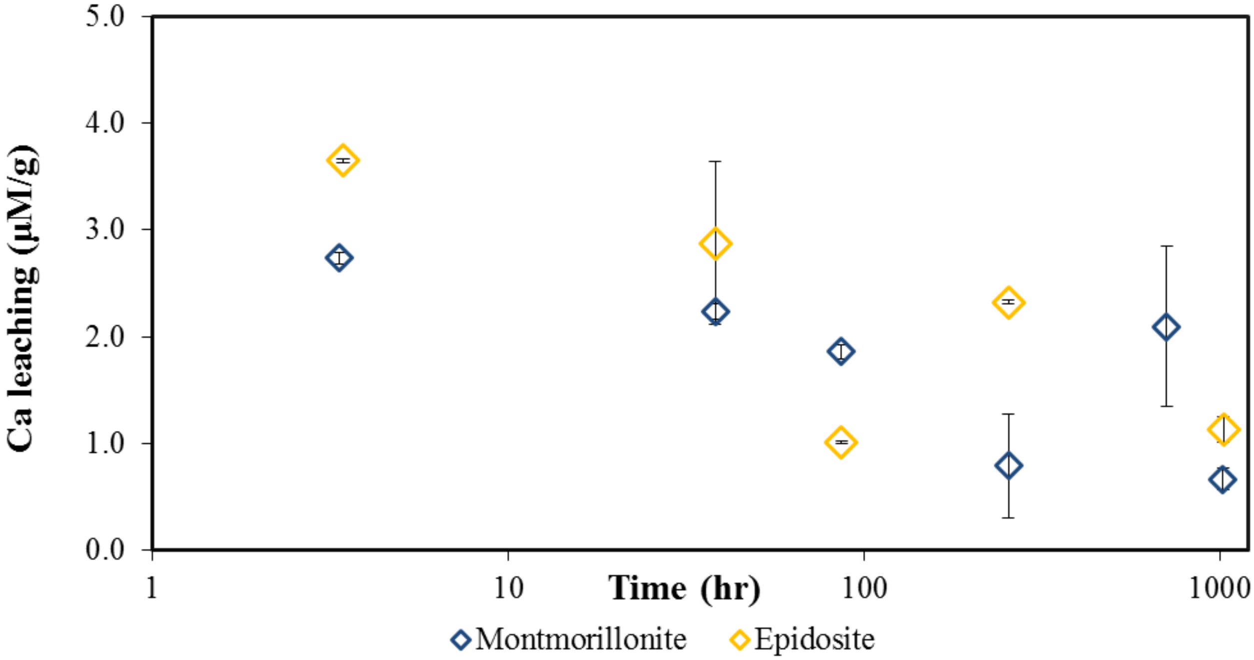

Figure 2-8. Calcium leaching [µM/g] (montmorillonite and epidosite) for anaerobic condition with 0.01 M NaOH in DIW as a function of time.

Experiments are also ongoing to quantify the cations associated with the minerals used during Ms. Di Pietro's PNNL summer 2016 internship and FIU experiments. The standard method consists of three parts: (1) soluble cations, (2) bound cations and (3) cation exchange capacity (CEC) of quartz; clay minerals muscovite, montmorillonite, illite; and feldspar minerals microcline and epidosite. By definition, CEC is the total negative charge on a mineral surface that may be exchanged with adsorbed (bound) cations. Generally, alkali and alkaline earth metals such as calcium (Ca), sodium (Na), magnesium (Mg), and potassium (K) are quantified for the aforementioned minerals (ASTM D7503-10, 2010). Data analysis for the three-part experiment is still ongoing and will be presented in the July monthly report.

References

1. ASTM D7503-10 Standard Test Method for Measuring the Exchange Complex and Cation Exchange Capacity of Inorganic Fine-Grained Soils, ASTM International, West Conshohocken, PA, 2010, https://doi.org/10.1520/D7503-10
2. Emerson, H.P., Di Pietro, S., Katsenovich, Y., Szecsody, J., 2017. Effects of ammonium on uranium partitioning and kaolinite mineral dissolution. Journal of Environmental Radioactivity, 167: 150-159.
3. Moyes, L. N., Parkman, R. H., Charnock, J. M., Vaughan, D. J., Livens, F. R., Hughes, C. R., & Braithwaite, A. (2000). Uranium uptake from aqueous solution by interaction with goethite, lepidocrocite, muscovite, and mackinawite: An X-ray absorption spectroscopy study. *Environmental Science & Technology*, 34(6), 1062-1068.
4. Szecsody, J. E., Truex, M. J., Zhong, L., Qafoku, N., Williams, M. D., McKinley, J. P., & Phillips, J. L. (2010). *Remediation of Uranium in the Hanford Vadose Zone Using Ammonia Gas: FY 2010 Laboratory-Scale Experiments* (No. *PNNL-20004*). Pacific

Northwest National Laboratory (PNNL), Richland, WA (US), Environmental Molecular Sciences Laboratory (EMSL).

5. Zachara, J.M. et al., 2007. A site-wide perspective on uranium geochemistry at the Hanford Site. Pacific Northwest National Laboratory, Hanford, WA.

Ammonia Gas Treated Batch Experiments without Pure Minerals

For the reporting period FIU completed the preparation for the new column experiments to evaluate the relative extractability from artificially prepared U-bearing precipitates. This experiment follows similar procedures to Smith and Szecsody's (2011) experiment. The method to evaluate the extractability is named "continuous leach" and uses a small volume (~1 cm^3) precipitate-filled cell and saturated flow.

Columns were set up for two types of precipitates. The procedures to prepare precipitates were outlined in the March monthly report. The general procedure to prepare samples containing the U-bearing precipitates was as follows: first, prepare tubes with a mixture containing measured volumes of Si and Al, add the corresponding amount of HCO_3 to create solutions at 3 mM and 50 mM. Then, pH was measured and adjusted to around 7-8 by adding small amounts (150-200 µL) of concentrated nitric acid (HNO_3). At this point, the pH was similar to Hanford Site soils. After this, ammonia gas was injected to the mixture in order to raise the pH to 11 and followed by the addition of measured volumes of U and Ca. All the tubes were then mixed well and set aside to settle for 1-2 days to allow the formation of precipitates. The final step was centrifuging the samples for 30 minutes, collecting the supernatant solutions in the centrifuge tubes for further analysis, and setting the precipitates to dry in the incubator at a temperature of 35°C.

Column 1 was filled with precipitates prepared from the solution composed of 50 mM Si, 5mMAl, 3 mM HCO_3 10 mM Ca and 2 ppm of U(VI). Column 2 was filled with a precipitate prepared from the solution composition of 50 mM Si, 5 mM Al, 50 mM HCO_3, 10 mM Ca and 2 ppm of U(VI). So, the only difference in the precipitate compositions was the concentration of bicarbonate: 3mM for a "low" concentration of bicarbonate in the precipitate for Column 1 and 50 mM for a "high" concentration of bicarbonate in the precipitate for Column 2. Precipitates were completely dried in the oven at 40^{o}C and the pump was set up to have an approximate flow of 1 mL/day. FIU was collecting 1 mL of sample per day in small vials to be further analyzed through KPA technology.

Figure 2-9. Experimental set up with mini columns (~1cm^3) filled with dried uranium-bearing precipitate

The analytical results for the first three weeks during continuous leach extraction experiments are presented in the Figures 2-10 and 2-11.

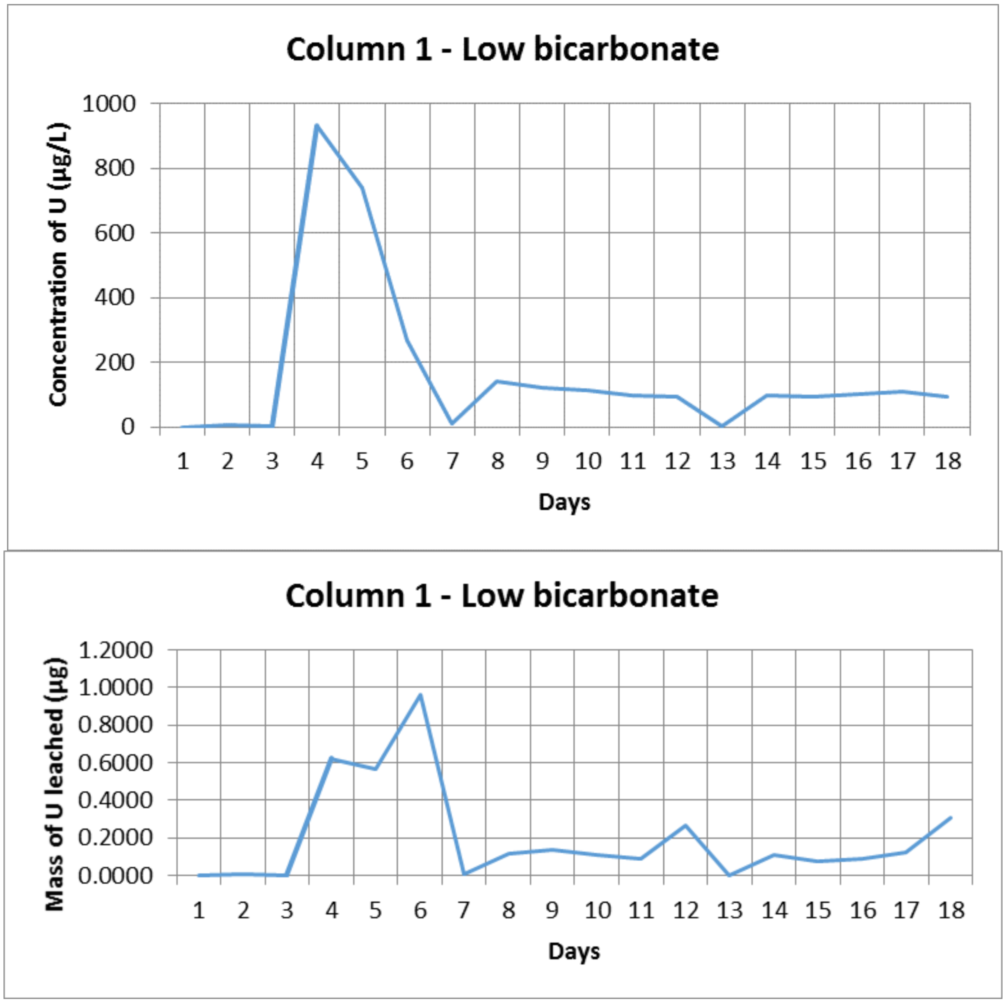

Figure 2-10. Uranium concentration and U(VI) mass leached out from column 1 with the precipitate composed of "low" bicarbonate concentration in the composition.

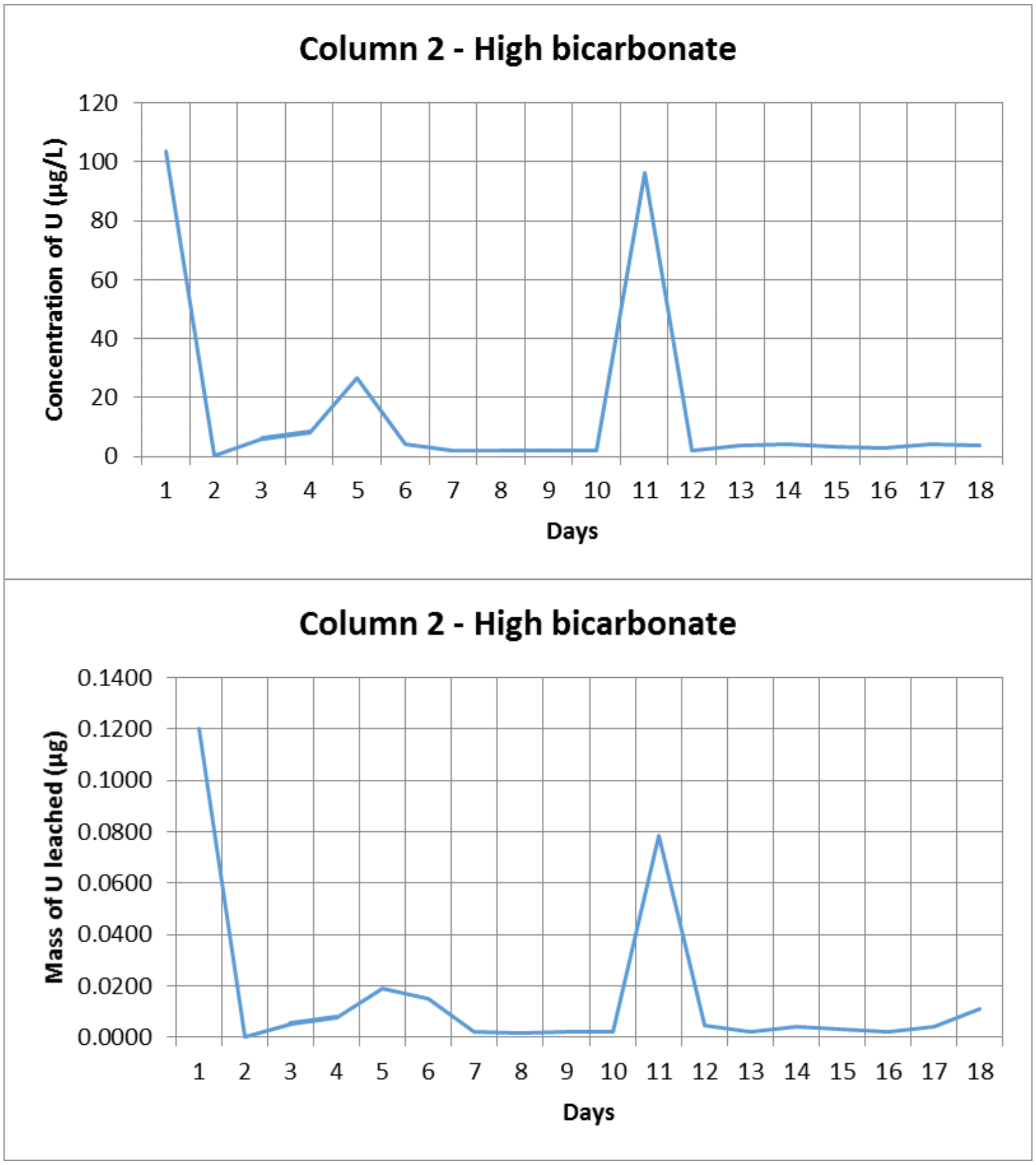

Figure 2-11. Uranium concentration and U(VI) mass leached out from column 1 with the precipitate composed of "high" bicarbonate concentration in the composition.

Observing the above figures, it can be noted that concentrations of U were high in the beginning and they seem to stabilize as days pass. The increase in the U concentrations observed between days 10-12 were due to a stop flow event and power interruptions lasting for two days. Analysis of the collected samples will be continued in order to establish conclusions and confirm trends. These experiments will also allow for calculating the cumulative U mass extracted.

<u>Experiment with Low Si/Al ratios</u>

FIU prepared an additional experiment with the low Si/Al ratio samples containing magnesium and calcium. Table 2-4 is a consolidation of the results on the uranium removal obtained from the KPA:

Table 2-4. U Removal in the Presence of Ca and Mg at Variable Bicarbonate Concentrations and Si/Al Ratios

Sample ID	Si/Al	HCO_3	Ca	Mg	C of U (ppb)	C of U In (ppb)	Removal	% Removal
1	3	3	0	0	999	2000	0.5005	50.05
2	3	3	5	0	34	2000	0.9830	98.30
3	3	3	10	0	29	2000	0.9854	98.54
4	3	50	0	0	1568	2000	0.2160	21.60
5	3	50	5	0	1534	2000	0.2328	23.28
6	3	50	10	0	1418	2000	0.2910	29.10
7	5	3	0	0	999	2000	0.5004	50.04
8	5	3	5	0	43	2000	0.9786	97.86
9	5	3	10	0	0	2000	1.0000	100.00
10	5	50	0	0	572	2000	0.7140	71.40
11	5	50	5	0	636	2000	0.6820	68.20
12	5	50	10	0	331	2000	0.8346	83.46
13	3	3	0	5	100	2000	0.9500	95.00
14	3	3	0	10	80	2000	0.9598	95.98
15	3	50	0	5	1378	2000	0.3111	31.11
16	3	50	0	10	1271	2000	0.3646	36.46
17	5	3	0	5	112	2000	0.9438	94.38
18	5	3	0	10	132	2000	0.9341	93.41
19	5	50	0	5	354	2000	0.8229	82.29
20	5	50	0	10	1297	2000	0.3515	35.15

This data reflects the average result of the triplicate samples for each sample ID. Currently, graphs are being prepared to present the results, illustrate the standard deviation, and draw conclusions. Furthermore, precipitates containing even lower Si concentrations (Si/Al 1.5 mM) and iron ($FeCl_3$ 0.2 mM and 5 mM) as a major cation instead of Ca or Mg are being prepared to be analyzed in order to complement these experiments. The complete results and conclusions for this experiment are expected to be presented in the following month.

The following graphs show the results obtained.

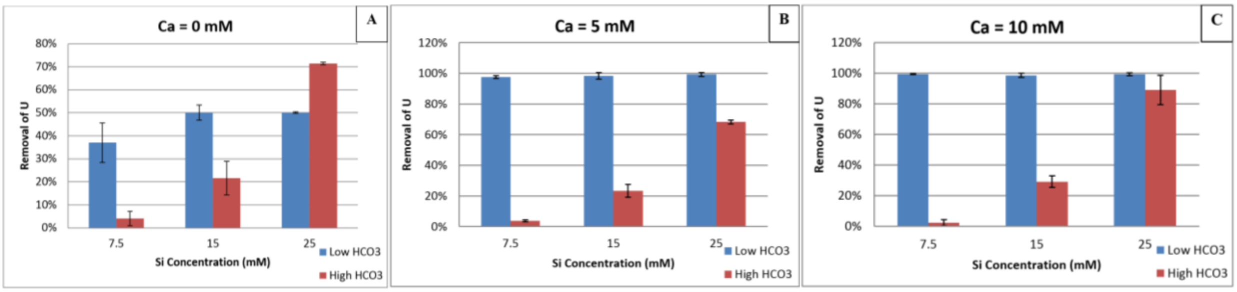

Figure 2-12. Percent removal of U (VI) tested at variable bicarbonate and silica concentrations in 5 mM Al amended solutions containing 2 mg/L U (VI) and (A) 0 mM; (B) 5 mM; and (C) 10 mM of Ca.

Generally, at a Ca concentration of 0 mM and a Si concentration of 15 mM, the removal efficiency of U resulted in relatively low values, averaging less than 50% ± 20% including both “low” and “high” bicarbonate concentrations (Figure 2-12A). Also, the presence in the solution composition of a “high” bicarbonate concentration (50 mM) appears to significantly reduce the removal efficiency of U at a Si concentration of 15 mM as opposed to a higher removal efficiency of U at a Si concentration of 25 mM (up to 72%). This trend was observed only at a Ca concentration of 0 mM in the solution composition (Figure 2-12A). This can be explained by the formation of calcium carbonates or calcium silicates, which could provoke Si coagulation and precipitation reactions leading to co-precipitation of uranium. In the absence of Ca, the co-precipitation of U can only occur by Si polymerization reactions that require much higher Si content, on the level of Si solubility concentrations at alkaline conditions. Furthermore, it is evident for all three Ca concentrations tested that, at “high” bicarbonate concentrations, the removal efficiency of U improves as concentration of Si increases (Figure 2-12A, 2-12B and 2-12C). Moreover, the data collected suggests that at both Si concentrations of 15 and 25 mM, U (VI) removal efficiency decreases as the concentration of bicarbonate increases; this reduction is smaller at Si concentrations of 25 mM (Figure 2-12B and 2-12C). According to Katsenovich, et al. (2016), at $HCO_3 > 25$ mM, stable soluble uranyl carbonate species such as $UO_2(CO_3)_3^{-4}$ become predominant at alkaline conditions. This might explain the relatively low removal efficiency of U compared to “low” bicarbonate concentrations where uranium is present in the uranyl hydroxide form. The highest removal efficiency of U, up to 99%, was achieved in the compositions containing “low” bicarbonate concentration for all Ca and Si concentrations tested (Figure 2-12).

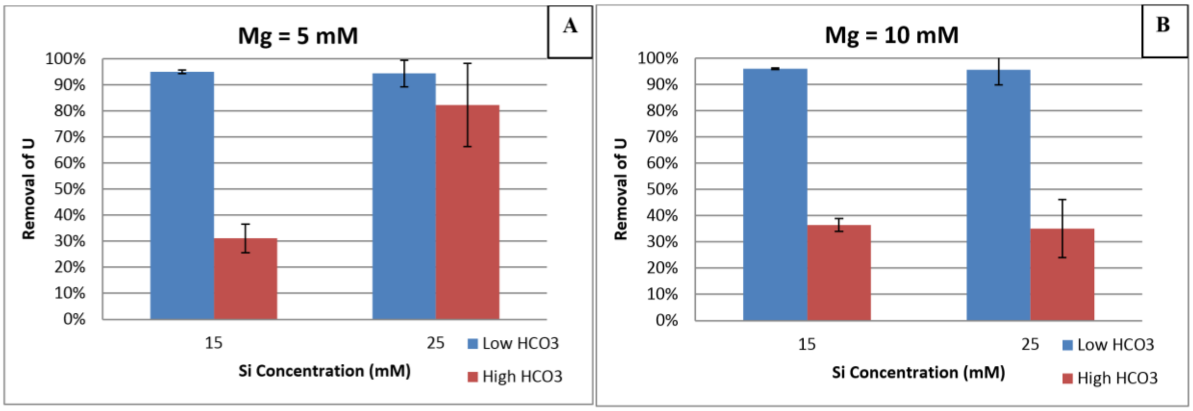

Figure 2-13. Percent removal of U (VI) tested at variable bicarbonate and silica concentrations in 5 mM Al amended solutions containing 2 mg/L U (VI) and (A) 5 mM; and (B) 10 mM of Mg.

Samples containing Mg, which is one of the major constituent in the pore water composition, showed similar trends in removal efficiency of U (VI) as previously was observed for samples containing Ca. First, at “low” bicarbonate concentrations, Si concentrations of 15 and 25 mM and Mg concentrations of 5 and 10 mM, the removal efficiency of U (VI) was greater than 94%. In addition, the data also demonstrated that the higher bicarbonate concentration correlates with a significantly lower removal efficiency of U (VI) at Si concentrations of 15 and 25 mM and Mg concentrations of 5 and 10 mM (Fig. 2-13A and 2-13B). Finally, higher Si concentrations improved the general removal efficiency of U (VI) at “low” bicarbonate and Mg concentrations of 5 mM.

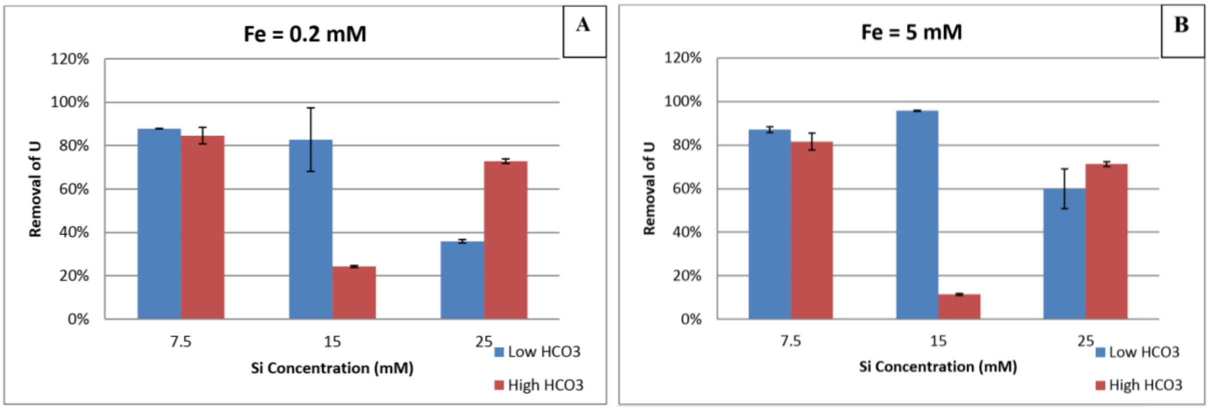

Figure 2-14. Percent removal of U (VI) tested at variable bicarbonate and silica concentrations in 5 mM Al amended solutions containing 2 mg/L U (VI) and (A) 0.2 mM; and (B) 5 mM of Fe.

The results of U removal in samples containing Fe showed a relatively different trend to those containing Ca and Mg (Figure 2-14). In the presence of low bicarbonate concentrations, the removal efficiencies of U tend to be higher, caused by possible formations of uranyl carbonates and iron oxides solid phases. Similar to the previous cases, with a "high" concentration of bicarbonate, removal efficiencies are lower, which can be attributed to the formation of stable soluble uranyl carbonates. FIU will initiate speciation modeling to predict the distribution of uranyl aqueous species and formation of uranium solid phases likely to be present in the tested compositions.

Additionally, in the month of June, new preparation of samples containing Fe as a major constituent were prepared, again to confirm results previously obtained in the month of May, considering the observed trends were different compared to the samples that contained Ca and Mg. Analysis with KPA is currently ongoing and results will be presented in the next monthly report.

Reference

Smith and Szecsody, 2011. Influence of contact time on the extraction of 233uranyl spike and contaminant uranium from Hanford Site sediment. Radiochim. Acta 99, 693–704.

Subtask 1.2. Investigation on Microbial-Meta-Autunite Interactions – Effect of Bicarbonate and Calcium Ions

In the month of April, FIU completed sampling of Na-autunite–bearing samples. The experimental bacteria, *Shewanella MRI*, were plated for each sample. From the plates, viable cells were counted by observing the number of colonies formed. Total cells were counted by placing 10-uL into a hemocytometer under a microscope. These measurements as a function of time can be seen in Figures 2-15 through 2-20 below. From the graph, it can be observed that the total number of cells is higher than the number of viable cells present. This is due to the presence of dead cells that do not grow on the agar plates but are visible under the microscope. Overall, the cell density was the same under each concentration of bicarbonate media, showing no change in amount of pattern.

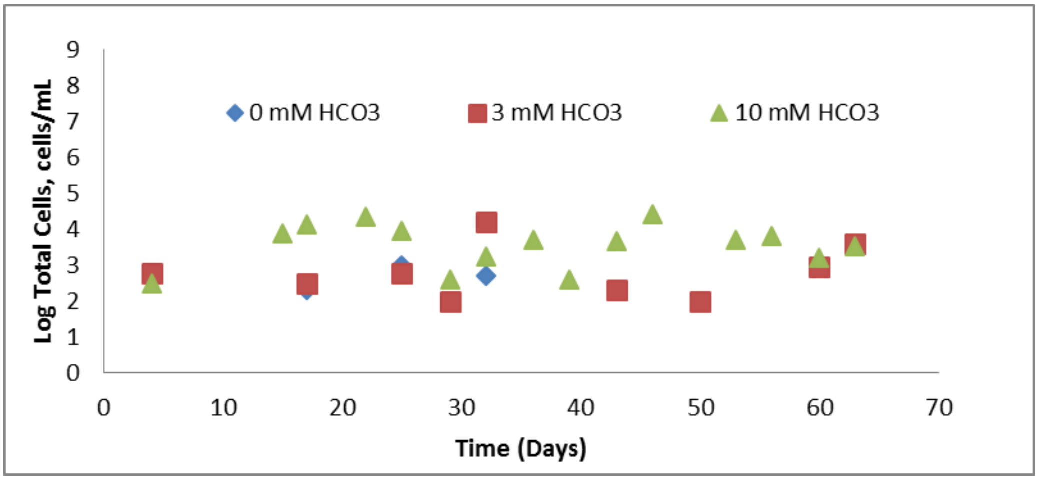

Figure 2-15. Viable cell concentration (log cells/mL) under different concentrations of HCO_3.

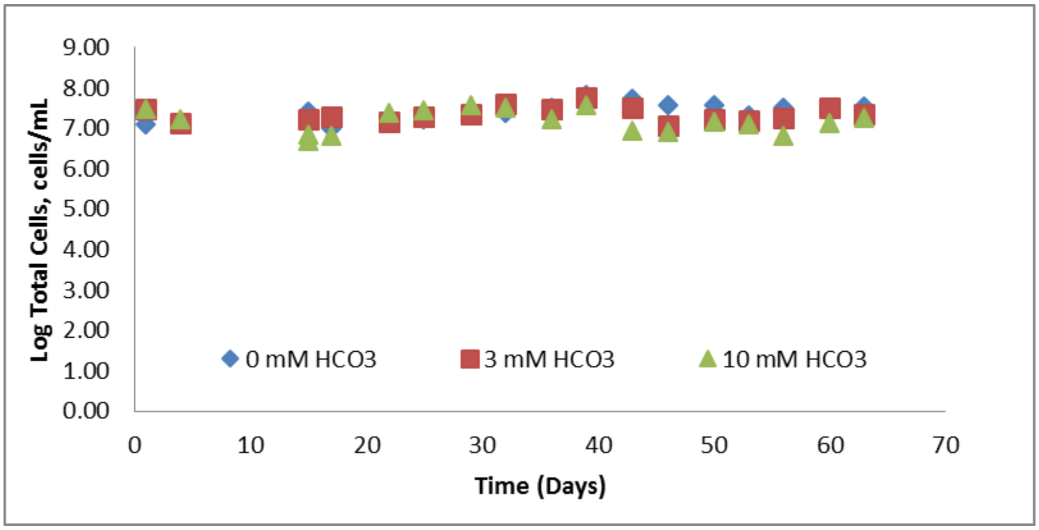

Figure 2-16. Total viable log cells/mL under different concentrations of HCO_3.

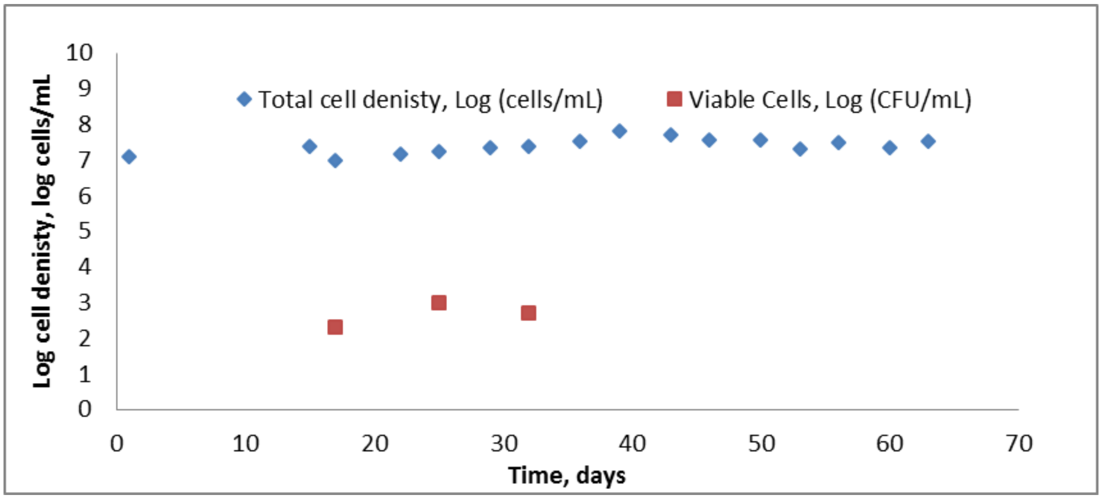

Figure 2-17. Log cell density for 0 mM HCO_3.

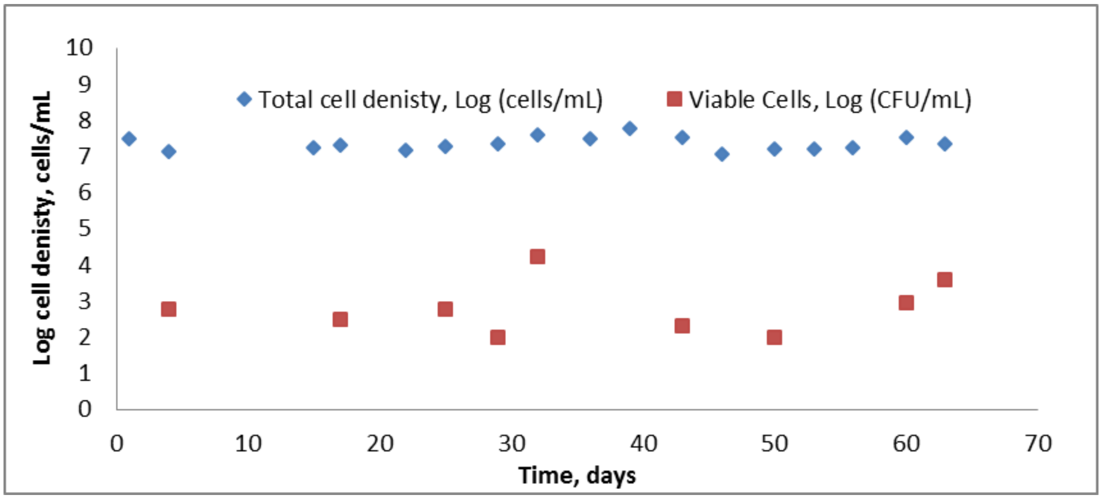

Figure 2-18. Log cell density for 3 mM HCO_3.

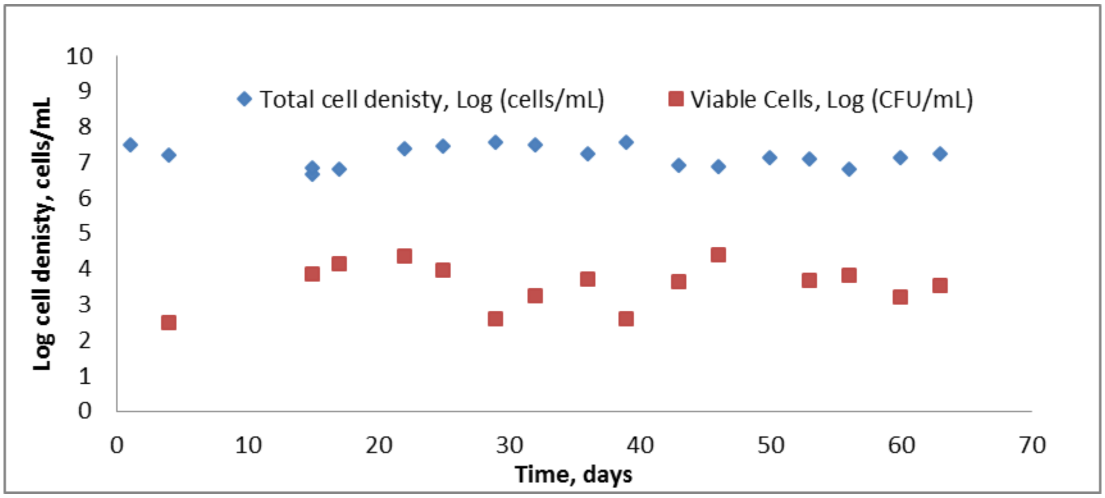

Figure 2-19. Log cell density for 10 mM HCO_3.

The 0.5-mL filtered samples that were taken in the anaerobic glove box using a 1-mL syringe and a 0.2-uL syringe filter were digested via wet and dry ashing. Wet digestion was performed by the addition of concentrated nitric acid (HNO_3) and concentrated hydrogen peroxide (H_2O_2) to each vial. The vials were placed on a heating plate until all the solution present was evaporated and a white solid precipitate was present. During the process, some samples turned yellow or brown so additional peroxide was added and the process was continued until a white precipitate was obtained. The dry samples were then placed in a furnace preheated to 450°C for 15 min and then allowed to cool at room temperature. Precipitates obtained in the drying step were dissolved in 1 mL of 2 mol/L nitric acid and analyzed by the kinetic phosphorescence analysis (KPA) instrument to determine uranium concentrations released into the aqueous phase as a function of time. This relationship can be seen in Figure 2-20. The uranium concentration for 0 mM and 3 mM bicarbonate samples stayed relatively the same from the first day of inoculation. The 10 mM bicarbonate samples increased a bit after about 10 days but then stabilized close to the original concentration afterwards.

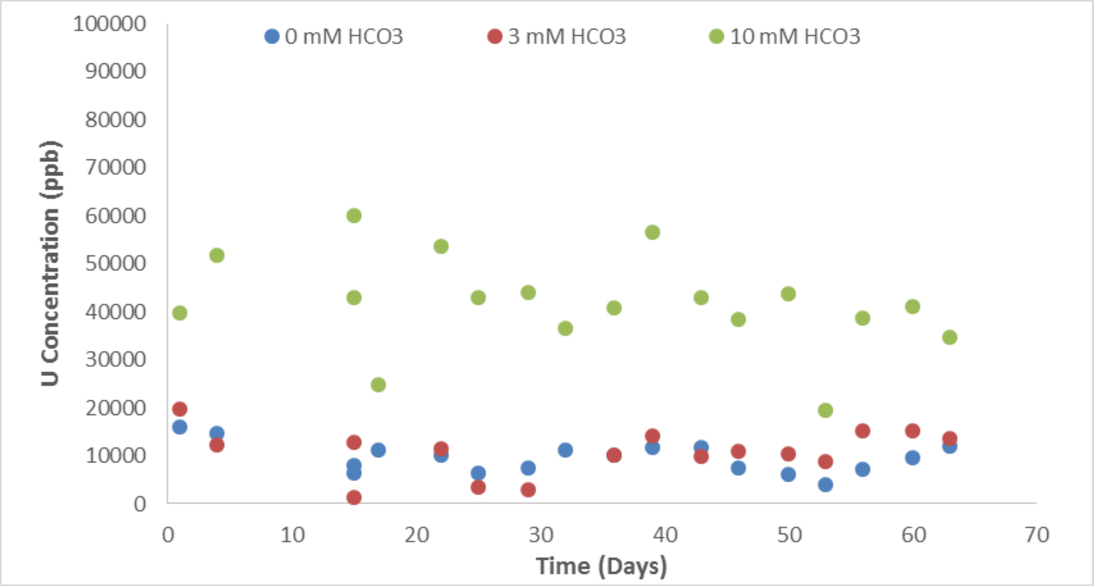

Figure 2-20. Uranium concentration under different concentrations of HCO_3.

FIU will begin the preparation process for determining phosphorous and sodium concentrations using inductively coupled plasma – optical emission spectroscopy (ICP) using phosphorous and sodium standards.

In the month of May, FIU continued analysis of the samples collected from the Na-autunite biodissolution experiments. The presence of organic content in the solutions can interfere with KPA measurements; so, samples collected during the biodissolution experiments were pre-processed by wet ashing followed by dry ashing procedures. Samples for uranium were analyzed by kinetic phosphorescence analysis (KPA-11, Chemchek Instruments Inc.) and sodium and phosphorous were determined by inductively coupled plasma - optical emission spectroscopy (ICP-OES 7300 Optima, Perkin Elmer) using sodium and phosphorous standards (Spex CertiPrep). Sodium concentration was also determined in the initial bicarbonate media solutions due to the presence of sodium lactate in the solution and sodium – Hepes buffer. This Na concentration was subtracted from the total sodium content obtained after the leaching experiments to measure its release from the synthetic autunite. Concentrations of phosphorus, sodium and uranium released into the aqueous phase as a function of time are presented in Figures 2-21, 2-22 and 2-23.

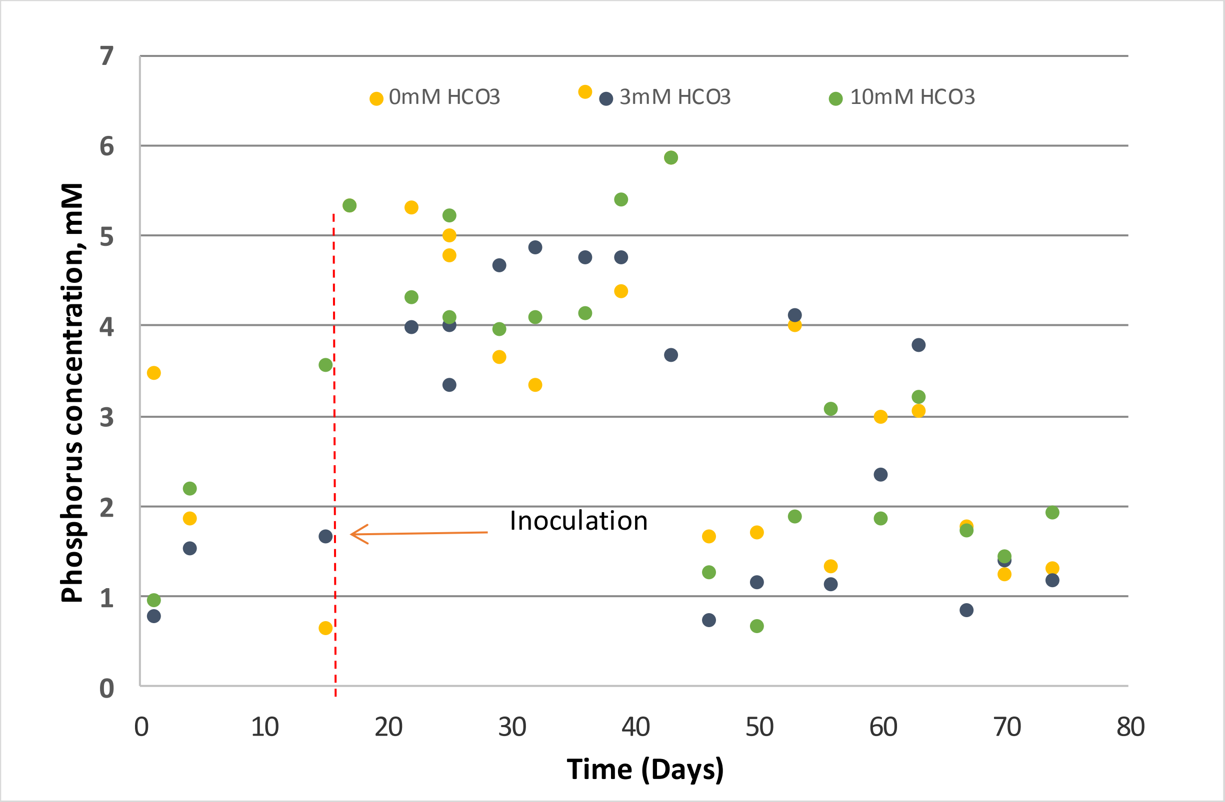

Figure 2-21. Concentrations of phosphorus released into the aqueous phase as a function of time under different HCO_3 concentrations.

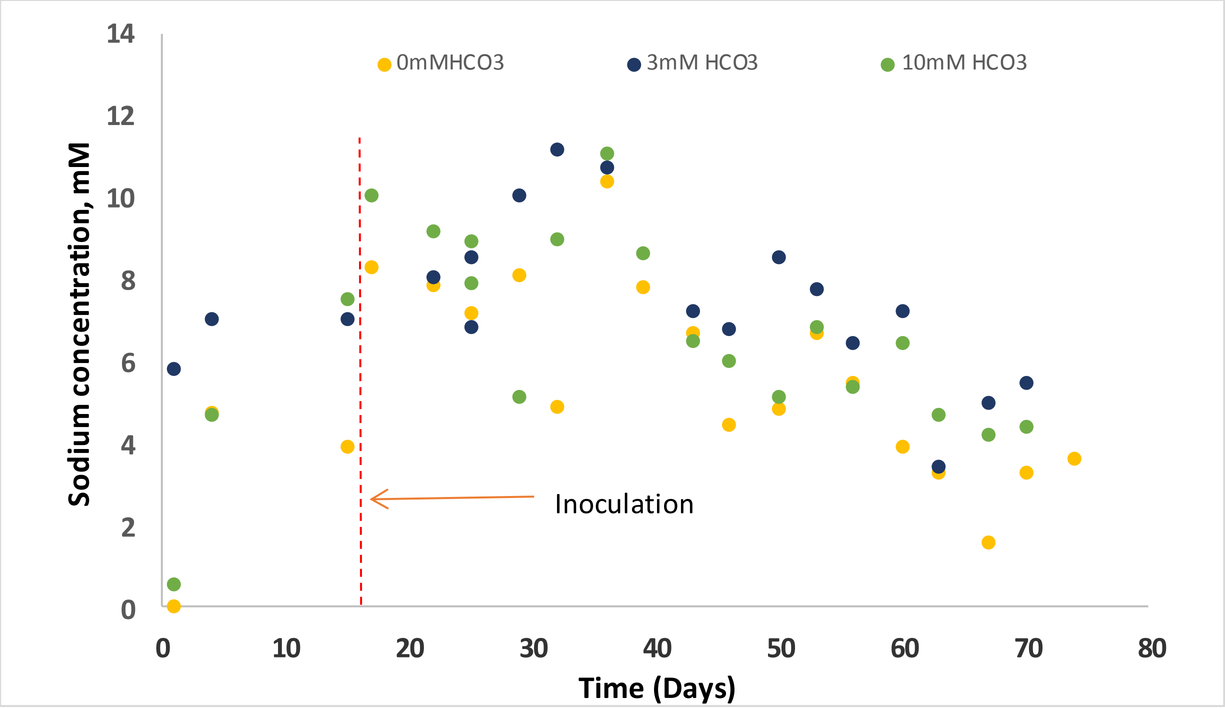

Figure 2-22. Concentrations of sodium released into the aqueous phase as a function of time under different HCO_3 concentrations.

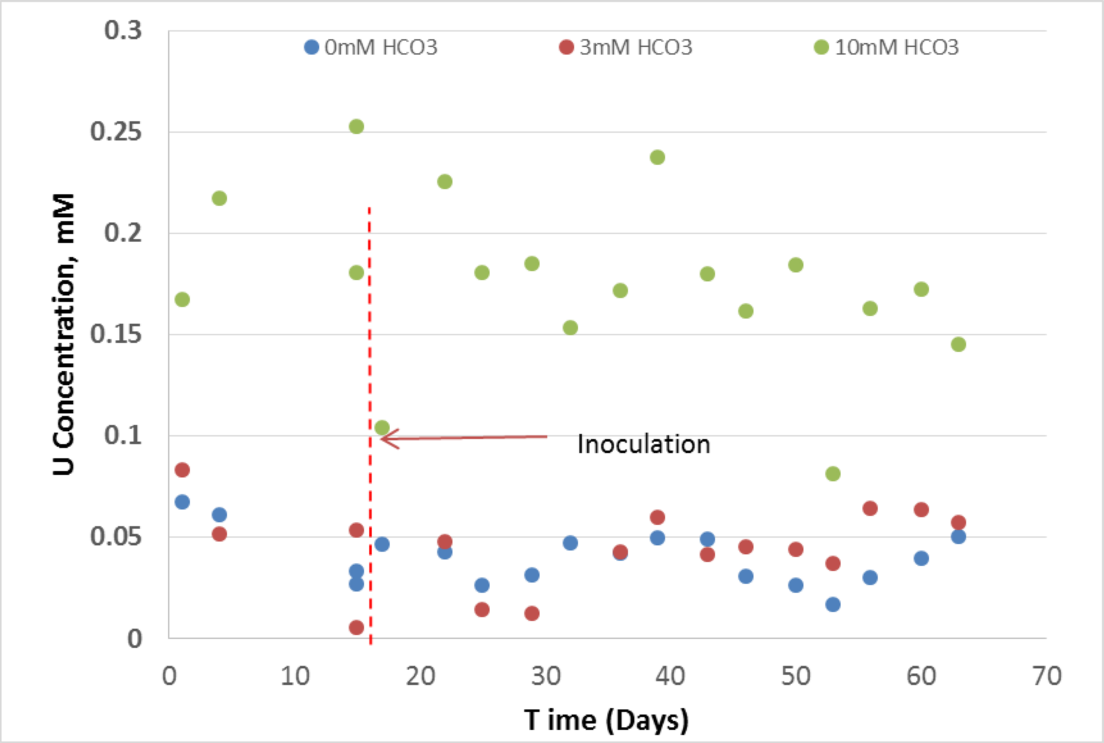

Figure 2-23. Concentrations of uranium released into the aqueous phase as a function of time under different HCO_3 concentrations.

Concentrations of sodium and phosphorus were increased after microbial inoculation of sacrificial samples and then gradually decreased. There is no significant difference of sodium concentrations between the 0 mM, 3 mM and 10 mM bicarbonate concentrations tested. The same is true for phosphorus concentrations. However, uranium concentrations for 0 mM and 3 mM bicarbonate stayed relatively the same from the first day of inoculation. The 10 mM bicarbonate samples slightly increased after about 10 days but then stabilized close to the original concentration. Concentrations determined during samples analysis do not correspond to an ideal empirical formula of $Na[UO_2PO_4]$ as 1:1:1 for Na, P and U. Data results suggest that the liberation of U(VI) from sodium autunite influences incongruent reactions to release Na and P from the mineral structure.

In the month of June, FIU initiated preparations for the natural autunite dissolution experiments in the presence of consortia culture enriched at Pacific Northwest National Laboratory (PNNL). The media solution for the dissolution studies was prepared in 1L of DIW buffered with 0.02M Na-Hepes buffer with pH adjusted to 7.1 with 0.1 mol/L HCl or NaOH. Sodium lactate ($C_3H_5NaO_3$, 60% w/w) was added to the solution with a concentration of 0.024 mol/L (3.4 mL/L). The solution was divided into three 500-mL bottles and sterilized by autoclaving at 121°C, 15 psi for 15 min and cooled at room temperature. As the experiment is based on the investigation of bacteria interactions in the presence of different bicarbonate concentrations, potassium bicarbonate salt was added to the autoclaved bottles to obtain one bottle each of 3 mM and 10 mM bicarbonate; the remaining bottle was kept bicarbonate-free. This accounts for a total of three concentrations of bicarbonate for the experiment tested. Next, the bicarbonate-bearing solutions were filter-sterilized into other sterile 500-mL bottles and the sterile bottles were stored in the anaerobic chamber until the beginning of the experiment. In addition, sixty sacrificial 20-mL glass scintillation vials were prepared for the experiments to have 10 duplicate vials for 10 sampling events for each bicarbonate concentration. Each vial was filled with 18 mg of autunite powder to provide a final U(VI) concentration of 4.4 mmol/L, which is similar to concentrations used in previous experiments. The vials were amended with 10 mL of sterile media solution containing 0, 3, and 10 mM $KHCO_3$. Each set, prepared using a specific bicarbonate concentration, includes duplicate sacrificial biotic vials and an abiotic control. Samples will be sacrificed at specific time intervals according to the sampling schedule. Frozen consortia-based culture enriched at PNNL was growing on LB and sterile hard and liquid media prepared with 250 mg/L of tryptone, 500 mg/L of yeast extract, 0.024M of sodium lactate, 0.6 g/L $MgSO_4.7H_2O$, and 0.07 g/L $CaCl_2.2H_2O$ (TYL). Hard media required an addition of 15.0 g/L of agar (Figure 2-24).

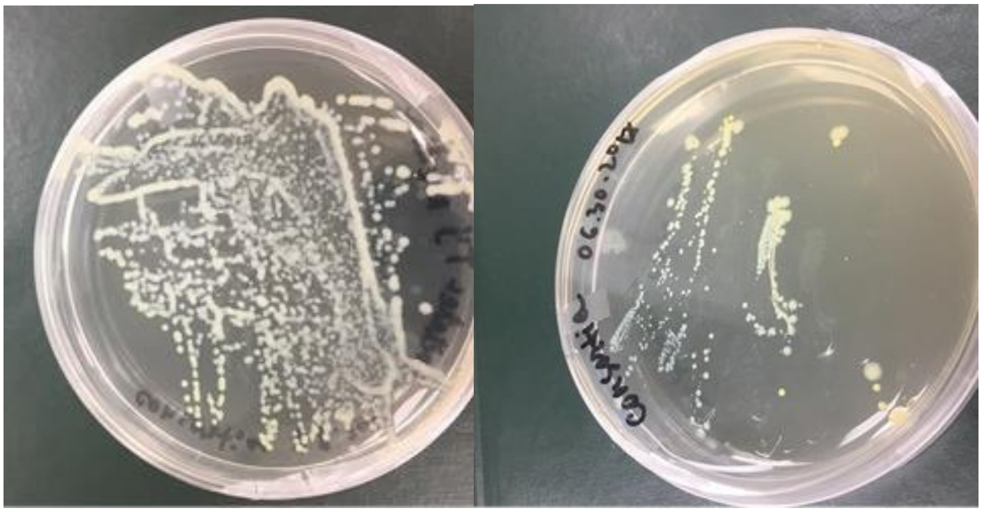

Figure 2-24. Consortia-based culture enriched at PNNL growing at TYL media (left) and LB media (right). Both cultures look very uniform with yellowish-white color colonies; however, the culture grown on LB media has in addition several yellowish colonies.

Subtask 1.3. Investigation of Electrical Geophysical Response to Microbial Activity in the Saturated and Unsaturated Environments

In month of April, FIU completed the sample collection from two columns related to the spectral induced polarization (SIP) signatures of microbial activity and obtained initial results from ICP-OES analysis of spring 2017 samples. Results for calcium are displayed in Figure 2-25 while results for phosphorous are displayed in Figure 2-26. Magnesium showed the same trend as calcium. Iron results were inconclusive possibly due to problems arising from the calibration. Aluminum was measured as well; however, there was no noticeable trend over time. Some of the results were erroneous and were thrown out; these may be repeated in the future to obtain cleaner data results.

In addition, FIU has completed preparation of the fall 2016 samples for ICP-OES. Future analysis will also include KPA for dissolved uranium as well as possibly re-running some ICP-OES samples.

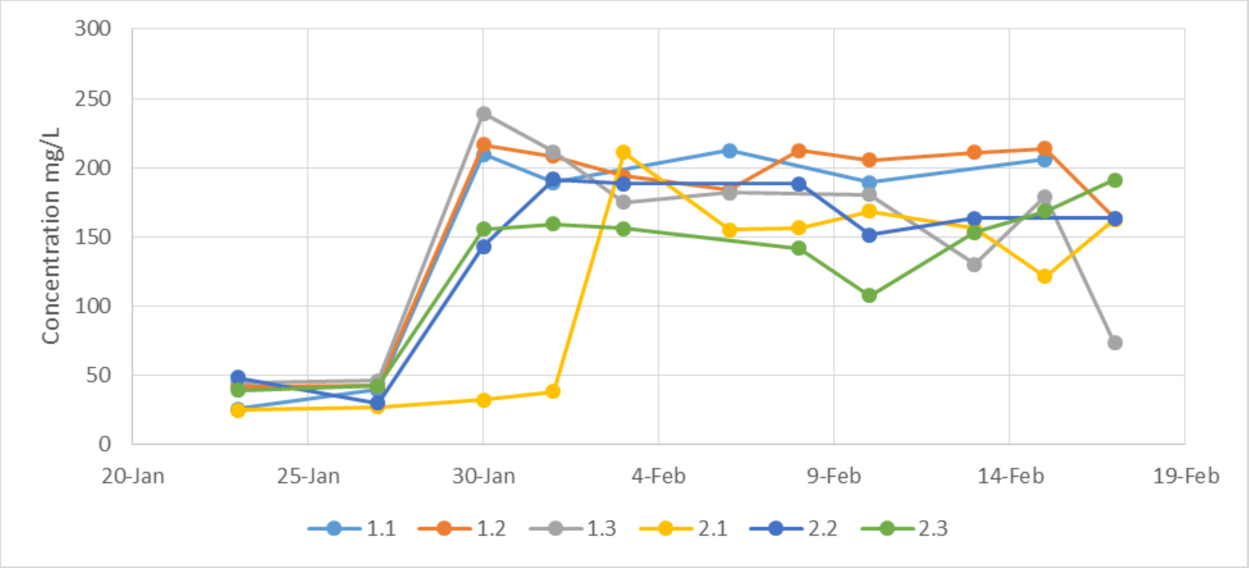

Figure 2-25. Calcium concentration for spring 2017 samples for columns 1 and 2 from ICP-OES.

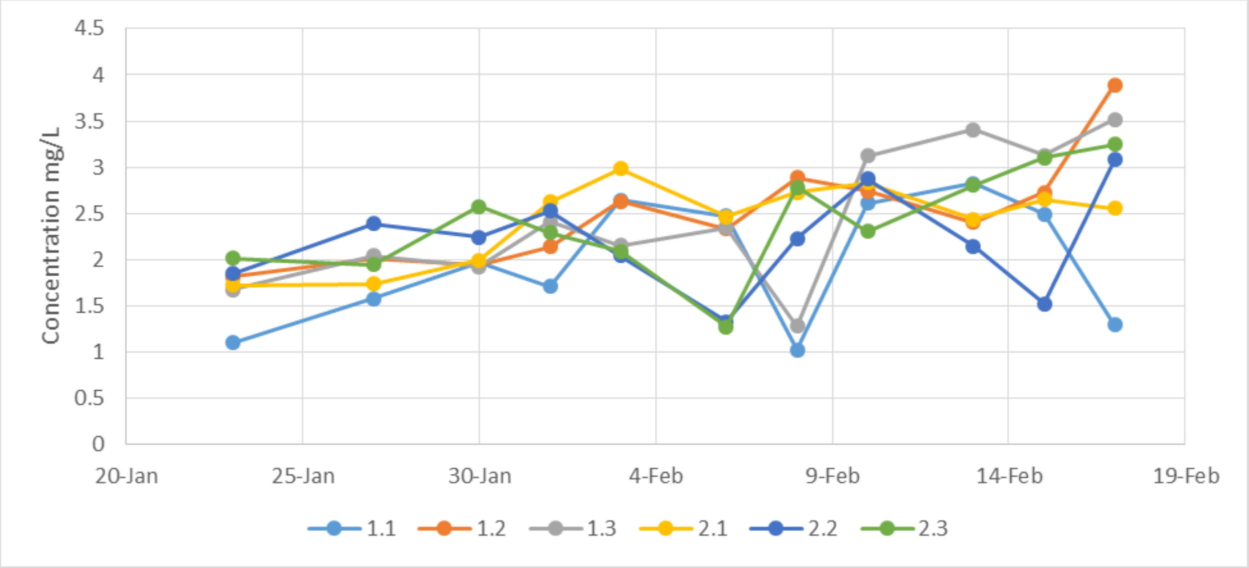

Figure 2-26. Phosphorous concentration for spring 2017 samples for columns 1 and 2 from ICP-OES.

In May, FIU completed ICP-OES analysis of samples collected in fall 2016. Elements measured include Fe, Ca, Mg, and P. Results for calcium are displayed in Figure 2-27. Phosphorous seems to show a downward trend; however, values this low may be below detection limits for the instrument. Magnesium showed the same trend as calcium. Both calcium and magnesium seem to correlate with the pore water conductivity taken with a microelectrode as well as the bulk resistivity taken with SIP. Iron showed a significant increase over time in columns where glucose was injected, although column 4 showed a slower response. Iron results for column 3 are displayed in Figure 2-28.

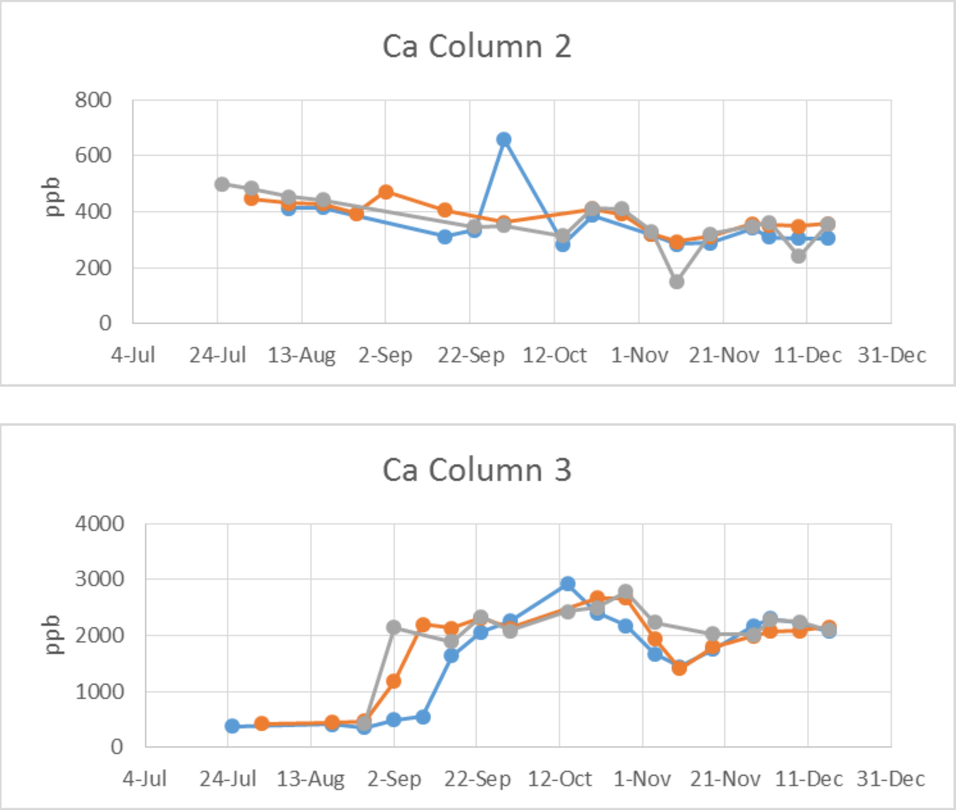

Figure 2-27. Calcium concentration for fall 2016 samples for columns 2 and 3 from ICP-OES, diluted 100x.

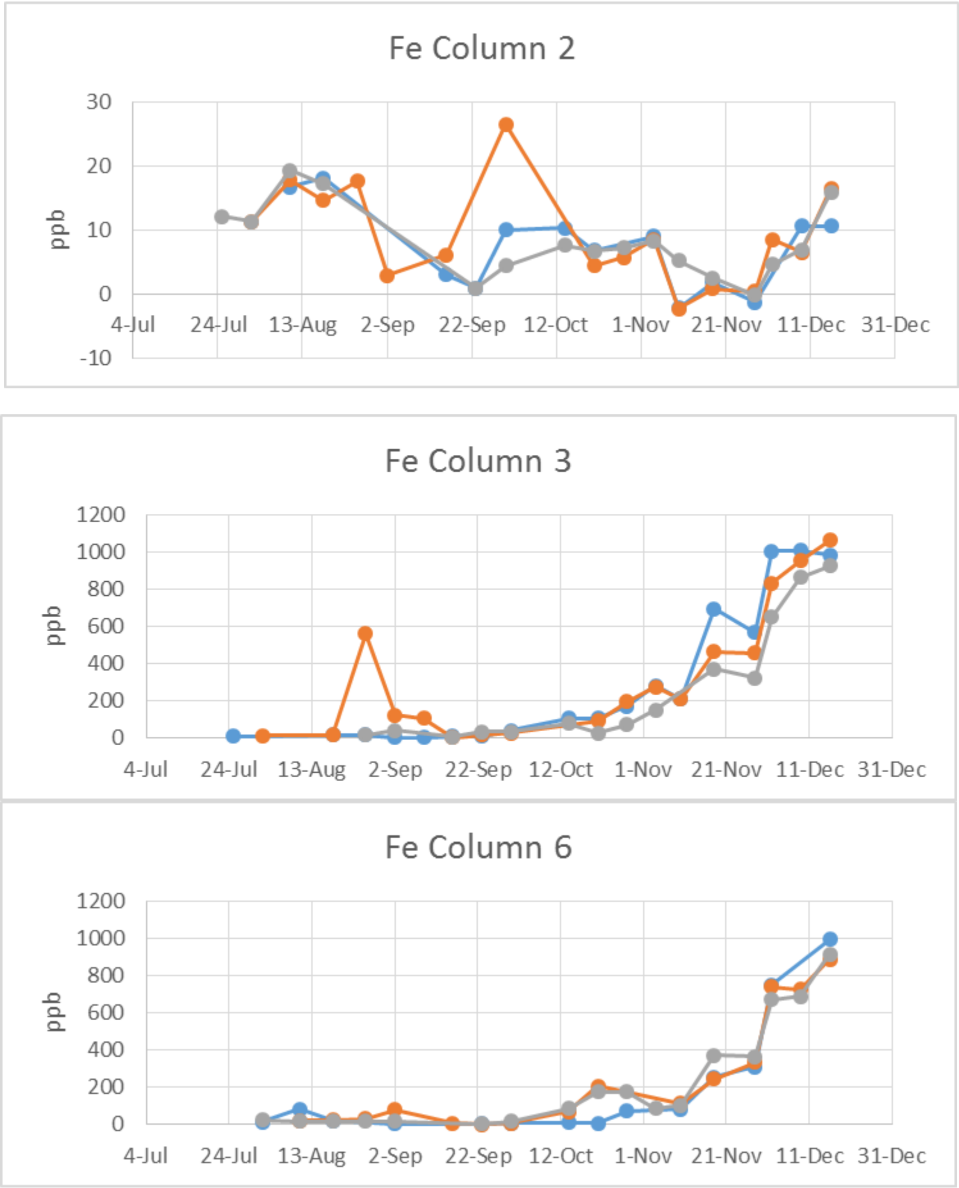

Figure 2-28. Iron concentration for fall 2016 samples for columns 2, 3, and 6 from ICP-OES, diluted 100x.

In June, uranium analyses were completed for the samples collected during spring 2017 using a Chemchek^{TM} kinetic phosphorescence analyzer (KPA). Samples were wet ashed prior to KPA using concentrated nitric acid and a 35% hydrogen peroxide solution and then dry ashed at 400°C in the furnace for 15 min. The ashed samples were then dissolved with 1M nitric acid and diluted with 1% nitric acid for the sample analysis via KPA. Due to the calibration prepared in the range of uranium concentrations up to 100 ppb, the dilutions factors of 10x, 100x, and 200x were used, depending on the sample. The ashing protocol is used to avoid interferences with KPA readings while processing organic-bearing samples as described previously in FIU monthly and year end reports.

The solutions flow to the columns also from the bottom; for this reason, the lowest uranium concentrations were observed at port 1 for both columns since the water never reached the autunite layer before being sampled. Column 2, which has bicarbonate in the solution composition, shows consistently lower values than column 1 at ports 2 and 3; these values also seem to be more stable. Column 1 seems to show a peak around the 30th of January; however, this may be erroneous since these values are above the maximum values used for KPA calibration. Column 1 also seems to show a downward trend over time, possibly indicating a reduction of uranium (VI) to U(IV) (Figure 2-29).

There may be a correlation of decreasing uranium concentration with the increase in ferrous iron concentration (Figure 2-30) and/or degree of reducing conditions in column 1 due to the fact that iron shows a positive increase over time.

The fall 2016 samples are currently being prepared for uranium analysis. The procedure for preparation of these samples will be the same as used for the spring 2017 samples.

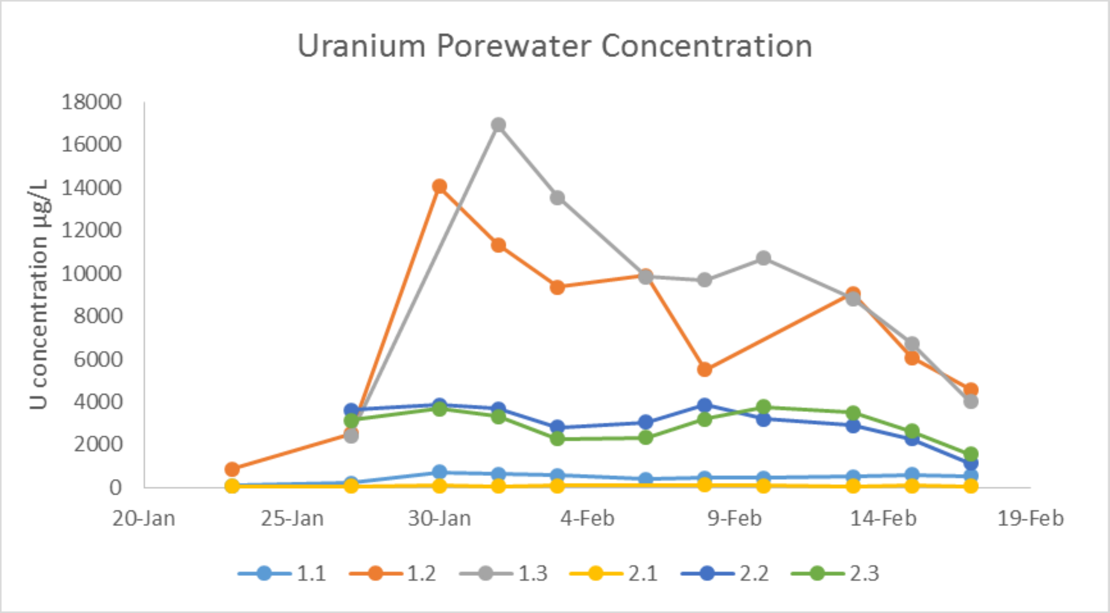

Figure 2-29.Changes in uranium concentrations for spring 2017 samples.

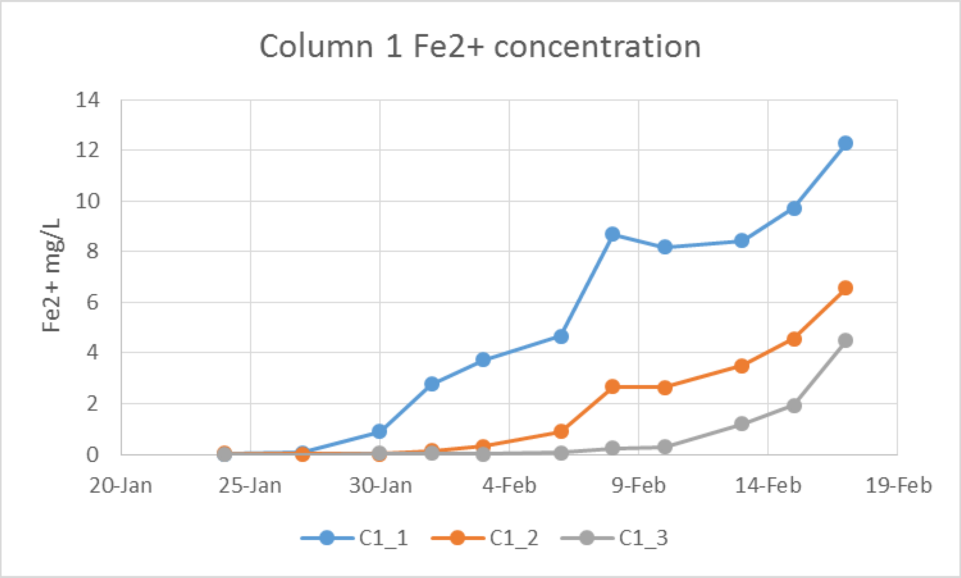

Figure 2-30. Changes in Fe^{2+} concentration using Ferrozine analysis for column 1, spring 2017.

Subtask 1.4. Contaminant Fate and Transport under Reducing Conditions

During the month of April, FIU managed to troubleshoot several technical factors that associate closely with studying Tc chemistry under anaerobic conditions. Specifically, the first issue addressed was creating an inert atmosphere in the anaerobic glovebox (Coy Labs, Figure 2-31). A mixture of nitrogen and hydrogen gas (5% H_2, balanced with N_2, AirGas) was introduced in the glovebox; nevertheless, a very high concentration of oxygen (~6,000 ppm O_2) inside the glovebox was observed. Oxygen and hydrogen levels were monitored through the Coy Lab Products CAM-12 dual reader (Figure 2-32).

Figure 2-31. Anaerobic glovebox at FIU-ARC Soil and Groundwater Laboratory.

Figure 2-32. Coy Lab CAM-12 O_2 and H_2 reader depicting current conditions inside the anaerobic glovebox.

The recorded amounts of oxygen do not allow the study of Tc chemistry under reducing conditions. The first step of troubleshooting was to examine the anaerobic glovebox for possible leaks and damage, with the aid of ARC engineers. The pump and airlock chamber valves were checked and the copper gas inlet wiring was changed to polypropylene tubing as a precaution in order to avoid potential future fractures due to the copper wiring's rigid nature. No leaks, punctures or other flaws were detected in the glovebox. After repeated trial and error experiments with 95% N_2 - 5% H_2 cylinders from the same vendor (AirGas) with similar results, a cylinder of the same gas concentrations was solicited from a new vendor (NexAir), accompanied by an analysis certificate for O_2 levels. This time, a stable oxygen reading was achieved (~25 ppm) with 1-1.5% hydrogen for several days (Figure 2-32). The anaerobic glovebox contains two stackable Pd catalysts that remove H_2O.

Once the inert atmosphere was regulated to acceptable levels, a set of mock samples was created using 1 gram of Hanford soil (mean particle diameter: $d<300$ μm) in 50 ml of DI water previously purged with N_2 under vigorous stirring for 2 hrs. The mock samples did not contain technetium or bicarbonate. The objective of preparing these samples was to test sodium dithionite, a reducing agent available in ARC's facilities, for ORP control and obtain preliminary understanding of the system before expanding the experiments to Tc-bearing solutions. The samples were spiked with the appropriate amount of $Na_2S_2O_4$ (sodium dithionite) and the final concentration of the reducing agent in the sample was 10^{-2} M. The oxidation reduction potential (ORP) was measured before and after the $Na_2S_2O_4$ addition to the samples as well as after a four-day equilibration period using MI-800 Redox Electrode (MicroElectrodes). ORP and pH measurements are presented in Table 2-5.

Table 2-5. ORP Measurements

Vials	ORP (mV)	pH	
1	358	7	Before addition of sodium dithionite
2	353	7.05	
3	352	7.1	
1	-330	6.5	After addition of sodium dithionite
2	-338	6.5	
3	-342	6.5	
1	240	6.5	4 days equilibration time after addition of sodium dithionite
2	246	6.5	
3	-395	6.5	

Upon initially introducing $Na_2S_2O_4$ to the samples, the ORP levels rapidly decreased. However, after the equilibration period, the ORP levels were significantly higher. An expected decrease in pH from 7 to 6.5 was also observed, since an aqueous solution of sodium dithionite is acidic and decomposes to sodium thiosulfate and sodium bisulfite (which decreases the pH), according to the reaction:

$$2\ Na_2S_2O_4 + H_2O \rightarrow Na_2S_2O_3 + 2\ NaHSO_3$$

On the other hand, in vial #3, 4 days after equilibration, the ORP still remained significantly low. This fluctuation in ORP values led to more frequent monitoring, which consequently led FIU to identify that the ORP electrode was malfunctioning (values for the same vial ranged from highly reducing to oxidizing within 20 minutes) and may have reached the end of its life span. To this end, a new HI36200 ORP electrode (Hannah Instruments) was purchased which is designed for field and industrial applications and is expected to be hardier and provide more reliable ORP readings when inserted in soil suspension samples. The ORP measurements in the samples will be repeated.

The presence of thiosulfate in acidic conditions based on the reaction above would induce the formation of technetium sulfide colloidal particles, which are not a focal point of this investigations. To this end, different inorganic and organic reducing agents will be investigated in preliminary experiments in order to assess the sustainability of reducing conditions within the solution. The potential reducing agents that will be investigated are summarized in Table 2-6.

Table 2-6. Reducing Agents

Name	Formula
Sodium Dithionite	$Na_2S_2O_4$
Sodium Thiosulfate	$Na_2S_2O_3$
Sodium Borohydride	$NaBH_4$
Oxalic Acid	$C_2H_2O_4$
Formic Acid	CH_2O_2
Ascorbic Acid	$C_6H_8O_6$
Ferrous Chloride	$FeCl_2$
Stannous Chloride	$SnCl_2$
Hydroquinone	$C_6H_6O_2$

Despite the fact that sodium dithionite and sodium thiosulfate may induce undesired reactions, they are included in the list for observational and comparison reasons. Weak acid reducing agents, such as formate, oxalate and ascorbic acid will be used for the stabilization of the ORP values in the system, along with inorganic reducing agents, such as ferrous chloride and stannous chloride. To the best of FIU's knowledge, there is no literature indicating a possible complexation between the chosen organic ligands and Tc under the conditions studied, despite Xia (Xia et al., 2006) reporting Tc complexation with oxalates in high ionic strength conditions. Hydroquinone has also been used as an ORP regulator achieving sub-oxic conditions at circumenutral pH values (Yalcintas et al., 2015). To this end, FIU is currently preparing more mock samples, which will contain fixed concentrations of bicarbonates (50 mM) and Tc-99 at pH 7.5 in the presence of different reducing agents. ORP and pH will be recorded as a function of time and, periodically, aliquots will be isolated and Tc(VII) and Tc(IV) concentrations in the aqueous phase will be determined. The experimental findings will be compared to the theoretical Pourbaix diagrams for Tc-O-H systems in an effort to identify if the presence of bicarbonate keeps Tc(IV) in the aqueous phase.

Furthermore, in future experiments, in order to ensure stable circumneutral pH conditions for the experiments (pH~7.5) and avoid pH fluctuation due to the introduction of several reducing agents, samples will be spiked with a small amount of an appropriate buffer. Acidification of the samples is not desirable in order to avoid degassing of CO_2 in acidic conditions within the glovebox. PIPES buffer has been used in the past for similar studies at circumneutral or slightly alkaline conditions (Yalcintas et al., 2015), whereas there have been studies indicating that reduced Tc products may be soluble in Tris buffer but they are not soluble in HEPES buffer (Shi et al., 2011). The same study concludes that the reduced Tc products in Tris buffer were a mixture of Tc(IV) and Tc(V) oxidation states, whereas in HEPES buffer, Tc was encountered only as Tc(IV). Hence, at this stage it seems that HEPES or PIPES would be the most appropriate buffer solutions for future use.

During the month of May, FIU initially prepared two suspensions containing 1g of Hanford soil (average particle diameter d<300μm) and 50 mL of aqueous phase with 50 μM final concentration of $^{99}TcO_4^-$. One sample was bicarbonate-free and the other sample was spiked with bicarbonate (final concentration of 3 mM HCO_3^-). Samples were created using N_2 purged solutions (N_2 purging time of 1h under vigorous stirring). The pH of all of the samples was adjusted to 7.5-8 using 0.001 M hydrochloric acid, and samples were placed in the anaerobic glove box in 99% N_2- 1% H_2. The samples were left to equilibrate and, during this period, aliquots were isolated and underwent solvent extraction ($CHCl_3$-TPPC) for the determination of Tc(IV) and Tc(VII) in the aqueous phase. Tc partitioning was measured by means of liquid scintillation counting.

After a month of equilibration under reducing conditions, Tc-99 was found in the +7 oxidation state in both samples (Figure 2-33) despite the significant presence of magnetite and ilmenite in the soil, as evidenced from the previous XRD analysis. Theoretically, the reaction is thermodynamically feasible under the reducing conditions observed. Furthermore, Cui and Eriksen (1996) reported the reduction of Tc(VII) to Tc(IV) by Fe(II) minerals, along with Peretyazhko et al. (2009) who suggested that Fe(II) minerals can be an effective heterogeneous reductant of Tc(VII). Peretyazhko proposed the following scheme to describe the affinity of the Tc(VII) heterogeneous reduction by Fe(II): aqueous Fe(II) ~ adsorbed Fe(II) in phyllosilicates [ion-exchangeable and some edge-complexed Fe(II)] << structural Fe(II) in phyllosilicates << Fe(II) adsorbed on Fe(III) oxides. Consequently, a third sample containing 1g of Hanford soil (average particle diameter d<300μm), 50 mL of aqueous phase with 50 μM final concentration of $^{99}TcO_4^-$ and 3 mM of bicarbonate was spiked with sodium dithionite (final concentration of 0.01 M). The Tc concentration in the aqueous phase was monitored for a period of two weeks and the results are presented in Table 2-7.

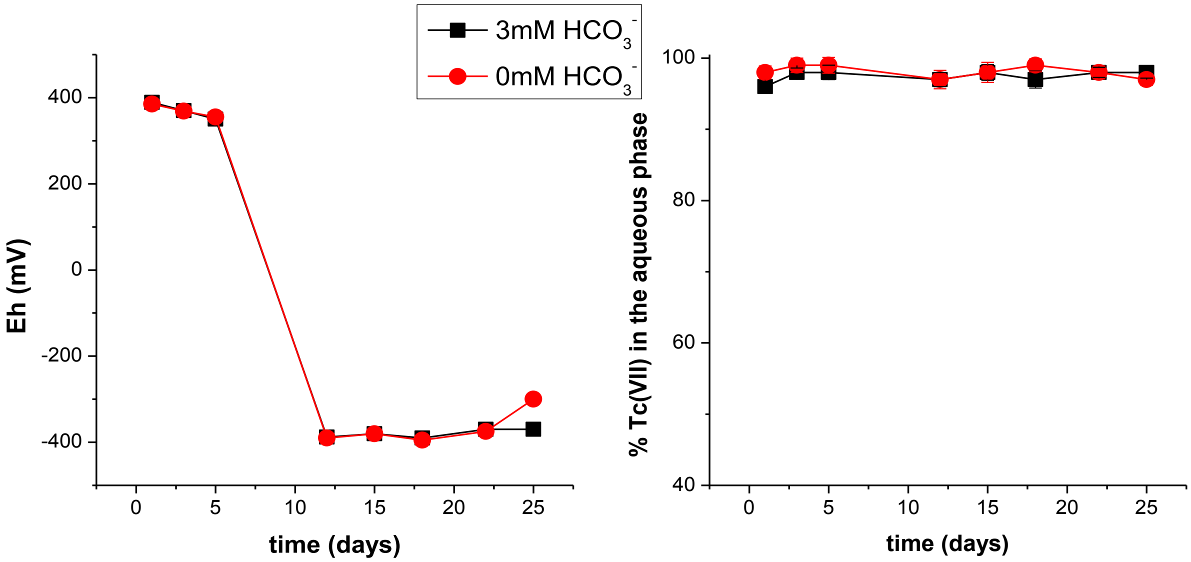

Figure 2-33. Eh (mV) values and Tc(VII) percentage detected in the aqueous phase as a function of time.

Table 2-7. Eh (mV) Values Percentage of Tc (VII) and Tc (IV) Soluble Species in the Sample Spiked with $Na_2S_2O_4$ (Final Concentration of 0.01 M)

	Day 1 from the preparation of the sample		**Day 5**		**Day 12**	
Oxidation State of Tc soluble species	Percentage %	Eh (mV)	Percentage %	Eh (mV)	Percentage %	Eh (mV)
4+	2 ± 1	260	11 ± 1	-300	3 ± 1	-310
7+	98 ± 1		5 ± 1		1 ± 0.5	

As can be seen in Table 2-7, a quantitative reduction of Tc(VII) is observed in the presence of sodium dithionite within 12 days, whereas the Eh values recorded are at the same levels as the samples that do not contain sodium dithionite. However, a lack of mass balance suggests that, in the presence of sodium dithionite, other reactions might be occurring that affect the Tc solubility. Such as the formation of insoluble Tc-sulfides complexes or precipitation of Tc (IV), this would be undetectable in the LSC as it can only detect radionuclides in solutions.

In order to identify the appropriate reducing agent, which will promote the reduction of Tc(VI) to Tc(IV), an experimental set up was designed that would evaluate different reducing agents under conditions relevant to the experiment. The samples were identical as described above except for the addition of Na-HEPES buffer (0.001 M) in order to maintain pH values within the desired range (7-8). The reducing agents tested included: sodium thiosulfate, sodium dithionite, formic acid, oxalic acid, ascorbic acid, sodium borohydride, hydroquinone, stannous chloride and ferrous chloride. The concentration of each reducing agent in all samples was 10^{-3} M. All reagents were prepared with N_2 purged deionized water and were placed inside the anaerobic glovebox. The Eh values were monitored for a period of 4 days and the results are presented in Figure 2-34.

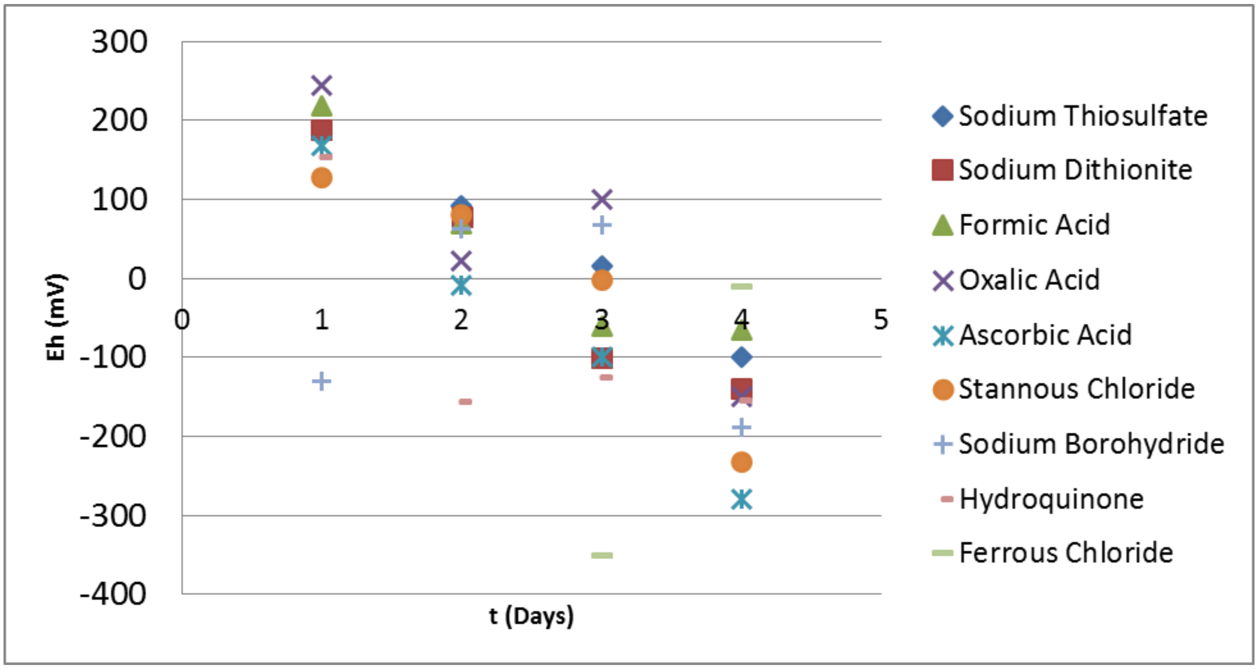

Figure 2-34 .Eh (mV) values as a function of time for different reducing agents used.

The experimental results revealed that all reducing agents maintained reducing conditions in the samples. Nevertheless, sodium dithionite was not deemed appropriate for future use due to the high fluctuation of Eh values during measurement, which is likely related to the degradation of $Na_2S_2O_4$ in circumneutral conditions (Lem and Wayman, 1970; Yalcintas, 2015a). Sodium thiosulfate was also excluded from future use due to the possible formation of technetium sulfides (Rard et al., 1999). The organic acids' capability to maintain stable Eh readings was found to be highly dependent on the hydrogen content of the anaerobic glovebox, as opposed to the rest of the reducing agents, where stable Eh readings were recorded despite H_2 content fluctuation (±0.5%) in the glovebox. Furthermore, stannous chloride and ferrous chloride were not chosen for future use due to the formation of a solid phase in circumneutral conditions. Quantitative reduction of Tc(VII) to Tc(IV) has been reported in the presence of Sn(OH)Cl solids (Yalcintas, 2015b) under circumneutral conditions. Nevertheless, the introduction of foreign solid phases to the system is not desirable. These preliminary experiments provided significant insight into the system's equilibration time and Eh stability due to the presence of reducing agents (and the absence of iron and titanium-bearing minerals present in Hanford soil). Next, experimental steps will include the repetition of the experiment, with the addition of Hanford soil, in the presence of hydroquinone and sodium borohydride. The Tc reduction rate will be monitored under different bicarbonate concentrations.

During the month of June, FIU continued investigating the chemistry of Tc under reducing conditions in the presence of Hanford soil. Specifically, five suspensions containing 1g of Hanford soil (average particle diameter d<300µm) and 50 mL of aqueous phase with 50 µM final concentration of $^{99}TcO_{4^-}$ and 10 mM HCO_3^- were prepared for the experiments. All samples contained 10^{-3} Na-HEPES and pH was adjusted to 7.5. Samples were spiked with small amounts of different reducing agents and the final concentration of each agent was: $NaBH_4$ 10^{-3} and $2·10^{-3}$ (A and B, respectively), 10^{-3} formic acid (sample C), 10^{-3}M hydroquinone (sample D) and 10^{-3}M $SnCl_2$ (sample E). Samples were created using N_2 purged solutions, such as Na-HEPES and

HCO_3^-, by purging with N_2 for 1 hr during vigorous stirring. The samples were placed in the anaerobic glove box in 99% N_2- 1% H_2 and aliquots were periodically isolated and underwent solvent extraction ($CHCl_3$-TPPC) for the determination of Tc(IV) and Tc(VII) in the aqueous phase. Eh (mV) and pH were also measured frequently by using a Hannah Instruments redox electrode and an Orion 9110D pH electrode, respectively. Tc partitioning was measured by means of liquid scintillation counting. In Figure 2-35, the fluctuation of Eh (mV) as a function of time for each sample is presented. No fluctuations of pH were monitored and no adjustment was required during the period of one month.

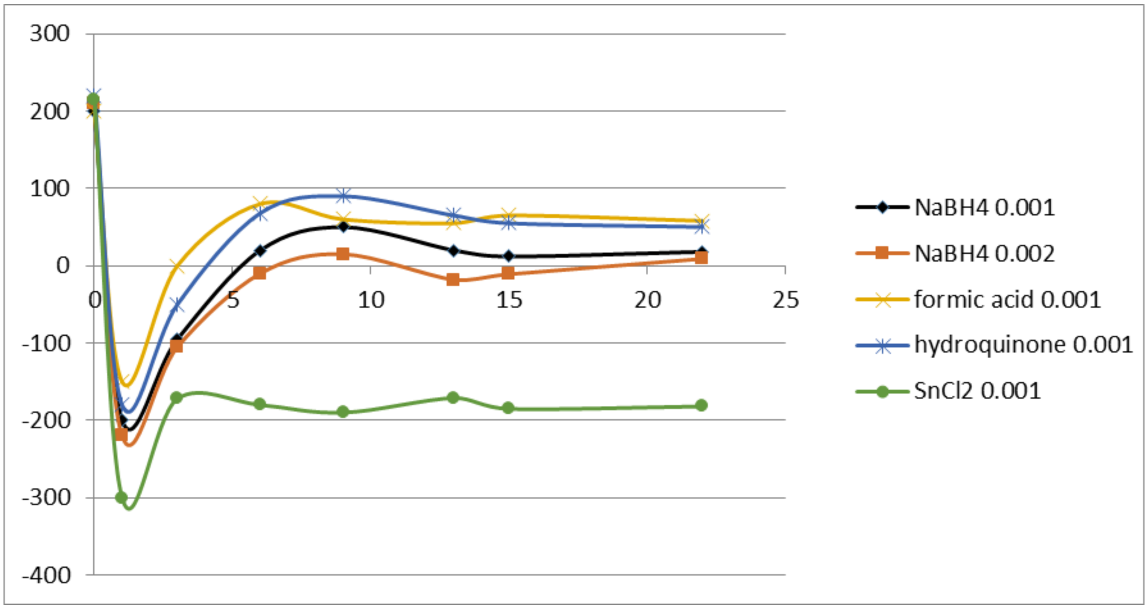

Figure 2-35. Eh (mV) as a function of time for each sample.

As can be seen from Figure 2-35, the introduction of a reducing agent in the aqueous phase incites an immediate plunge of the Eh values and then equilibration takes place and Eh values stabilize in a time period of 5-7 days. $SnCl_2$ is one of the strongest reducing agents and managed to keep the Eh values very low, slightly above the border of water reduction (Yalçintaş 2015). All reducing agents induce conditions that favor the reduction of Tc(VII) to Tc(IV), which in circumneutal conditions will usually take place for Eh values below 100 mV (Icenhower et al., 2008).

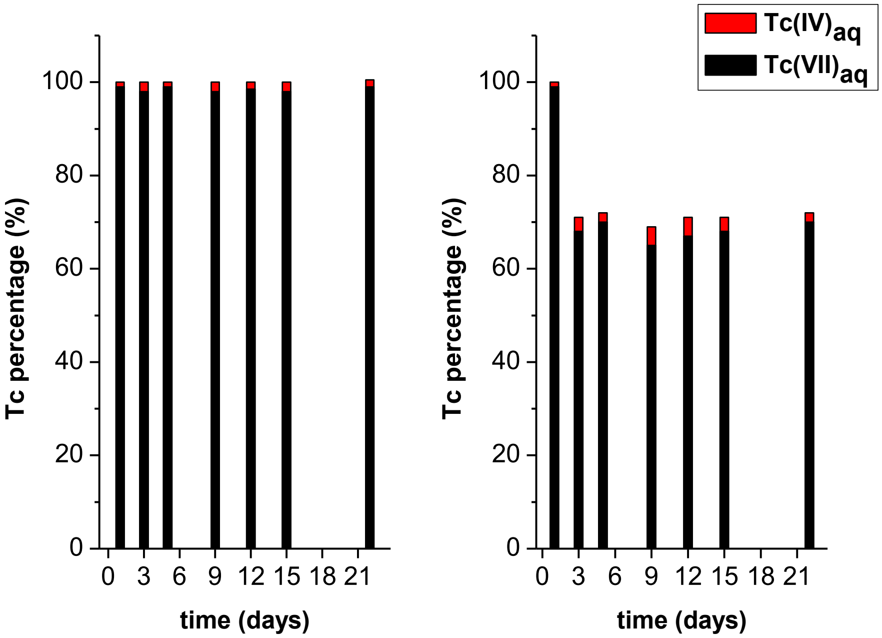

Figure 2-36. Tc percentage in the aqueous phase as a function of time for Hanford soil suspensions in the presence of hydroquinone, formic acid and in plain N_2-H_2 atmosphere (left) and in the presence of $NaBH_4$ (right).

As can be seen in Figure 2-36, despite the recorded reducing conditions, the presence of reducing agents such as formic acid and hydroquinone, as well as in the absence of a reducing agent in the aqueous phase (plain N_2-H_2 atmosphere), Tc-99 is overwhelmingly found in the +7 oxidation state. Despite this seemingly paradox, Tc can be encountered as pertechnetate even under reducing conditions, since the steric distribution of electron donors is more important for the redox reaction Tc(7+) to Tc(4+) rather than the overall Eh values (Icenhower et al., 2008). Similar results have been recorded in plain Tc solutions in the presence of hydroquinone (in the absence of a mineral or a solid phase) by Yalçintaş (2015) and Kobayashi (2013) in the presence of hydroquinone in diluted NaCl systems. Overall, it was concluded that the oxidized form of hydroquinone was incapable of providing the 3 e^- needed for the reduction of pertechnetate to Tc(4+). In the case of $SnCl_2$, a fast and complete reduction was observed within 3 days, where all the quantity of technetium was removed from the aqueous phase. Similar results have been reported in literature (Yalçintaş et al., 2015), where a complete reduction was observed within 7 days. $SnCl_2$ was used for comparison reasons, since the undesirable formation of an insoluble salt under circumenutral conditions based on the reaction $SnCl_2$ (aq) + H_2O (l) ⇌ Sn(OH)Cl (s) + HCl (aq) would render its use very limited. In the case of $NaBH_4$ after 3 days, the concentration of Tc_{aq} decreased by 35%; nevertheless, the remaining technetium in the aqueous phase is encountered in the +7 oxidation state. This is an additional indication of the importance of electron donation for the reduction of pertechnetate to Tc(IV), since the reaction took place by 35% and since day 3 remained in a steady state. The concentration of $NaBH_4$ did not seem to affect the outcome of the reaction under the conditions studied. Finally, it should be noted that all samples contained a ratio of Tc:HCO_3^- equal to 200:1, much higher than the 30:1 cited in literature (Eriksen et al., 1992), which would likely favor the formation of Tc(IV)-carbonate complexes under circumneutral conditions and prevent the precipitation of TcO_2. In order to investigate this phenomenon further, FIU has initiated samples containing 0.01 M $NaBH_4$ (higher concentration than used previously) in an effort to identify if the reaction is going to take place at 100%. Furthermore, since no reduction has been observed in the samples that contain no reducing agents (plain N_2-H_2 atmosphere) despite the presence of magnetite and ilmenite in the soil, FIU will initiate batch experiments using pure minerals in comparison with the samples containing actual Hanford soil. Different quantities as well as different forms of the same mineral will be investigated (magnetite nanoparticles versus microparticles), since the quantity and the specific surface area play an important role in a heterogeneous reaction such as the reduction of TC(VII) to Tc(IV) in the presence of minerals (McBeth et al., 2011).

References

Cui D and Eriksen TE (1996) Reduction of pertechnetate in solution by heterogeneous electron transfer from Fe(II)-containing geological material. Environ. Sci. Technol. 30, 2263– 2269.

Eriksen T.E., Ndalamba P., Bruno J., Caceci M., 1992. The solubility of $TcO_2 \cdot nH_2O$ in neutral to alkaline solutions under constant p_{CO2}. Radiochimica Acta, 58/59, 67-70

Icenhower, J.P., Martin, W.J., Qafoku, N.P., Zachara, J.M., 2008. The geochemistry of technetium: a summary of the behavior of an artificial element in the natural environment, PNNL, Richland, WA.

Kobayashi T., Scheinost A., Fellhauer D., Gaona X., Altmaier M., 2013. Redox behavior of Tc(VII)/Tc(IV) under various reducing conditions in 0.1M NaCl solutions. Radiochimica Acta 101, 323-332

Lem WJ and Wayman MD (1970) Decomposition of aqueous dithionite. 1. Kinetics of decomposition of aqueous sodium dithionite. Can. J Chem. 48, 782-790

McBeth JM, Lloyd JR, Law GT, Livens FR, Burke IT, Morris K, 2011. Redox interctions of technetium with iron bearing minerals. Mineralogical Magazine 75(4), 2419-2430

Peretyazhko T, Zachara JM, Heald SM, Jeon BH, Kukkadapu RK, Liu C, Moore D, Resch CT (2009) Heterogeneous reduction of Tc(VII) by Fe(II) at the solid–water interface. Geochim. Cosmochim. Acta 72, 121-1539

Rard, J., Rand, M., Anderegg, M., Wanner, H., 1999. Chemical Thermodynamics of Technetium, OECD Nuclear Energy Agency.

Shi L, Belchik SM, Plymale AE, Heald S, Dohnalkova AC, Sybirna K, Bottin H, Squier TC, Zachara JM, Fredrickson JK. “Purification and Characterization of the [NiFe]-Hydrogenase of *Shewanella oneidensis* MR-1”. Applied and Environmental Microbiology 77(16):5584-5590.

Xia Y, NJ Hess, and AR Felmy. 2006. “Stability Constants of Technetium(IV) Oxalate Complexes as a Function of Ionic Strength.” Radiochimica Acta 94:137-141.

Yalcintas E, Gaona X, Scheinost AC, Kobayashi T, Altmaier M, Geckeis H. 2015 "Redox chemistry of Tc(VII)/tc(IV) in dilute to concentrated NaCl and $MgCl_2$ solutions. Radiochimica Acta 103(1):57-72

Yalçintaş E. 2015a. Redox, solubility and sorption chemistry of technetium in dilute to concentrated saline systems. KIT Scientific Report 7703, KIT Scientific Publishing, Karlsruhe, Germany

Yalcintas E, Gaona X, Scheinost AC, Kobayashi T, Altmaier M, Geckeis H., 2015b. Redox chemistry of Tc(VII)/Tc(IV) in dilute to concentrated NaCl and $MgCl_2$ solutions. Radiochimica Acta 103(1), 57-72

Task 2: Remediation Research and Technical Support for Savannah River Site

Task 2 Overview

The acidic nature of the historic waste solutions received by the F/H Area seepage basins caused the mobilization of metals and radionuclides, resulting in contaminated groundwater plumes. FIU is performing basic research for the identification of alternative alkaline solutions that can amend the pH and not exhibit significant limitations, including a base solution of dissolved silica and the application of humic substances. Another line of research is focusing on the evaluation of microcosms mimicking the enhanced anaerobic reductive precipitation (EARP) remediation method previously tested at SRS F/H Area.

Task 2 Quarterly Progress

Subtask 2.1. Investigation on the Properties of Acid-Contaminated Sediment and its Effect on Contaminant Mobility

During April, FIU determined the specific surface area and pore volume of the different acidified soil profiles, which were prepared during March. Soil samples isolated after 7, 30 and 50 days of contact are given the code names A, B and C, respectively, and the soil samples that went through 1 cycle of acidification and the supernatant was not replenished (hence, saturation was allowed and secondary mineral precipitation took place) are named Sat, for the purposes of the present report. The specific surface areas and pore distributions of each profile are summarized in Table 2-8.

Table 2-8. Specific Surface Areas and Pore Distribution for Each Acidified Soil Profile, Followed by Relative Standard Deviation

Acidified soil profile	Specific Surface Area (m^2/g)	Pore volume (mm^3/g)
A	0.14 ± 0.02	0.89 ± 0.1
B	0.07 ± 0.01^a	0.35 ± 0.2^b
C	0.07 ± 0.03^a	0.50 ± 0.1^b
Sat	0.23 ± 0.02	2.1 ± 0.4^c
Background (untreated)	0.41 ± 0.02	2.1 ± 0.3^c

Note: The same superscripts (a, b and c) denote statistically the same values (t-test, P>0.05 for 95% confidence level)

The experimental findings indicate a clear trend of decreases in the specific surface area and pore volume of the acid exposed soil, when compared to background (untreated soil). The specific surface area and the pore volume values of the acidified soil that contains secondary precipitates fall in between of those of the background soil and category A, indicating both competing mechanisms: a balance between acidification (mineral loss) and secondary mineral contribution/precipitation.

Samples of each category were used in batch experiments in order to assess their sorptive capacities for U(VI). 200 mg of each soil were brought in contact with 10 ml of the aqueous phase (pH 3 and 4.5), containing 0.5 mg/L U(VI). The samples were equilibrated for 24 hrs on a platform shaker (120 rpm) at room temperature. After 24 hrs, aliquots were isolated from the supernatant and were diluted 1:10 with 1% HNO_3. The U(VI) residual concentration in the supernatant was determined by means of kinetic phosphorescence analysis (KPA). The results are presented in Table 2-9.

Table 2-9. U(VI) Uptake by the Different Profiles of Acidified Soil, Expressed in Terms of Uranium Percent Removal, at pH Values 3 and 4.5

Acidified soil profile	% U(VI) Removal	
	pH 3	**pH 4.5**
A	0	11 ± 3
B	0	5 ± 1
C	0	0
Sat	0	11 ± 2
Background (untreated)	0	20 ± 2

Table 2-9 revealed that retention of U(VI) at pH 3 by SRS F/H Area soil (acidified or background) is negligible, whereas at pH 4.5, a trend seems to be taking place, indicating that the longer the soil is exposed to acid (and loses its content in Fe), sorption decreases. Nevertheless, the percent removal is quite limited and a similar trend may be more obvious when sorption is performed at higher pH values. To this end, in the future FIU will perform identical experiments at circumneutral conditions (pH~6.5) and pH 8.

The concentrations of Fe, Al and Si in the aqueous phase, as a result of soil-aqueous phase contact for a 24-hr equilibration, were determined by means of ICP-OES and are presented in Table 2-10.

Table 2-10. Al, Fe and Si Concentrations (ppb) Detected in the Aqueous Phase for Each Acidified Soil for pH Values 3 and 4.5

Acidified soil profile	pH 3			pH 4.5		
	Al	Si	Fe	Al	Si	Fe
A	439 ± 12	188 ± 20	380 ± 80	485 ± 60	155 ± 20	412 ± 38
B	346 ± 50	204 ± 25	460 ± 100	330 ± 10	150 ± 37	400 ± 10
C	269 ± 40	123 ± 30	420 ± 40	275 ± 70	120 ± 14	410 ± 51
Sat	312 ± 25	119 ± 22	460 ± 109	277 ± 50	117 ± 18	570 ± 100

The experimental findings of Table 2-10 show that the amount of Al, Fe and Si released in the supernatant under the conditions the sorption experiments were performed are independent of the pH values. The pH values studied are quite close, nevertheless they are in the strong acidic region, where more leaching is theoretically expected than pH 6.5 that will be studied in the future. Finally, future experiments will also include the characterization of the samples using SEM-EDS and normalization of all sorption data in mg U(VI)/m^2 of soil, as well as K_d.

During the month of May, FIU continued investigating the sorptive capacities of the different acidified soil profiles created in the previous months. To this end, batch sorption experiments were conducted at circumneutral conditions (pH~6.8) and pH 8. The experimental conditions were identical to the previous sorption experiments: 200 mg of each soil were brought in contact with 10 ml of the aqueous phase, containing 0.5 mg/L U(VI). The samples were equilibrated for 24 hr at room temperature on a platform shaker (110 rpm). Aliquots isolated after 24 hr were diluted 1:10 with 1% HNO_3 and were analyzed for Al, Fe and Si with ICP-OES. The results are presented in Table 2-11. Uranium analysis by means of KPA is scheduled to take place during the first week of June, upon arrival of the Uraplex, a complexing agent required for uranium analysis, from the Chemchek Company. Soil samples isolated after 7, 30 and 50 days of contact have been titled A, B and C, respectively.

Table 2-11. Al, Fe and Si Concentrations (ppb) Detected in the Aqueous Phase for Each Acidified Soil Batch Sorption Experiment for pH Values 6.8 and 8

Acidified soil profiles	pH 6.8			pH 8		
	Al	Si	Fe	Al	Si	Fe
A (7 days)	2330 ± 100	5400 ± 100	1497 ± 63	4481 ± 80	9870 ± 200	2314 ± 42
B (30 days)	1620 ± 300	5000 ± 600	986 ± 200	1602 ± 295	6011 ± 650	2384 ± 51
C (50 days)	552 ± 40	1230 ± 30	420 ± 40	1178 ± 70	4693 ± 200	2204 ± 101
Sat	3782 ± 54	6778 ± 150	2503 ± 30	3739 ± 259	8810 ± 421	2864 ± 221

The results of the ICP analysis revealed several interesting trends. The concentration of Al, Fe and Si at pH 6.8 and 8 is at least 5 times higher than the concentrations detected when sorption experiments took place at pH 3 and 4.5 (results were reported in the April monthly report). Furthermore, a decrease in each element's concentration was observed for both pH values going from soil profile A towards C, which is rather expected since the amount of kaolinite and goethite decreases as well. Finally, the concentrations detected for the soil profile where secondary mineral precipitation was allowed during leaching experiments were at similar levels as soil profile A.

FIU also performed elemental analysis of each soil profile by means of SEM-EDS at the Florida Center for Analytical Electron Microscopy (FIU, Modesto Maidique Campus). The results of elemental analysis are presented in Table 2-12. The percentage of Al and Fe decreased in soil profiles A to C, which is in agreement with the preliminary leaching kinetic experiments, which revealed that the longer the exposure of the soil in acidic environment, the higher the leaching of Al and Fe, due to kaolinite and goethite dissolution.

Table 2-12. Percentage of Al, Fe and Si in Each Soil Profile

Acidified soil profiles	Percentage elemental composition (%)		
	Al	**Si**	**Fe**
A	8.8 ± 3	38 ± 5	5.7 ± 2
B	2.9 ± 2	47 ± 3	1.8 ± 0.8
C	1.0 ± 0.7	52 ± 1	0.4 ± 0.2
Sat	4.3 ± 2	42 ± 0.5	5.6 ± 0.6

On the other hand, the percentage of Si increased for soil profiles A to C, showing that the longer the exposure of the soil to acid, the higher the removal of Al and Fe due to dissolution; acidified soil profile C resembles pure quartz. In Figure 2-37, EDS spectra for soil profiles A and C are presented.

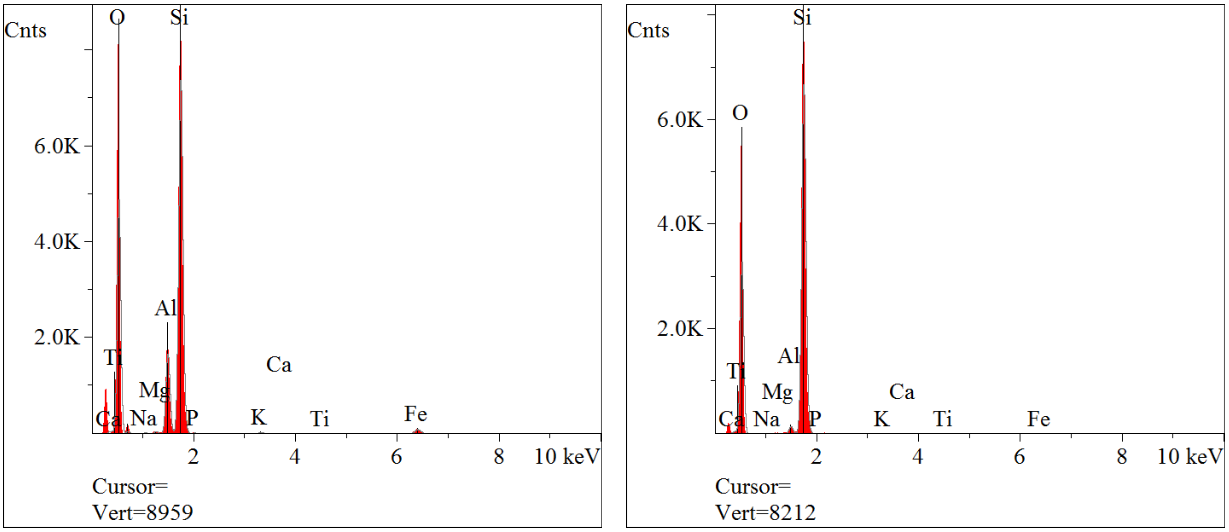

Figure 2-37. EDS spectrum for soil profile A (left) and soil profile C (right).

As it can be seen in Figure 2-37, the peak of Al diminishes and the already small peak for Fe is almost absent; soil profile C consists mostly of quartz. For the soil profile where secondary precipitation was allowed (i.e., the "Sat" soil profile), the percentage of Si and Fe remain at the same levels as compared to soil profile A. This may be due to the precipitation of hematite and amorphous silica, as predicted by speciation studies conducted earlier this year using Visual

Minteq software. On the other hand, no secondary aluminum precipitates were predicted by the software.

Future studies include the normalization of the SEM-EDS percentage results as mg of Al, Fe and Si per g of soil. Furthermore, uranium sorption results at pH 6.8 and 8 will be evaluated and compared to the respective values from experiments using background (non-acidified) soil.

During the month of June, FIU continued investigating the sorptive capacities of the different acidified soil profiles created the previous months. Furthermore, FIU received soil from the core of the plume located to SRS F/H Area (FAW-5). FIU performed elemental analysis of the plume soil by means of SEM-EDS at the Florida Center for Analytical Electron Microscopy (FIU, Modesto Maidique Campus). The results of elemental analysis are presented in Table 2-13 and Figure 2-38, where the results of the elemental analysis of the different acidified soil profiles are also included for comparison reasons.

Table 2-13. Concentration of Al, Fe and Si in Each Acidified Soil Profile and Plume Soil

Acidified soil profile	**Elemental concentration (mg g^{-1} soil)**		
	Al	**Si**	**Fe**
A (7 days)	88 ± 30	380 ± 50	57 ± 20
B (30 days)	29 ± 20	470 ± 30	18 ± 8
C (50 days)	10 ± 7	520 ± 10	4 ± 2
Sat	43 ± 20	420 ± 5	56 ± 6
Plume soil (FAW-5)	131 ± 28	745 ± 66	87 ± 9

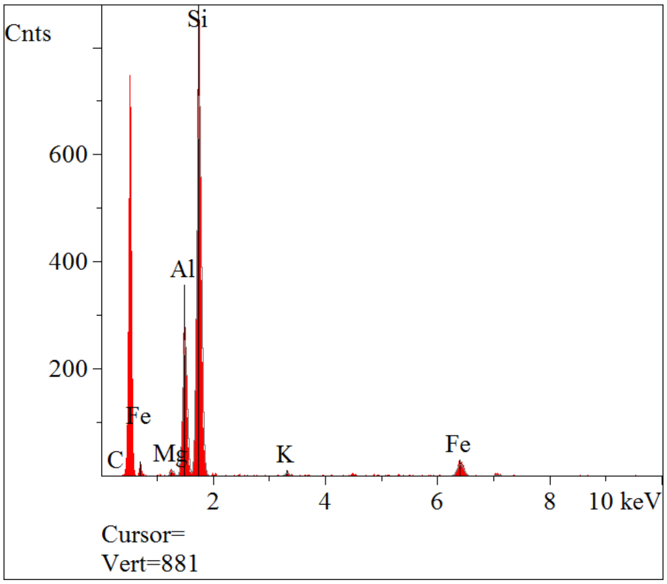

Elt.	**Line**	**Intensity (c/s)**	**Conc**	**Units**	**Error 2-sig**	**MDL 3-sig**	
C	Ka	0.00	0.000	wt.%	0.000	0.000	
Mg	Ka	11.14	0.863	wt.%	0.302	0.388	
Al	Ka	254.64	18.876	wt.%	0.795	0.412	
Si	Ka	740.49	70.337	wt.%	1.668	0.505	
K	Ka	7.84	0.985	wt.%	0.405	0.518	
Fe	Ka	36.04	8.939	wt.%	1.074	0.789	
			100.000	wt.%			Total

Figure 2-38. EDS spectrum and analysis for plume soil.

The concentrations of Al, Fe and Si in the plume soil are significantly higher than the acidified soil profiles. The levels of Fe in the plume soil are similar when compared to background soil from the SRS F/H Area (89±2 and 70±7 for mean particle diameter $d<63\mu m$ and $63<d<180\mu m$, respectively), whereas the concentrations of Al and Fe are practically double (Anagnostopoulos et al., 2017).

During June, batch sorption experiments were conducted at pH 3, 4.5, 7 and 8. The experimental conditions were identical to past sorption experiments performed: 200 mg of plume soil were brought in contact with 10 ml of aqueous phase, containing 0.5 mg/L U(VI) in the pH range mentioned above. pH was adjusted as necessary with the addition of small amounts of NaOH during equilibration. Samples were equilibrated for 24h at room temperature on a platform shaker (110 rpm). Aliquots isolated after 24 h were diluted 1:10 with 1% HNO_3 and were analyzed for Al, Fe and Si with ICP-OES. The results are presented in Table 2-14.

Table 2-14. Al, Fe and Si Concentrations (ppb) Detected in the Aqueous Phase after 24h Equilibration of Plume Soil with 0.5 ppm U(VI) at pH Values 3, 4.5, 7 and 8

Soil profile	**pH 3**			**pH 4.5**			**pH 7**			**pH 8**		
	Al	**Si**	**Fe**	**Al**	**Si**	**Fe**	**Al**	**Si**	**Fe**	**Al**	**Si**	**Fe**
FAW-5 (plume soil)	2386 ± 238^{a}	1284 ± 79^{b}	843 ± 103^{c}	2671 ± 567^{a}	1400 ± 99^{b}	941 ± 255^{c}	2916 ± 640^{a}	1519 ± 708^{b}	1225 ± 281^{c}	5083 ± 74	6046 ± 601	2478 ± 20

Note: Same superscripts (a, b and c) denote statistically the same values (t-test, P>0.05 for 95% confidence level)

It is evident from Table 2-14 that the concentrations of Al, Fe and Si in the supernatant are higher when samples were equilibrated at pH 8, a trend that was noticed in the equilibrium studies with acidified soil performed the past months as well. Congruent kaolinite dissolution has been cited in literature for pH<4 (as opposed to incongruent dissolution pH 5-10) (Huertas et al., 1999); nevertheless, the levels of Al and Fe in the supernatant in circumneutral and mildly alkaline conditions may be affected by precipitation of aluminum and iron secondary phases (Carroll and Walther, 1990; Huertas et al., 1999). Furthermore, the levels of Al, Fe and Si as presented in Table 2-14 are significantly higher than the levels in background soil equilibrated for 24h at pH 3 and 7 (Anagnostopoulos et al., 2017).

Uranium residual concentration in the supernatant was determined by using kinetic phosphorescence analysis (KPA). The results are presented in Table 2-15.

Table 2-15. U(VI) Uptake by the Different Profiles of Acidified Soil, Expressed in Terms of Uranium Percent Removal, at pH Values 3, 4.5, 7 and 8

Acidified soil profile	**% U(VI) Removal**			
	pH 3	**pH 4.5**	**pH 7**	**pH 8**
FAW-5	0	15 ± 2	72 ± 6	70 ± 12
A (7 days)	0	11 ± 3	38 ± 1	29 ± 5
B (30 days)	0	5 ± 1	39 ± 2	24 ± 3
C (50 days)	0	0	20 ± 4	18 ± 4
Sat	0	11 ± 2	44 ± 9	24 ± 2
Background	0	18 ±2	61 ± 6	

Interestingly, the soil profiles show zero and very low sorptive capacity at pH 3 and 4.5, respectively. At pH 7, the plume soil removes a similar amount of U(VI) from the aqueous phase to the background soil, a fact that may be attributed to their similar iron content. At pH 8, the plume soil exhibits a far higher retention of uranium compared to the acidified soil, which is rather expected due to iron content (Table 2-13).

Future work includes the comparison of the sorptive capacities of the different soil profiles in mass of U(VI) per surface unit, as well as running speciation software for the pH conditions studied in order to investigate the role of speciation in sorption.

References

Anagnostopoulos, V.A., Katsenovich, Y., Denham, M., 2017. Sodium silicate treatment for the attenuation of U(VI) by iron-bearing sediments in acidic groundwater plumes. Journal of Chemical Technology & Biotechnology, 92(8): 1919-1927.

Carroll, S.A., Walther, J.V., 1990. Kaolinite dissolution at 25°C, 60°C and 80°C. American Journal of Science, 290: 797-810.

Huertas, F.J., Chou, L., Wollast, R., 1999. Mechanism of kaolinite dissolution at room temperature and pressure Part II: kinetic study. Geochimica et Cosmochimica Acta, 63(19): 3261-3275.

Subtask 2.2: The Synergistic Effect of Humic Acid and Colloidal Silica on the Removal of Uranium (VI)

FIU finished experiments with batches 2, 3, 5 and 6 for pH values of 3-8 by preparing triplicate samples with 30 ppm humic acid, 3.5 mM of silica, 400 mg of sediment and 30 ppm uranium. The pH of these samples was adjusted with a stock solution of 0.01M HCl and 0.05M NaOH to the appropriate pH conditions and samples were placed on a platform shaker and pH of samples was measured daily and adjusted to desired pH if needed. Samples were centrifuged at 2700 rpm for 30 minutes to allow the separation of the solids from the solution. After being centrifuged, the filtered samples were diluted using 1% HNO_3 by a dilution factor of 240, filtered using a 0.45 μm syringe filter, and 6 mL was placed in each KPA vial. The unfiltered samples were diluted using 1% HNO_3 by a dilution factor of 240 and 6 mL was placed in each additional KPA vial. Each filtered and unfiltered sample was prepared for analysis via KPA to measure the concentration of uranium. The percent of average and standard deviation of uranium removal for both unfiltered and filtered samples at pH 3-8 are shown in Tables 2-16 and 2-17. Lowest uranium removal was observed at pH 3 for all batches for both filtered and unfiltered samples. Uranium removal increased with an increase in pH till pH 6 with highest removal of 69% for batch 5 and the uranium removal dropped with increase in pH range from 7 to 8.

Table 2-16. Unfiltered Uranium Concentrations KPA Samples

Unfiltered Uranium Concentration Samples; 30 pmm Uranium								
pH	Si, HA, U (Batch 2)		HA, U (Batch 3)		Si, HA, Sediment, U (Batch 5)		HA, Sediments, U (Batch 6)	
	Uranium removal	Standard Dev	Uranium removal	Standard Dev	Uranium removal	Standard Dev	Uranium removal	Standard Dev
3	21%	0.073	71%	0.056	6%	0.084	15%	0.040
4	18%	0.040	16%	0.042	27%	0.043	38%	0.010
5	26%	0.057	32%	0.053	46%	0.079	53%	0.013
6	43%	0.028	24%	0.108	49%	0.009	42%	0.042
7	35%	0.028	24%	0.047	41%	0.019	40%	0.007
8	29%	0.119	69%	0.099	35%	0.030	43%	0.031

Table 2-17. Filtered Uranium Concentration KPA Samples

Filtered Uranium Concentration Samples; 30 pmm Uranium								
pH	Si, HA, U (Batch 2)		HA, U (Batch 3)		Si, HA, Sediment, U (Batch 5)		HA, Sediments, U (Batch 6)	
	Uranium removal	Standard Dev	Uranium removal	Standard Dev	Uranium removal	Standard Dev	Uranium removal	Standard Dev
3	17%	0.015	27%	0.029	16%	0.002	20%	0.021
4	27%	0.048	29%	0.006	28%	0.035	28%	0.020
5	45%	0.096	47%	0.009	63%	0.027	55%	0.012
6	59%	0.011	35%	0.087	69%	0.016	57%	0.052
7	56%	0.032	33%	0.113	63%	0.015	45%	0.024
8	44%	0.118	68%	0.059	52%	0.037	48%	0.040

Control (samples with no HA) triplicate samples of batches containing 3.5 mM of silica, 400 mg of sediment and 30 ppm uranium at pH 3 and 4 were prepared by mixing a known amount of various constituents, except uranium, as shown in Tables 2-18 to 2-21. Uranium was added prior to the pH adjustment and specific amounts of deionized water were added with the addition of acid/base so the final volume totaled approximately 20 ml. The pH of the samples was adjusted with a stock solution of 0.01M HCl and 0.1M NaOH to the desired pH; samples were then placed on a platform shaker. The pH of the samples were measured periodically and readjusted if there was a change in pH. Tables 2-19 and 2-21 show the data for the daily change of pH for each batch sample. FIU completed the experiments with pH 3 and 4 batch samples which are currently being stored for preparation of KPA analysis. Once pH 3-4 adjustments are completed, the batches will be prepared for dilution, filtration and KPA analysis.

Table 2-18. Overall pH Adjustments for pH 3 Batch Samples

pH 3 Adjusted Set		Constituents						
		SiO2	Sediments	Uranium, U (VI)	Volume of acid/ base	DIW, H2O	pH	
		mL	mg	mL	mL	mL	Initial pH	Final pH
Batch No. 1	1.1	2.10	0.00	0.50	4.55	13.75	1.73	3.05
	1.2				4.65	13.75	1.69	3.03
	1.3				4.75	13.75	1.63	3.00
Batch No. 4	4.1	2.10	400.00	0.50	4.85	13.75	1.58	3.02
	4.2				4.80	13.75	1.56	3.02
	4.3				4.80	13.75	1.54	3.04
Batch No. 7	7.1	0	400.00	0.50	2.95	15.50	2.16	3.00
	7.2				2.90	15.50	2.18	3.02
	7.3				2.90	15.50	2.18	3.01

Table 2-19. Daily Change of pH 3 Batch Samples

Sample #		pH 3						
		Day 1	Day 2	Day 3	Day 4	Day 5	Day 6	Day 7
Batch No. 1	1.1	1.73	3.33	3.07	3.07	3.06	3.02	3.05
	1.2	1.69	3.42	3.06	3.06	3.06	3.02	3.03
	1.3	1.63	3.43	3.04	3.04	3.04	3.00	3.00
Batch No. 4	4.1	1.58	3.42	3.03	3.05	3.06	3.02	3.02
	4.2	1.56	3.42	3.04	3.05	3.07	3.03	3.02
	4.3	1.54	3.44	3.04	3.06	3.06	3.02	3.04
Batch No. 7	7.1	2.16	2.94	2.94	2.97	3.01	2.98	3.00
	7.2	2.18	2.95	2.96	2.99	3.03	3.01	3.02
	7.3	2.18	2.95	2.95	2.98	3.02	2.99	3.01

Table 2-20. Overall pH Adjustments for pH 4 Batch Samples

pH 4 Adjusted Set		Constituents						
		SiO2	Sediments	Uranium, U (VI)	Volume of acid/ base	DIW, H2O	pH	
		mL	mg	mL	mL	mL	Initial pH	Final pH
Batch No. 1	1.1	2.10	0.00	0.50	3.61	13.50	2.09	4.05
	1.2				7.14	10.00	2.15	3.95
	1.3				3.37	12.00	2.20	4.02
Batch No. 4	4.1	2.10	400.00	0.50	3.92	12.00	2.14	4.02
	4.2				3.50	12.00	2.14	4.00
	4.3				3.50	12.00	2.14	4.04
Batch No. 7	7.1	0	400.00	0.50	3.95	15.00	2.16	4.02
	7.2				4.00	15.00	2.15	4.03
	7.3				3.96	15.00	2.15	4.05

Table 2-21. Daily Change of pH 3 Batch Samples

Sample #		pH 4						
		Day 1	Day 2	Day 3	Day 4	Day 5	Day 6	Day 7
Batch No. 1	1.1	2.09	4.06	4.09	3.92	3.88	4.02	4.05
	1.2	2.15	3.89	3.98	3.98	3.94	3.94	3.95
	1.3	2.20	3.84	4.05	4.02	4.02	4.01	4.02
Batch No. 4	4.1	2.14	3.91	4.01	4.03	4.00	4.00	4.02
	4.2	2.14	3.98	3.99	4.02	3.99	4.00	4.00
	4.3	2.14	4.03	4.04	4.07	4.02	4.03	4.04
Batch No. 7	7.1	2.16	4.04	4.18	4.32	4.11	4.13	4.02
	7.2	2.15	4.08	4.24	4.35	4.17	4.18	4.03
	7.3	2.15	3.97	4.14	4.37	4.19	4.18	4.05

Subtask 2.3: Humic Acid Batch Sorption and Column Experiments with SRS Soil

Humic Acid Batch Sorption Experiments

During the month of April, FIU performed sorption kinetic experiments of uranium onto SRS sediments at pH 4. For the kinetic experiments, an initial U(VI) concentration of 0.5 mg L^{-1} was allowed to equilibrate with SRS sediment for different time periods at pH 4 and constant ionic strength (0.01M $NaClO_4^-$). The samples were vortex mixed, placed on a platform shaker, and centrifuged. The supernatant was analyzed by KPA. It is important to note that prior to the addition of uranium, sediments were pre-equilibrated for three days. For the sediments amended with Huma-K, initially 20 mL of Huma-K solution with a fixed concentration (200 mg L^{-1}) at pH 4 was brought in contact with 1 g of SRS sediment for five days to be equilibrated on the platform shaker. After five days, samples were centrifuged, and the supernatant was replaced by deionized water (ionic strength 0.01M $NaClO_4^-$) at pH 4. Uranium with an initial metal concentration of C_0 = 0.5 mg L^{-1} was spiked in the samples, which were vortex mixed, placed on a platform shaker, and centrifuged. The supernatant was analyzed by KPA.

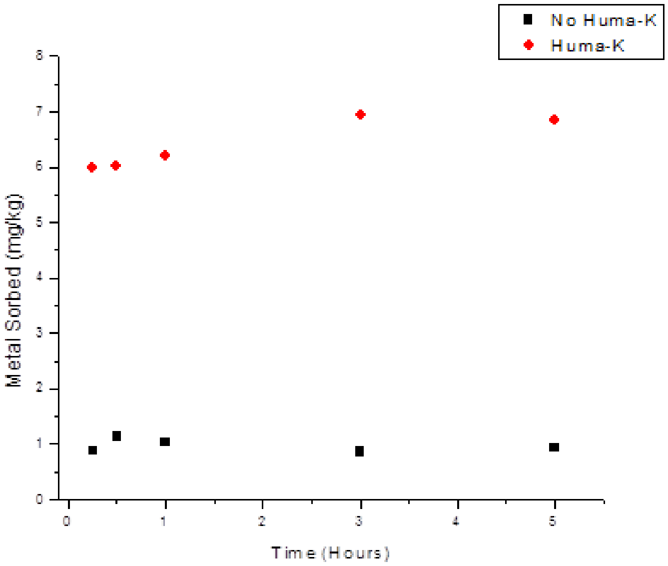

Figure 2-39. Uranium sorption for sediment with and without amended Huma-K.

The results showed that uranium sorption for both sediment with and without amended Huma-K reaches equilibrium sorption very fast (less than 15 min) (Figure 2-39). Also, sediments amended with Huma-K significantly enhanced the extent of uranium removal (70%) compared to plain sediments (10%) at pH 4.

In addition, a manuscript titled, “Unrefined humic substances as a potential low-cost remediation method for acidic groundwater contamination” authored by DOE Fellow Hansell Gonzalez-Raymat in collaboration with Vasileios Anagnostopoulos, Miles Denham, Yong Cai, and Yelena Katsenovich was submitted to the Chemosphere journal.

During the month of May, the sorption kinetic experiment of uranium onto SRS sediments at pH 4 was repeated due to the fact that the previous kinetic experiment results showed that the reaction rate was too fast (equilibrium reached in less than 15 min). In order to have a better representation of the sorption kinetics, a lower amount of sediment was used in the experiment (200 mg). For the kinetic experiments, an initial uranium concentration of 0.5 mg L^{-1} was allowed to equilibrate with SRS sediment for different time periods at pH 4 and constant ionic strength (0.01 M $NaClO_4^-$). The samples were vortex mixed, placed on a platform shaker, and centrifuged. The supernatant was analyzed by KPA.

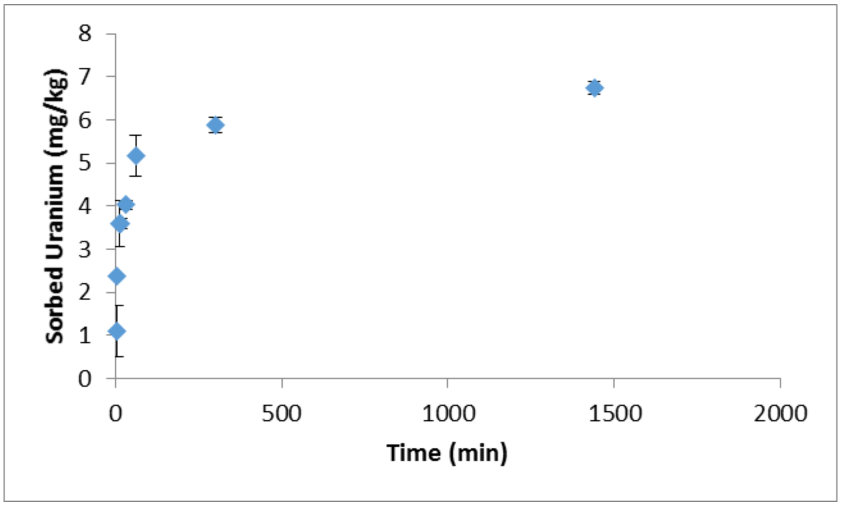

Figure 2-40. Kinetics of uranium sorption onto SRS sediments.

During the month of June, experiments investigating sorption kinetic behavior of uranium onto SRS sediments with Huma-K coating at pH 4 were performed. Initially, 20 mL of Huma-K solution with a fixed concentration (20 mg L^{-1}) at pH 4 was brought in contact with 200 mg of SRS soil for five days. After five days, the samples were centrifuged and the supernatant was replaced by deionized water (ionic strength 0.01M $NaClO_4^-$).) at pH 4. Samples were left to be equilibrated on the platform shaker for three days prior to the addition of uranium (0.5 mg L^{-1}). Samples were then vortex mixed, placed on a platform shaker, and centrifuged. The supernatant was analyzed by KPA. The results are shown in Figure 2-41. In addition, different kinetic models were used (first, second, pseudo-first, and the pseudo-second order), and the model that best described the experimental data in both cases was the pseudo-second order, which suggests that the mechanism of sorption of uranium is a chemisorption.

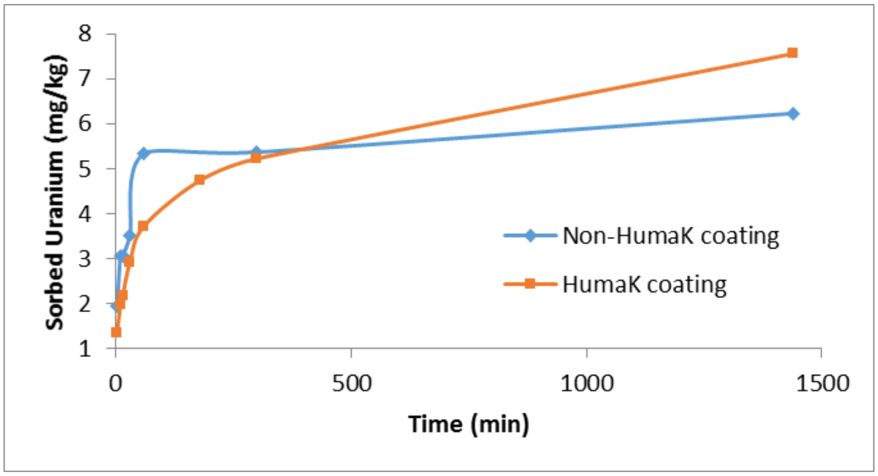

Figure 2-41. Kinetics of uranium sorption onto SRS sediments at pH 4.

The results from Figure 2-41 suggest that the kinetics of sorption of uranium on sediments with non-Huma-K coating is fast reaching almost an equilibrium stage at 1 hour. In the case of sediments with Huma-K coating, it was noted that the kinetics seemed to be slower and not have reached equilibrium after 24 hours. This is attributed to several factors such as affinity of humic molecules for metal ions, its hydrophobicity, and aggregation properties, which can affect transport and adsorption mechanisms of metals. Probably, uranium experiences a slow migration to more deeply hidden binding sites in the solid phase and within adsorbed or aggregated humic molecules in the solid phase, in order to form inner sphere complexes.

Humic Acid Column Experiments

FIU performed a column experiment to study the sorption and desorption of modified humic acid onto SRS sediment and to evaluate the effect of sorbed modified humic acid on uranium mobility. Approximately 260 grams of SRS soil was oven dried at 35°C and used to fill the column. Glass wool was used in the column end adapters to retain the soil inside the column and to avoid flushing of the soil during the injection process. The bottom of the column was sealed with a Teflon adapter and a small amount of soil was carefully added and compacted with the same amount of force. Once the column was filled and compacted, the column was sealed using another adapter and deionized water was injected from the bottom of the column to avoid air bubbles. After the column was saturated, the flowrate of the effluent solution was measured and adjusted to flow at 2 ml//min. A tracer test was performed using 250 ppm of rhenium solution; approximately 0.7325 mg of rhenium was injected into the column and 60 samples were collected at 4 and 7 minute intervals. Samples were analyzed to determine the concentration of rhenium using ICP-OES. The data analysis concluded that 0.75 mg of rhenium was recovered from the column at 102% recovery with an effective flow rate of 1.97 mL/min. The breakthrough curve from the tracer test is shown in Figure 2-42. Optimal recovery of rhenium through the tracer test was met and set parameters such as a residence time of 52.6 minutes, a pore volume of 0.104 L, and a peclet number of 8.32 (Table 2-22).

Table 2-22. Parameters of the Column Obtained during the Tracer Test

Percent Recovery (%)	102.81
Time effective flow rate (mL/min)	1.97
Pore volume (L)	0.104
Residence Time (min)	52.60
Peclet Number	8.32
U (m/s)	6.69E-05
Da (m^2/s)	2.41E-07

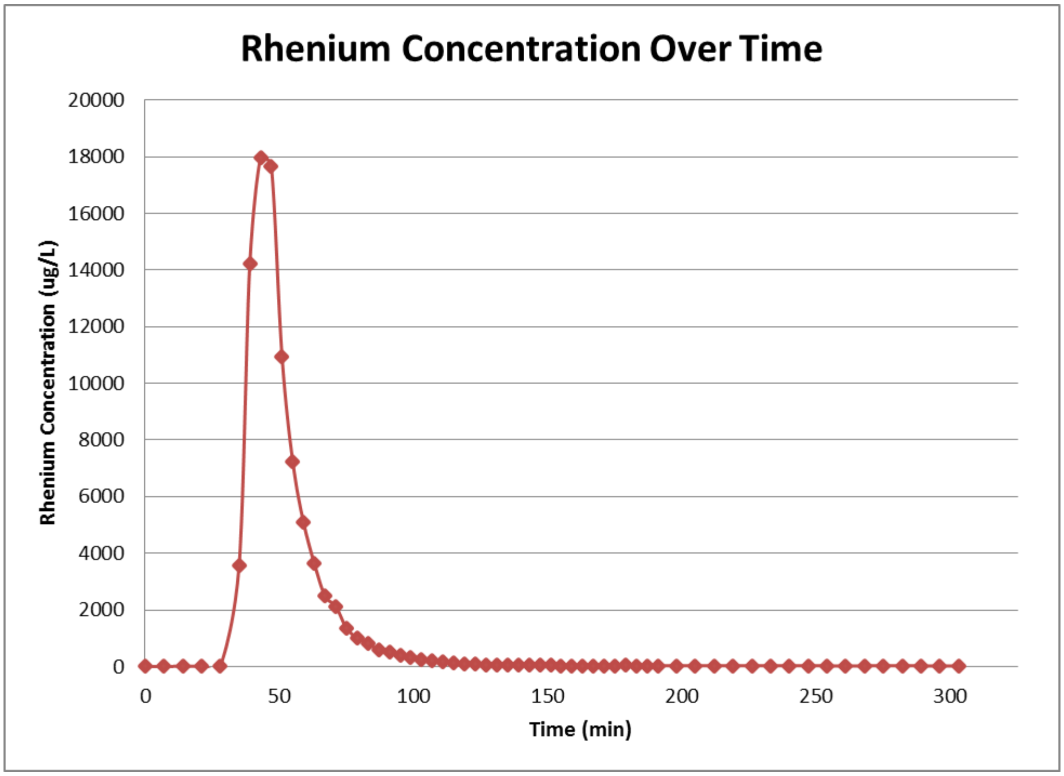

Figure 2-42. Rhenium breakthrough curve during the tracer test.

After performing the tracer test, the column was conditioned with artificial ground water (AGW) adjusted to pH 3.5 to mimic the SRS water conditions. After reaching a steady pH of 3.46, approximately 80 mL of 10,000 ppm modified humic acid was injected into the column followed by AGW at pH 3.5 while collecting samples at 5 minute intervals. pH and humic acid concentrations (via UV-Vis) were immediately measured in the collected samples to estimate humic acid loading. After the concentration of humic acid reached around 2% of the initial concentration, 2 PV of 100 ppb uranium solution was injected into the column followed by 2 PV of AGW at pH 3.5, 4.5, and 5.5. Table 2-23 shows the data for the samples collected during the experiment.

Table 2-23. Modified Humic Acid and Uranium Sorption/Desorption

Injection Scenario	Sample Number	Time (min)	Total Time (min)	Wt of Empty Vial (g)	Wt with Sample (g)	Sample Volume (ml)	Total Volume (ml)	pH	Pore Volume Fraction
Mod-HA Injection	1	5.00	5.00	5.324	15.555	10.231	10.231	3.42	0.10
	2	5.00	10.00	5.425	15.676	10.251	20.482	3.39	0.20
	3	5.00	15.00	5.329	15.567	10.238	30.72	3.4	0.30
	4	5.00	20.00	5.424	15.671	10.247	40.967	3.4	0.40
	5	5.00	25.00	5.425	15.838	10.413	51.38	3.43	0.50
	6	5.00	30.00	5.427	15.966	10.539	61.919	3.42	0.61

	7	5.00	35.00	5.295	15.617	10.322	72.241	3.45	0.71
	8	5.00	40.00	5.386	15.576	10.19	82.431	6.34	0.81
Huma-K desorption	9	5.00	45.00	5.453	15.61	10.157	92.588	6.77	0.91
	10	5.00	50.00	5.309	15.393	10.084	102.672	6.96	1.01
	11	5.00	55.00	5.449	15.548	10.099	112.771	7.15	1.11
	12	5.00	60.00	5.404	15.495	10.091	122.862	7.34	1.20
	13	5.00	65.00	5.319	15.418	10.099	132.961	7.46	1.30
	14	5.00	70.00	5.395	15.52	10.125	143.086	7.62	1.40
	15	5.00	75.00	5.386	15.511	10.125	153.211	7.82	1.50
	16	5.00	80.00	5.414	15.533	10.119	163.33	7.95	1.60
	17	5.00	85.00	5.389	15.563	10.174	173.504	7.74	1.70
	18	5.00	90.00	5.389	15.597	10.208	183.712	7.6	1.80
	19	5.00	95.00	5.386	15.558	10.172	193.884	7.49	1.90
	20	5.00	100.00	5.418	15.576	10.158	204.042	7.36	2.00
	21	5.00	105.00	5.387	15.535	10.148	214.19	7.26	2.10
	22	5.00	110.00	5.407	15.558	10.151	224.341	7.18	2.20
	23	5.00	115.00	5.307	15.446	10.139	234.48	7.14	2.30
	24	5.00	120.00	5.407	15.523	10.116	244.596	7.14	2.40
	25	5.00	125.00	5.407	15.494	10.087	254.683	7	2.50
	26	5.00	130.00	5.407	15.488	10.081	264.764	7.13	2.60
	27	5.00	135.00	5.407	15.48	10.073	274.837	7	2.69
	28	5.00	140.00	5.307	15.428	10.121	284.958	6.99	2.79
	29	5.00	145.00	5.407	15.388	9.981	294.939	6.95	2.89
	30	5.00	150.00	5.307	15.39	10.083	305.022	6.89	2.99
	31	5.00	155.00	5.407	15.471	10.064	315.086	6.85	3.09
	32	5.00	160.00	5.407	15.391	9.984	325.07	6.81	3.19
	33	5.00	165.00	5.307	15.509	10.202	335.272	6.9	3.29
	34	5.00	170.00	5.407	15.478	10.071	345.343	6.73	3.39
	35	5.00	175.00	5.407	15.39	9.983	355.326	6.72	3.48
	36	5.00	180.00	5.407	15.476	10.069	365.395	6.74	3.58
	37	5.00	185.00	5.407	15.46	10.053	375.448	6.7	3.68
	38	5.00	190.00	5.307	15.465	10.158	385.606	6.77	3.78
	39	5.00	195.00	5.307	15.456	10.149	395.755	6.96	3.88
	40	5.00	200.00	5.407	15.511	10.104	405.859	7.05	3.98
	41	5.00	205.00	5.407	15.451	10.044	415.903	7.01	4.08
	42	5.00	210.00	5.407	15.493	10.086	425.989	6.92	4.18
	43	5.00	215.00	5.507	16.299	10.792	436.781	6.61	4.28
Injection of 100 ppb Uranium	44	5.00	220.00	5.307	15.513	10.206	446.987	7.02	4.38
	45	5.00	225.00	5.407	15.446	10.039	457.026	6.94	4.48
	46	5.00	230.00	5.407	15.383	9.976	467.002	6.94	4.58
	47	5.00	235.00	5.307	15.278	9.971	476.973	6.84	4.68

	48	5.00	240.00	5.407	15.374	9.967	486.94	6.81	4.77
	49	5.00	245.00	5.407	15.378	9.971	496.911	6.83	4.87
	50	5.00	250.00	5.407	15.378	9.971	506.882	6.78	4.97
	51	5.00	255.00	5.407	15.3	9.893	516.775	6.73	5.07
	52	5.00	260.00	5.307	15.419	10.112	526.887	6.79	5.17
	53	5.00	265.00	5.407	15.273	9.866	536.753	6.81	5.26
	54	5.00	270.00	5.407	15.353	9.946	546.699	6.78	5.36
	55	5.00	275.00	5.307	15.371	10.064	556.763	6.72	5.46
	56	5.00	280.00	5.407	15.289	9.882	566.645	6.74	5.56
	57	5.00	285.00	5.407	15.344	9.937	576.582	6.73	5.65
	58	5.00	290.00	5.407	15.382	9.975	586.557	6.78	5.75
	59	5.00	295.00	5.407	15.335	9.928	596.485	6.77	5.85
	60	5.00	300.00	5.407	15.39	9.983	606.468	6.79	5.95
	61	5.00	305.00	5.407	15.356	9.949	616.417	6.85	6.04
	62	5.00	310.00	5.407	15.268	9.861	626.278	6.76	6.14
	63	5.00	315.00	5.307	15.448	10.141	636.419	6.73	6.24
Injection of pH 3.5 SRS GW	64	5.00	320.00	5.307	15.46	10.153	646.572	6.92	6.34
	65	5.00	325.00	5.307	15.498	10.191	656.763	6.82	6.44
	66	5.00	330.00	5.407	15.392	9.985	666.748	6.73	6.54
	67	5.00	335.00	5.307	15.465	10.158	676.906	6.73	6.64
	68	5.00	340.00	5.307	15.338	10.031	686.937	6.71	6.73
	69	5.00	345.00	5.307	15.439	10.132	697.069	6.59	6.83
	70	5.00	350.00	5.407	15.417	10.01	707.079	6.64	6.93
	71	5.00	355.00	5.407	15.367	9.96	717.039	6.67	7.03
	72	5.00	360.00	5.407	15.426	10.019	727.058	6.57	7.13
	73	5.00	365.00	5.407	15.437	10.03	737.088	6.53	7.23
	74	5.00	370.00	5.407	15.494	10.087	747.175	6.44	7.33
	75	5.00	375.00	5.507	15.349	9.842	757.017	6.45	7.42
	76	5.00	380.00	5.407	15.487	10.08	767.097	6.78	7.52
	77	5.00	385.00	5.407	15.455	10.048	777.145	6.51	7.62
	78	5.00	390.00	5.307	15.412	10.105	787.25	6.5	7.72
	79	5.00	395.00	5.307	15.473	10.166	797.416	6.48	7.82
	80	5.00	400.00	5.307	15.417	10.11	807.526	6.57	7.92
	81	5.00	405.00	5.307	15.386	10.079	817.605	6.56	8.02
	82	5.00	410.00	5.307	15.349	10.042	827.647	6.52	8.11
	83	5.00	415.00	5.307	15.498	10.191	837.838	6.3	8.21
	84	5.00	420.00	5.407	15.349	9.942	847.78	6.51	8.31
Injection of pH 4.5 SRS GW	85	5.00	425.00	5.307	15.375	10.068	857.848	6.43	8.41
	86	5.00	430.00	5.507	15.472	9.965	867.813	6.46	8.51
	87	5.00	435.00	5.307	15.446	10.139	877.952	6.48	8.61
	88	5.00	440.00	5.407	15.452	10.045	887.997	6.43	8.71

	89	5.00	445.00	5.407	15.422	10.015	898.012	6.44	8.80
	90	5.00	450.00	5.407	15.444	10.037	908.049	5.74	8.90
	91	5.00	455.00	5.407	15.366	9.959	918.008	5.97	9.00
	92	5.00	460.00	5.407	15.429	10.022	928.03	6.41	9.10
	93	5.00	465.00	5.307	15.348	10.041	938.071	6.27	9.20
	94	5.00	470.00	5.407	15.358	9.951	948.022	6.44	9.29
	95	5.00	475.00	5.407	15.461	10.054	958.076	6.65	9.39
	96	5.00	480.00	5.407	15.391	9.984	968.06	5.6	9.49
	97	5.00	485.00	5.407	15.302	9.895	977.955	5.4	9.59
	98	5.00	490.00	5.407	15.314	9.907	987.862	5.34	9.68
	99	5.00	495.00	5.307	15.419	10.112	997.974	5.39	9.78
	100	5.00	500.00	5.407	15.322	9.915	1007.889	5.37	9.88
	101	5.00	505.00	5.407	15.388	9.981	1017.87	5.41	9.98
	102	5.00	510.00	5.407	15.32	9.913	1027.783	5.34	10.08
	103	5.00	515.00	5.407	15.458	10.051	1037.834	5.33	10.17
	104	5.00	520.00	5.307	15.464	10.157	1047.991	5.36	10.27
Injection of pH 5.5 SRS GW	105	5.00	525.00	5.407	15.402	9.995	1057.986	5.25	10.37
	106	5.00	530.00	5.307	15.309	10.002	1067.988	5.26	10.47
	107	5.00	535.00	5.307	15.402	10.095	1078.083	5.24	10.57
	108	5.00	540.00	5.407	15.349	9.942	1088.025	5.21	10.67
	109	5.00	545.00	5.407	15.483	10.076	1098.101	5.26	10.77
	110	5.00	550.00	5.407	15.327	9.92	1108.021	5.25	10.86
	111	5.00	555.00	5.407	15.417	10.01	1118.031	5.18	10.96
	112	5.00	560.00	5.307	15.465	10.158	1128.189	5.21	11.06
	113	5.00	565.00	5.307	15.404	10.097	1138.286	5.32	11.16
	114	5.00	570.00	5.407	15.312	9.905	1148.191	5.44	11.26
	115	5.00	575.00	5.407	15.41	10.003	1158.194	5.4	11.35
	116	5.00	580.00	5.407	15.43	10.023	1168.217	5.4	11.45
	117	5.00	585.00	5.407	15.386	9.979	1178.196	5.54	11.55
	118	5.00	590.00	5.407	15.401	9.994	1188.19	5.6	11.65
	119	5.00	595.00	5.307	15.319	10.012	1198.202	5.65	11.75
	120	5.00	600.00	5.407	15.434	10.027	1208.229	5.53	11.85
	121	5.00	605.00	5.407	15.292	9.885	1218.114	5.44	11.94
	122	5.00	610.00	5.407	15.316	9.909	1228.023	5.42	12.04

FIU completed analysis of samples collected during the column experiment with modified humic acid; a UV-Vis spectrophotometer was used to measure humic acid concentration and total recovery was calculated. Approximately 820 mg of humic acid was injected into the column while 1,233 mg of humic acid was recovered, this could be due to interference caused by something in the sample. Upon reviewing the MSDS, it was noted that there is 0.5-3.0% of crystalline silica in present in modified humic acid. To see if crystalline silica present in the samples interfered with VU-Vis and caused higher absorbance while measuring the samples, resulting in increased humic acid concentrations, 25 ppm of modified HA and Huma-K were prepared and analyzed along with pH adjusted 25 ppm of modified HA (same samples used in the experiment). Figure 2-43 represents the scan of the samples over a wavelength of 190 to 1100 nm while humic acid was measured at 254 nm (blue vertical line). The difference in the absorbance at 254 nm between Huma-K and modified humic acid is negligible, indicating that there is no significant influence of crystalline silica on absorbance.

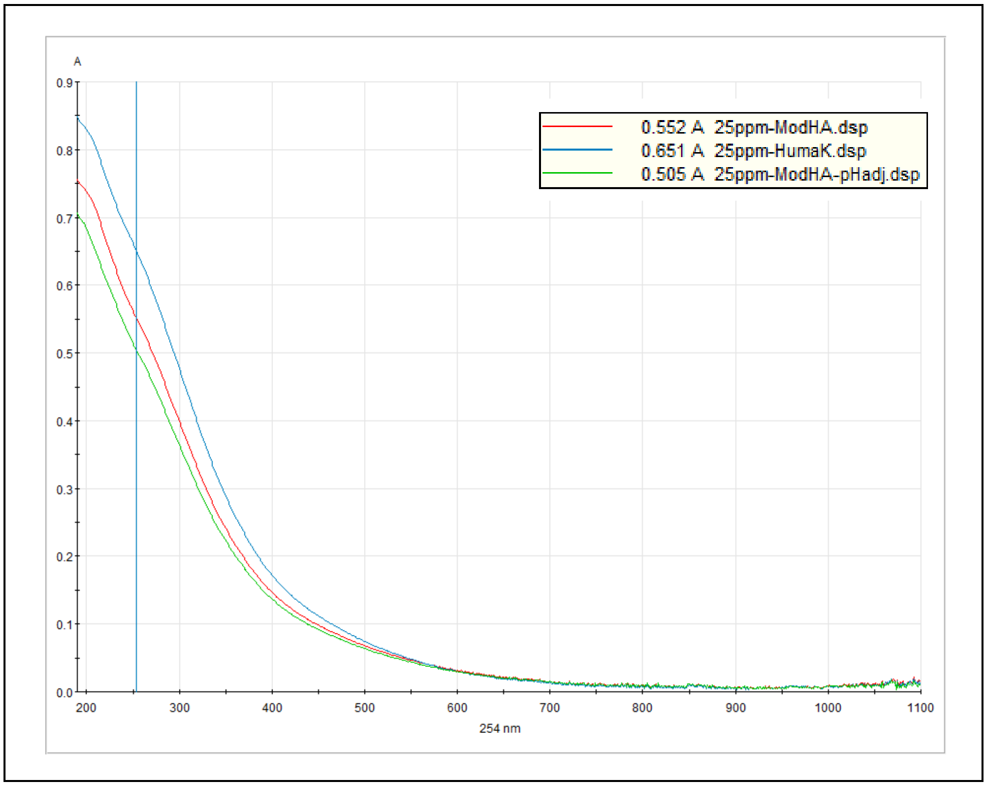

Figure 2-43. Absorbance spectra of Huma-K and modified humic acid material

Some samples collected during the experiment were centrifuged at 2700 rpm for 30 mins at 23°C and analyzed for humic acid concentration to compare results with pre-centrifuged humic acid concentrations (Table 2-24). As shown in Figure 2-44, the concentration of humic acid in the samples decreased significantly following the centrifugation process, which could be due to the removal of precipitates and tiny sediment particles. It is postulated that some sediment particles flushed out of the column and caused interference with analysis via UV-Vis. To avoid this difference, some samples will be analyzed via TOC analyzer to confirm this theory.

Table 2-24. Concentration of Humic Acid in the Samples Before and After Centrifugation

Sample ID	Concentration of modified humic acid (ppm)	
	Pre centrifuged	Post centrifuged
8	4255.96	3709.09
9	7273.20	6368.18
10	8178.27	7407.73
11	8816.36	8109.20
12	9123.86	8352.27
13	9051.70	8635.11
14	9551.36	8795.34
15	8882.39	8410.23
16	6895.57	6081.93
17	7462.61	3678.98
18	6588.07	1843.98
19	5544.20	1177.27
20	3878.18	845.34
21	2871.93	456.07
22	2192.27	316.36

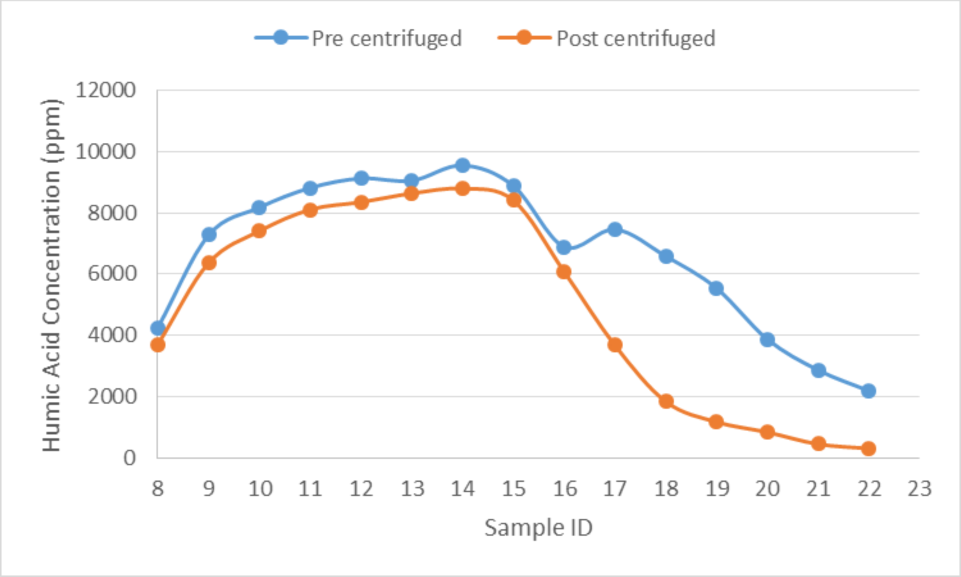

Figure 2-44. Effect of centrifugation on the samples' humic acid content.

Task 3: Surface Water Modeling of Tims Branch

Task 3 Overview

This task will perform modeling of surface water, and solute/sediment transport specifically for mercury and tin in Tims Branch at the Savannah River Site (SRS). This site has been impacted by 60 years of anthropogenic events associated with discharges from process and laboratory facilities. Tims Branch provides a unique opportunity to study complex systems science in a full-scale ecosystem that has experienced controlled step changes in boundary conditions. The task effort includes developing and testing a full ecosystem model for a relatively well defined system in which all of the local mercury inputs were effectively eliminated via two remediation actions (2000 and 2007). Further, discharge of inorganic tin (as small micro-particles and nanoparticles) was initiated in 2007 as a step function with high quality records on the quantity and timing of the release. The principal objectives are to apply geographical information systems and stream/ecosystem modeling tools to the Tims Branch system to examine the response of the system to historical discharges and environmental management remediation actions.

Task 3 Quarterly Progress

Subtask 3.1. Modeling of Surface Water and Sediment Transport in the Tims Branch Ecosystem

The overall objective of this subtask is to develop an integrated surface water, infiltration loss, and contaminant transport model to investigate the fate and transport of contaminants such as mercury and tin in Tims Branch at SRS. The MIKE SHE/MIKE 11 model being developed for Tims Branch can be used as a tool to better understand the effect of extreme weather on flow in Tims Branch. The results of the hydrology model will be used to assess the fate and transport of remedial by-products, such as tin dioxide or other existing solutes (uranium, plutonium), that may have direct or indirect impact on the environment in SRS. The outcome of such a model can determine spatial and temporal distribution of suspended particles or contaminants in the area when storms or heavy rainfalls occur.

During the month of April, focus on this task was primarily on resolving errors occurring during the simulations carried out during the model calibration and sensitivity analyses. Although the source of the initial error was identified and resolved, the simulations were still experiencing constant termination when running for longer time periods. Necessary corrective actions have been taken to resolve these numerical errors.

MIKE SHE Model Calibration and Sensitivity Analysis:

Initial water depth was applied as one of the initial conditions to improve model stability and performance. The results were observed to understand the effect of various water depth conditions on the model results. Introducing the initial condition, however, created some numerical instability. The errors were due to the file format on the edge of the watershed boundary. The issue was resolved by changing the boundary conditions on the edge.

Simulations for long periods of time were performed to establish the initial water depth that can be used in the model. It is suspected that imposing initial water depth may be the source of new numerical errors in long simulations. Corrective actions were taken to resolve the issue.

MIKE 11 model development, calibration and sensitivity analysis for Tims Branch and A-014 is in progress and will be completed by applying ground survey data of Tims Branch cross sections. This data will be available after the field work planned during DOE Fellow Ron Hariprashad's summer internship at SRS. Ron's summer internship scope of work was drafted and submitted in April to Dr. John Seaman at SREL who will serve as Ron's mentor in collaboration with Dr. Brian Looney from SRNL. The document will serve to provide guidance for Ron during his internship at SRS which is focused on sampling and in situ data collection to support the hydrology and transport modeling task.

Several training sessions on water sampling and sediment quantification were implemented to prepare Ron for his internship in the summer. The training mostly focused on sample collection and laboratory preparation methods.

During the month of May, FIU continued working on resolving errors that occurred during the MIKE SHE simulations. Although the initial source of error was identified and removed, the simulations were still experiencing constant termination for longer run times (i.e., 10-yr, 1993-2003, as opposed to 9-mth). Necessary corrective actions were taken to resolve these numerical errors. The 10-yr simulations were performed to establish the initial water depth that can be used in the model. It was suspected that imposing initial water depth was the source of the new numerical errors encountered in the long run time simulations, so corrective actions were taken to resolve the issue.

Snapshots of the MIKE SHE model simulations are depicted in Figures 2-45 to 2-47. These simulation results are inconclusive as the model is still being calibrated. Figure 2-45 illustrates overland flow in the y direction in the downstream portion of Tims Branch near its confluence with Upper Three Runs. The vectors indicate the direction of the flow. The negative sign refers to flow direction downstream. Figure 2-46 shows the preliminary simulated results of discharge in the y direction from 1993 to 2003 in the vicinity of a former USGS monitoring station near the junction of Tims Branch and Upper Three Runs. Although no calibration was performed with these results, they provide basic information on how flow may change during a rainfall event. Figure 2-47 shows the depth of water simulation for a 10-yr period (1993 to 2003) at the former USGS station located downstream of Tims Branch. These results reflect the values that were measured during the fieldwork performed last August along this downstream area of Tims Branch. Substantial calibration is required to fully develop the model and minimize the uncertainty factors associated with numerical simulation.

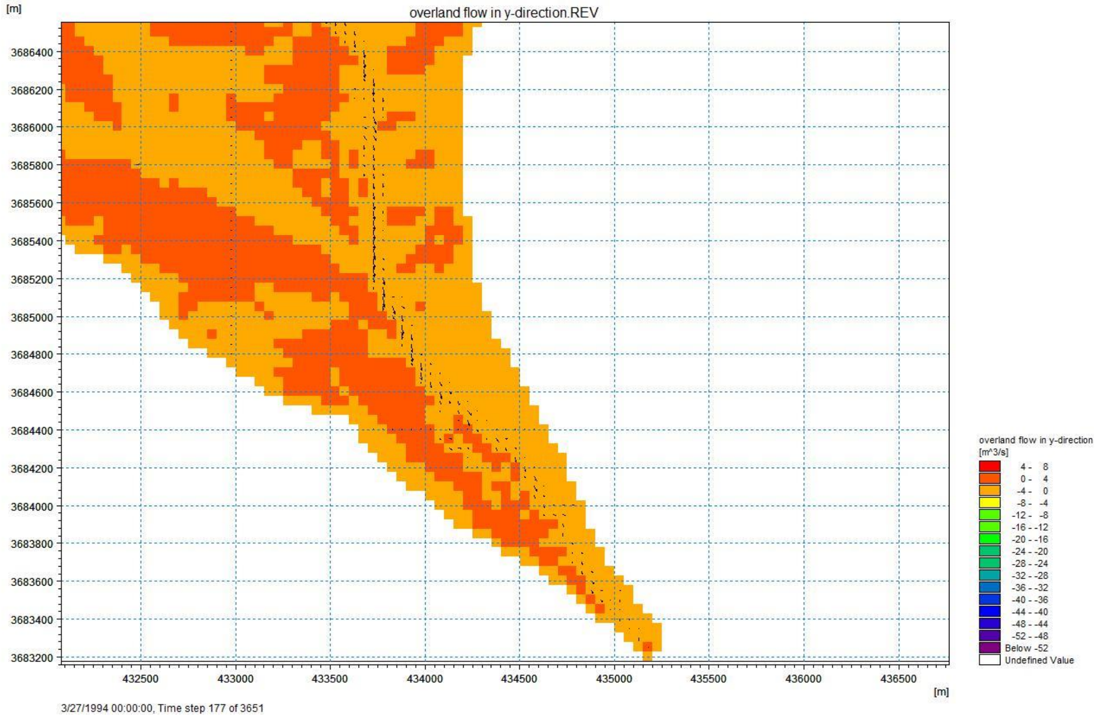

Figure 2-45. MIKE SHE simulated results of overland flow in the y direction in the downstream portion of Tims Branch near its confluence with Upper Three Runs. The vectors indicate the routing direction of the flow from overland into the Tims Branch stream.

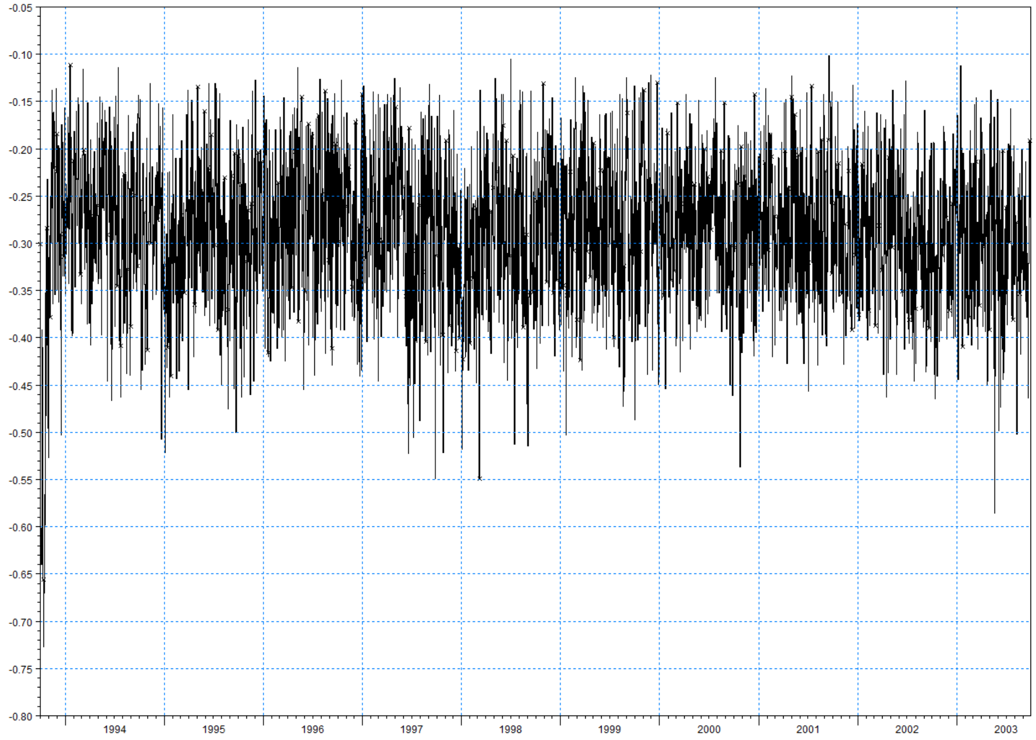

Figure 1-46. Daily value of simulated discharge (m^3/s) in the vicinity of a former USGS station (node 85, 5) for the period 1993 - 2003. The negative sign indicates that the value is downstream.

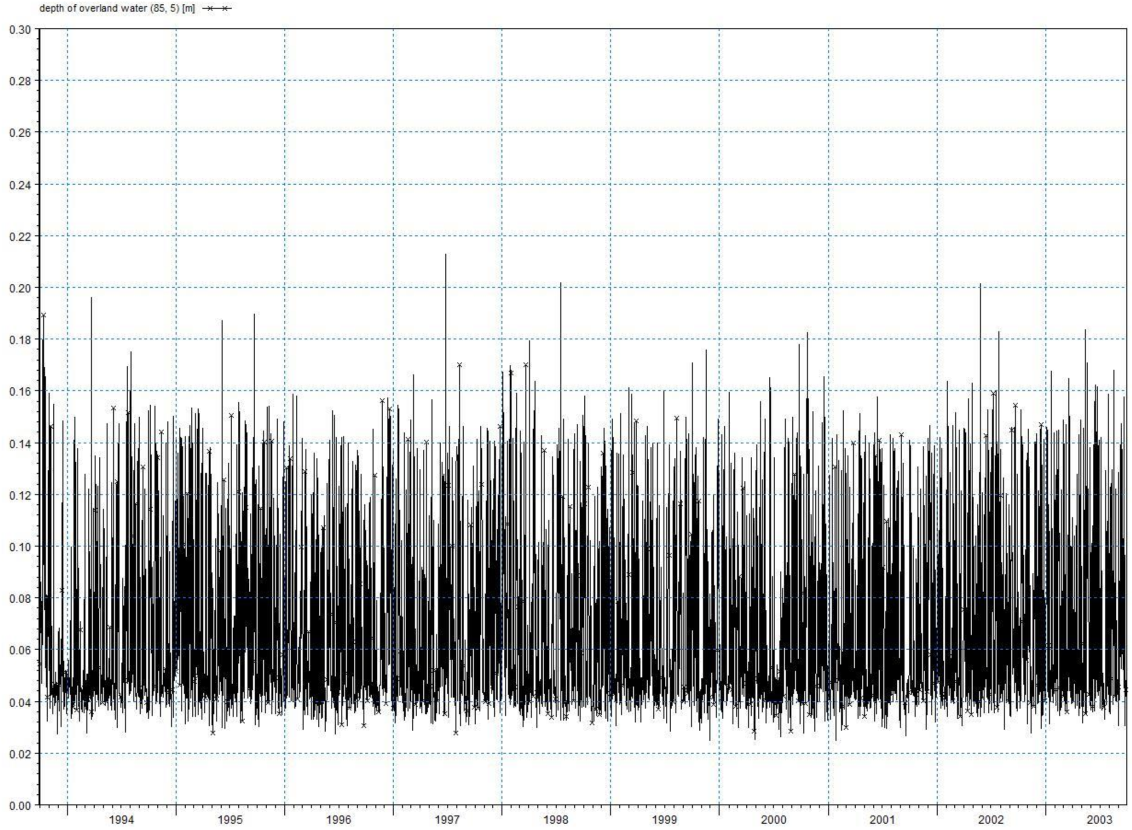

Figure 2-47. Daily value of simulated depth of overland flow in the vicinity of a former USGS station (node 85, 5) for the period 1993 – 2003.

In order to complete the overland flow model of Tims Branch watershed, it is necessary to incorporate the Tims Branch stream into the overland flow model. This part requires coupling of the MIKE 11 stream model of Tims Branch with the MIKE SHE overland flow model as stream flow plays an important role in overland flow simulation in the watershed. Additional cross section measurements along the main Tims Branch stream were collected during a visit by Dr. Mahmoudi to SRS in June 2017. She was assisted by DOE Fellow, Ron Hariprashad, during his 2017 summer internship at SREL which includes collection of in situ field data. This data will be used to develop the MIKE 11 stream flow model for the main Tims Branch stream during FIU Performance Year 8.

Most of the work in the month of June focused on revision of the MIKE 11 stream model of the A-014 outfall tributary, and planning and preparation for the follow-up field trip to SRS which took place from June 12-16, 2017. The MIKE 11 model input data and parameters were reviewed and some minor adjustments and corrections were made. Ground survey data collected in August 2016 has been implemented in the model. The work plan for the next few months will focus on calibrating this model and performing sensitivity analyses.

Subtask 3.2. Application of GIS Technologies for Hydrological Modeling Support

The data collected during FIU ARC's visit to SRS in June 2017 is currently being integrated into the SRS geodatabase. The raw data coordinate data of the sample locations will be imported into

ArcGIS for conversion to a point shapefile, which will then be merged with the other locations formerly sampled in August 2016. The cross section profile measurements will also be imported using ArcGIS and MIKE HYDRO tools for implementation in the MIKE 11 model of the main Tims Branch stream which will be developed during FIU Performance Year 8. The use of GIS tools will remain a continuous integrated component of the hydrological model development. Over the next few months, GIS will be used for cross section delineation and for preparing maps and charts of the study area that depict model results.

Subtask 3.3. Biota, Biofilm, Water and Sediment Sampling in Tims Branch

In April, FIU began discussions with SREL and SRNL scientists to plan for DOE Fellow Ron Hariprashad to participate in a 10-week summer 2017 internship which incorporates some of the sampling and data collection required for this task. A second follow-up field trip to the one conducted in August 2016 was also considered for Dr. Mahmoudi to train Ron and collect water samples and water quality data, as well as measure cross section profiles along the main Tims Branch stream. The plan was to have Ron guided and mentored primarily by Dr. John Seaman from SREL in collaboration with Dr. Brian Looney from SRNL, not only in field sampling and data collection but also laboratory analysis of water (and possibly sediment and biofilm) samples collected in the field. FIU also held discussions with SRNL personnel regarding implementation of monitoring stations in Tims Branch to collect timeseries water quality and flow data at strategic points along the stream; however, this would be subject to available funding through the cooperative agreement.

In May, FIU worked in coordination with SREL and SRNL scientists to finalize the work scope for DOE Fellow Ron Hariprashad's internship, which would focus on field sampling, data collection and laboratory techniques to support the collaborative research being conducted by DOE labs (SREL and SRNL) and FIU's Applied Research Center. The internship would involve collecting in-situ water quality parameters that are important in hydrology and transport modeling development, calibration and application. Several training sessions on water sampling, and sediment quantification were conducted to prepare Ron for this internship. The training mostly focused on sample collection and laboratory preparation methods. Planned tasks included:

1. Cross section profiling along Tims Branch stream
2. Collecting water, sediment and biota samples
3. Field measurement of water quality parameters and flow characteristics
4. Laboratory analysis of water, sediment, and biota
5. Implementing long-term monitoring station/s for flow discharge

Dr. Mahmoudi also confirmed her visit to SRS in June 2017 to collect additional field data along the main Tims Branch stream. She made plans to work with Ron to collect cross section measurements along the main Tims Branch stream as well as flow and water quality parameters in the study area. During FIU's visit to SRS, there were also plans to implement remote monitoring stations in Tims Branch to collect timeseries water quality and flow data at strategic points along the stream, for which FIU purchased a HOBO RX3000 Remote Monitoring System coupled with a KPSI model 720 pressure transducer to collect timeseries water level data.

Dr. Noosha Mahmoudi and FIU student, Ron Hariprashad (DOE fellow), conducted fieldwork in Tims Branch at Savannah River Site with assistance from Dr. John Seaman and his research team at the Savannah River Ecology Lab (SREL) from June 12-16, 2017. As previously mentioned, the aim was to measure cross-section profiles along the main Tims Branch stream, and to collect in situ water quality and flow data to assist in calibration of the hydrological models being developed by ARC. Water and biofilm samples were also collected for chemical analysis of radiological and other contaminants of concern, and to monitor the chemical by-product of a tin-based DOE-EM implemented remediation technology. These samples were cleared by SRS RadCon prior to release for laboratory analysis. FIU ARC, SREL and SRNL have been working collaboratively to fill data and knowledge gaps to support the complementary environmental remediation research projects being conducted by each center. The following photos show Dr. Mahmoudi providing hands-on training to the student intern, Ron, on the collection of water samples and the utilization of various field measurement devices including a YSI multi-parameter probe and a handheld flow tracker to record in situ water quality and flow velocity measurements. The water samples that were collected are currently being processed in the SREL laboratory via ICP-MS/ICP-OES analyses. The biofilm samples will undergo XRF analysis for tin compounds.

Figure 2-48. FIU ARC researcher, Dr. Noosha Mahmoudi, providing hands-on fieldwork training to FIU student Ron Hariprashad (DOE Fellow).

Mr. Hariprashad is also being trained by Dr. John Seaman and his research team on how to set-up, calibrate and deploy a dedicated monitoring station (i.e., ISCO sampler, batteries, solar panel, etc.) in Tims Branch just below Steed Pond to provide estimates of discharge rates that will dictate sampling, and a turbidity sensor to provide estimates of sediment loading. Once the station is operational, stream samples representing base flow and episodic precipitation events will be collected during the summer for extensive characterization. In addition, FIU ARC is planning to establish long-term discharge monitoring stations along Tims Branch and the A-014 outfall tributary. The aim is to install stage gauges at locations where old USGS gauges were formerly stationed and download data periodically with support from SREL personnel during their field research. This requires installing an automated remote monitoring stage gauge (HOBO Onset RX3000 Remote Monitoring System). Installation of these remote monitoring devices is subject to SRS site approval. SREL has submitted the required paperwork for permit approval.

Task 5 Quarterly Progress

During the month of May, a deliverable in the form of a progress report was finalized based on the variable ionic strength batch sorption and column experimental results for the Nd-dolomite system. During the month of June, DOE Fellow Frances Zengotita began her 10-week summer internship at LANL CEMRC. Postdoc Hilary Emerson traveled to LANL CEMRC as well to help initiate her internship experiments. Internship results will be presented in a full report in the fall. The focus of Ms. Zengotita's experiments is to understand the mobility of lanthanides and Cs in the presence of *Chromohalobacter* and dolomite mineral via column and batch kinetics experiments.

Back at FIU, the collection of samples from 0.1 and 5 M ionic strength (IS) columns and sequential batch experiments was continued and 0.5 and 3.0 M IS batch kinetics experiments were completed as described in previous reports. Samples are currently awaiting analysis at LANL-CEMRC for 0.5 and 3.0 M IS batch kinetics, 0.1 and 5 M IS sequential batch, and 0.1 and 5 M IS column effluent sampling. In the coming weeks, solids reacted with Nd in column and sequential batch experiments will be characterized via microscopy (SEM-EDS, TEM, EMPA). Preliminary experiments and speciation modeling were also initiated to prepare for DOE Fellow Frances Zengotita's internship beginning June 3 with results presented below.

Aqueous speciation modeling for Nd, Th, and U in the presence of EDTA

EDTA has previously been identified in the WIPP waste stream and may be the strongest complexant present in the system (Brush, 1990; Dunagan et al., 2007). Therefore, the effects of complexation of actinides and lanthanides by EDTA on sorption to dolomite will be a major focus of DOE Fellow Frances Zengotita's internship. Initial modeling was completed to predict speciation and solubility of actinides and lanthanides in the presence of EDTA in order to design relevant experiments.

Figure 2-49 and Figure 2-50 below depict the total concentration of Nd, Th, and U in the absence and presence of ethylenediaminetetraacetic acid (EDTA), respectively. These predictions were modeled in Geochemist Workbench under the following conditions: 0.003 M $NaHCO_3$, 0.097 M NaCl, pH 6-10, and 5 mg/L EDTA. This model suppressed the formation of ThO_2 but allowed formation of the $Th(OH)_4$ solid species as the hydrolysis species is expected to control solubility based on the timeframe of experiments in this system. It should be noted that solubility of Th and

U are similar in the presence and absence of EDTA, but aqueous Nd is significantly increased above pH 7 in the presence of EDTA.

The speciation of Nd is most impacted by EDTA under the conditions modeled (as compared to Th and U) likely due to its relatively stronger complexation by EDTA. In the presence of EDTA, $Nd(EDTA)^-$ is the major species (>99.9%) across the pH range investigated. The complexation constant is based on previous work (Gritmon et al., 1977). It is consistent with previous values measured for other trivalent actinides and lanthanides including Am, Cm, and Eu (Rizkalla et al., 1989).

The speciation of Th is significantly affected by EDTA below pH 8 where the major aqueous species is ThEDTA. However, above pH 8, EDTA cannot compete with hydrolysis and carbonate complexation. The major species predicted is $Th(OH)_3CO_3^-$ in the model with >99%.These predictions are consistent with previous modeling efforts by Langmuir and Herman based on the complexation constant measured by Bottari and Anderegg (Bottari and Anderegg, 1967; Langmuir and Herman, 1980).

EDTA species compose < 0.1% of the total U above pH 8. The major species at pH 8.5 are $UO_2(CO_3)_3^{-4}$ at ~96% and $UO_2(CO_3)_2^{-2}$ at ~4%. Therefore, EDTA is not expected to play a significant role in sorption and complexation processes of uranium in the WIPP-dolomite system. Previous work confirms the weak complexation with EDTA above neutral pH and shows that ionic strength does not significantly affect complexation up to 5.0 m (Pokrovsky et al., 1998).

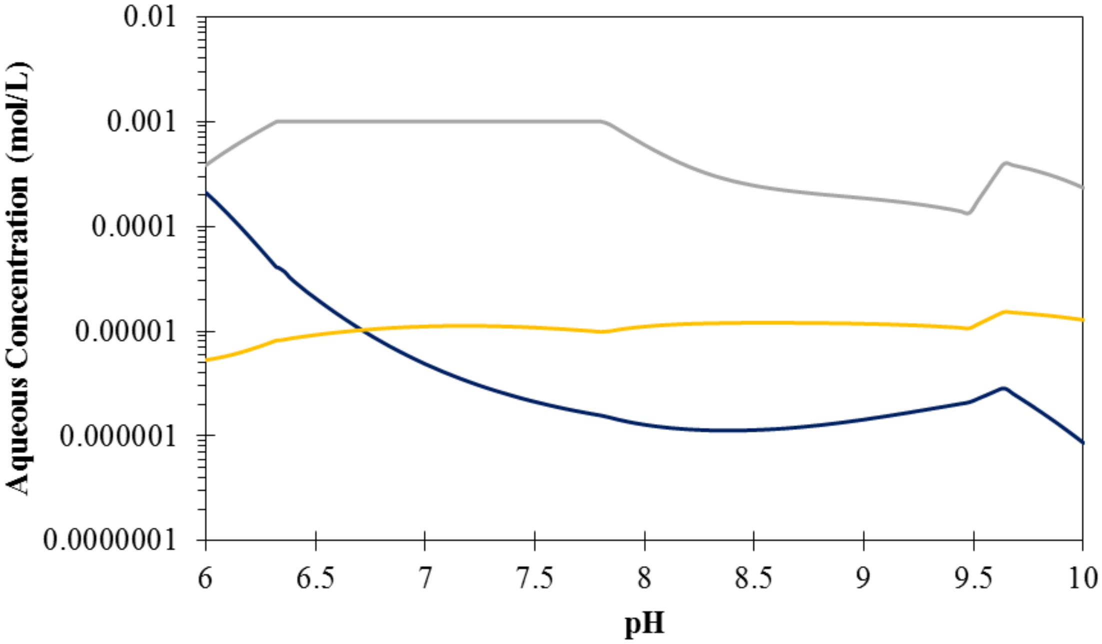

Figure 2-49. Solubility of Nd (blue), Th (yellow) and U (gray) in the presence of 0.003 M $NaHCO_3$ and 0.097 M NaCl at variable pH, Note: formation of ThO_2 is suppressed.

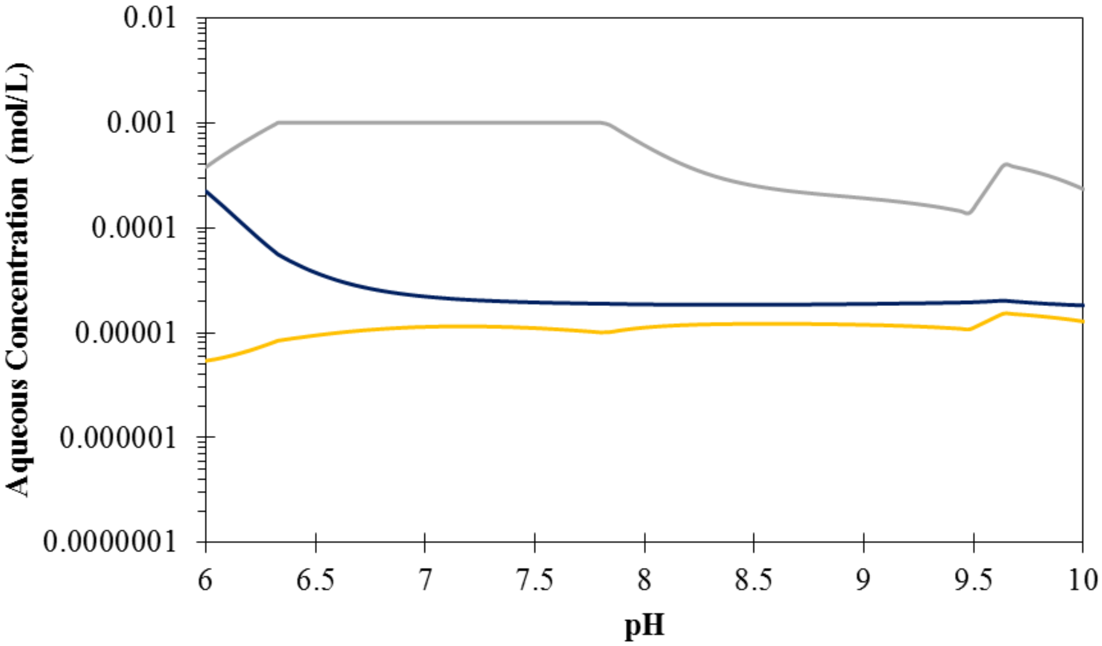

Figure 2-50. Solubility of Nd (blue), Th (yellow) and U (gray) in the presence of 0.003 M $NaHCO_3$, 0.097 M NaCl, and 5 mg/L EDTA at variable pH, Note: formation of ThO_2 is suppressed.

Sorption of Nd, Th, and U to dolomite in the presence of EDTA

Preliminary batch experiments were conducted for 1000 ppb Nd, Th, and U sorption to 5 g/L dolomite in the presence of 5 mg/L EDTA, 0.003 M $NaHCO_3$, and 0.097 M NaCl. Results are presented in Figure 2-51 following 24 hours of equilibration and removal of a 1.3 mL homogenous aliquot for centrifugation to removal particles >100 nm. Nd, Th, U, Ca, and Mg were analyzed via ICP-OES with analytical limits of detection as shown in Table 2-25 below. It should be noted that there is an interference for U in the presence of high levels of Ca.

Measured Nd K_d values are greater than an order of magnitude less than those in the absence of EDTA (724±105 mL/g at pH 8.6). Although previous experiments in the absence of EDTA were at a much lower concentration of Nd (20 ppb), it is expected that there are still ample sites available for sorption on dolomite based on column saturation experiments. These results show that EDTA significantly decreases sorption (increases mobility) of trivalent lanthanides and actinides due to its strong complexation as discussed in the above modeling section.

Due to carbonate complexation, significant sorption of U is not expected in this system. Th will also likely be significantly decreased. Their sorption may also be somewhat decreased due to minor EDTA complexation. U and Th controls without EDTA will be conducted in the near future for comparison.

Table 2-25. Limits of Detection (ppb) for Major Elements Analyzed by ICP-OES

Element	LOD (ppb)
Nd	6.1
Th	7.7
U	6.4
Al	5.9
Fe	9.4
Ca	9.4
Mg	7.0
Si	11.9

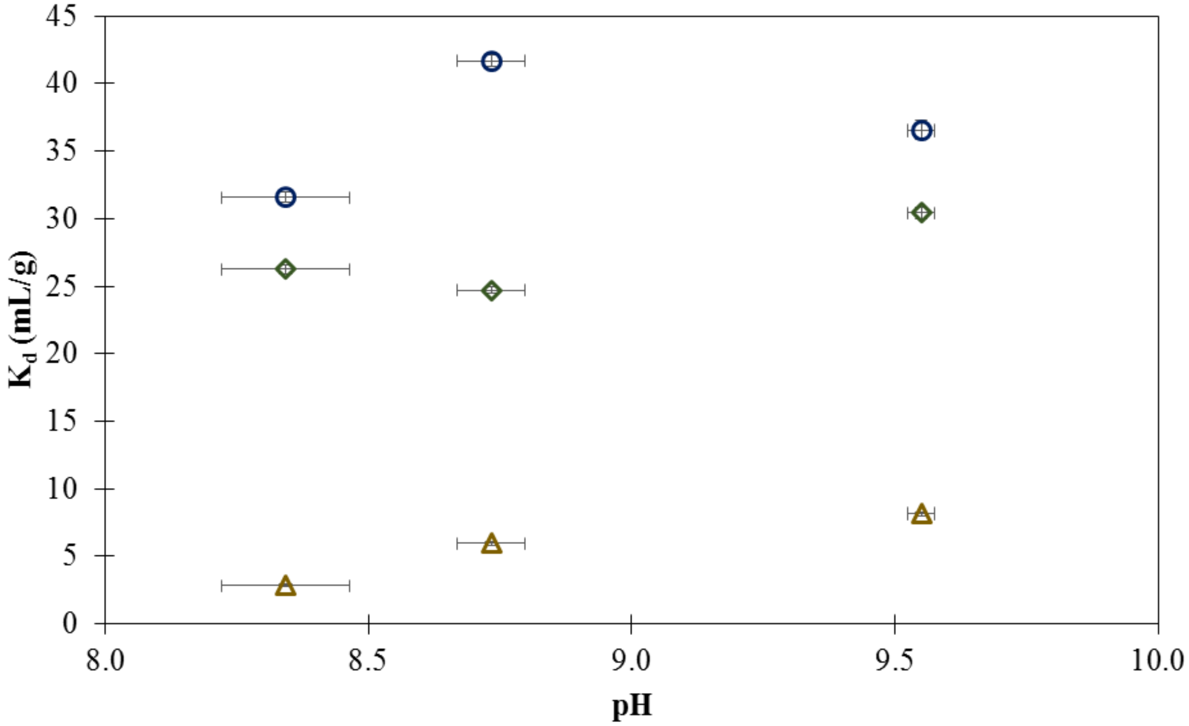

Figure 2-51. Results for sorption of initially 1000 ppb Nd (blue), Th (green), and U (yellow) as a K_d (mL/g) in the presence of 5 g/L dolomite, 5 mg/L EDTA, 0.003 M $NaHCO_3$, and 0.097 M NaCl with error bars based on triplicate samples.

Dissolution of dolomite in the presence of EDTA

A small fraction of dolomite is dissolving in the presence of 0.003 M $NaHCO_3$, 0.097 M NaCl, and 5 mg/L EDTA as shown by Figure 2-52. There is a clear dependence of dissolution on pH with an increase in dissolution as the pH decreases. This trend is consistent with the expected solubility of dolomite. Furthermore, dissolution is congruent as both Ca and Mg are dissolving in similar ratios. Therefore, secondary precipitates are likely not forming in this system.

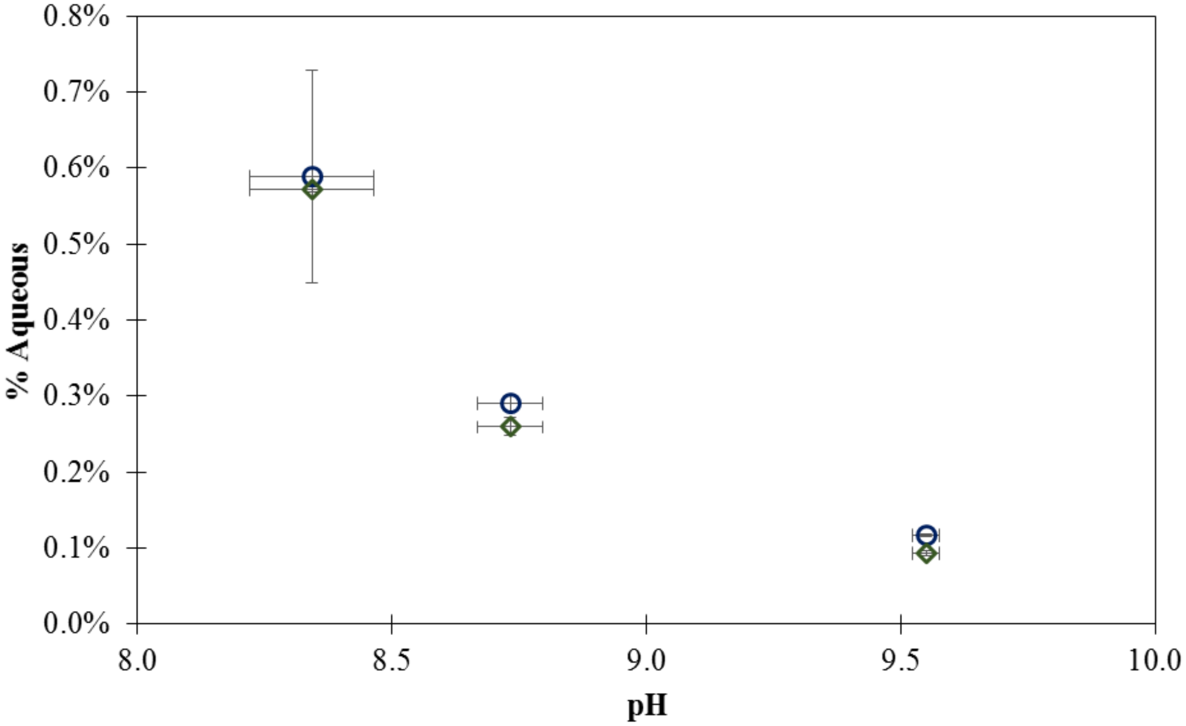

Figure 2-52. Dissolution of dolomite based on ICP-OES measurement of Ca (blue) and Mg (green) in the aqueous phase during batch experiments, error bars are based on measurement of triplicate samples.

<u>References</u>

1. Bottari, E., Anderegg, G., 1967. Complexons. XLII. Investigation of the 1:1 complex of some tri- and tetravalent metal ions with polyaminocarboxylates by means of redox measurements. Eidgenoessisches Technische Hochschule, Zurich.
2. Brush, L., 1990. Test plan for laboratory and modeling studies of repository and radionuclide chemistry for the Waste Isolation Pilot Plant. Sandia National Labs., Albuquerque, NM (USA).
3. Dunagan, S., Roselle, G., Vugrin, E., Long, J., 2007. Analysis Report for the Shielded Container Performance Assessment. Revision 1, Analysis Report, November, p. 2007.
4. Gritmon, T., Goedken, M., Choppin, G., 1977. The complexation of lanthanides by aminocarboxylate ligands—I: Stability constants. Journal of Inorganic and Nuclear Chemistry 39, 2021-2023.
5. Langmuir, D., Herman, J.S., 1980. The mobility of thorium in natural waters at low temperatures. Geochimica et Cosmochimica Acta 44, 1753-1766.
6. Pokrovsky, O.S., Bronikowski, M.G., Moore, R.C., Choppin, G.R., 1998. Interaction of neptunyl (V) and uranyl (VI) with EDTA in NaCl media: Experimental study and Pitzer modeling. Radiochimica Acta 80, 23-30.
7. Rizkalla, E., Sullivan, J., Choppin, G.R., 1989. Calorimetric studies of americium (III) complexation by amino carboxylates. Inorganic chemistry 28, 909-911.

Milestones and Deliverables

The milestones and deliverables for Project 2 for FIU Performance Year 7 are shown on the following table. Milestone 2016-P2-M5, under subtask 1.4, was completed with trial-and-error experiments for separations and determination of Tc(IV) and Tc(VII). Milestone 2016-P2-M4, investigation of acidified sediment and contaminant mobility for SRS, was completed and notification sent via email on May 9, 2017 to all project points of contact. Milestone 2016-P2-M9, complete batch experiments on the biodissolution of Na-autunite (subtask 1.2), was also completed with a notification email being sent out on May 8. In addition, FIU submitted the technical report deliverable on the effect of ionic strength on the sorption of neodymium to dolomite (Task 5) on May 15. Milestone 2016-P2-M7, column experiments using modified humic acid for subtask 2.3, was completed and notification sent via email on June 29, 2017 to all project points of contact.

The following changes have been communicated to both the site collaborators, who have agreed to the revised dates and/or format, and DOE HQ via email as well as during regular project teleconferences. The results for the research under subtask 2.3, originally planned to be included in a technical report (investigation of the removal of uranium by Huma-K sorbed on SRS sediments via batch experiments) will be included in the Year End Report. In addition, FIU is reforecasting, the completion of the coupling of the MIKE SHE and MIKE 11 models (milestone 2016-P2-M10 for subtask 3.1) to the next performance year. In addition, a deliverable on the surface water modeling of Tims Branch (Task 3) has been reforecast from June 15, 2017 to August 17, 2017.

FIU Performance Year 7 Milestones and Deliverables for Project 2

Task	Milestone/ Deliverable	Description	Due Date	Status	OSTI
Project	2016-P2-M1	Submit three draft papers to Waste Management 2017 Symposium	11/4/16	Complete	
Task 1: Hanford Site	2016-P2-M2	Submit abstract to ACS Spring Conference (Subtask 1.1)	11/30/16	Complete	
	2016-P2-M5	Complete training on LSC analytical technique and trial-and-error experiments for separations and determination of Tc(IV) and Tc(VII) (Subtask 1.4)	1/27/17	Complete	
	2016-P2-M9	Complete batch experiments on the biodissolution of Na-autunite (Subtask 1.2)	3/20/17	Complete	
	Deliverable	Technical report on the results of columns monitoring using geochemical and SIP analyses (Subtask 1.3)	1/30/17	Complete	
Task 2: SRS	2016-P2-M4	Complete the creation of acid-impacted soil samples through conditioning of SRS F/H Area soil with acidified water in columns	12/15/16	Complete	

		(Subtask 2.1)			
	Deliverable	Technical report on the Investigation on the Properties of Acid-Contaminated Sediment and its Effect on Contaminant Mobility (Subtask 2.1)	2/13/17	Complete	
	2016-P2-M6	Complete batch experiments of uranium removal by Huma-K sorbed on SRS sediments (Subtask 2.3)	2/15/17	Reforecast to 8/18/17	
	2016-P2-M7	Complete a set of column experiments using modified humic acid (Subtask 2.3)	2/28/17	Complete	
	Deliverable	Technical report on the synergy between colloidal Si and HA on the removal of U(VI) (Subtask 2.2)	3/31/17	Reforecast to be included in Year End Rpt	
	Deliverable	Technical report on the Investigation of the Removal of Uranium by Huma-K Sorbed on SRS Sediments via Batch Experiments (Subtask 2.3)	4/3/17	Reforecast – to be included in Year End Rpt	
Task 3: Tims Branch	2016-P2-M3	Complete development of MIKE 11 stream flow model for A-014 outfall (Subtask 3.1)	12/8/16	Complete	
	2016-P2-M8	Complete calibration of MIKE SHE and MIKE 11 models (Subtask 3.1)	3/1/17	Complete	
	2016-P2-M10	Complete coupling of MIKE SHE and MIKE 11 models (Subtask 3.1)	5/5/17	Reforecast to FIU Performance Year 8	
	Deliverable	Technical report on the surface water modeling of Tims Branch (Task 3)	6/15/17	Reforecast to 8/17/17	
Task 5: WIPP	Deliverable	Technical report on the effect of ionic strength on the sorption of neodymium to dolomite (Task 5)	5/12/17	Complete	

Work Plan for Next Quarter

Project-wide:

- Draft the Year End Report (YER) for FIU Performance Year 7.
- Draft the Project Technical Plan (PTP) for FIU Performance Year 8.

Task 1: Remediation Research and Technical Support for the Hanford Site

Subtask 1.1 – Remediation Research with Ammonia Gas for Uranium

- Conduct final batch experiments with ammonia gas injection into mineral suspensions
- Analyze solids treated with ammonia gas via SEM and prepare in epoxy for EMPA
- Finalize experimental data in the presence of minerals including statistical comparison of results for each treatment
- Develop publication for Ms. Di Pietro's summer 2016 internship investigating mineral dissolution kinetics with basic treatment
- Finalize publication comparing treatment of batch samples with NaOH, NH_4OH and NH_3 gas on mineral dissolution/precipitation and uranium removal
- Continue with flow-through dissolution experiments using mini columns filled with uranium- bearing precipitates and process collected samples
- Repeat experiments at low Si/Al ratios and variable HCO_3^-/Fe to determine the minimum concentration of Si in the system that causes coagulation reactions with U after ammonia gas applications

Subtask 1.2. Investigation on Microbial-Meta-Autunite Interactions - Effect of Bicarbonate and Calcium Ions

- Conduct microscopy analysis via SEM/EDS on prepared post reacted Na-autunite samples
- Culture microbial consortia for vials inoculation
- Continue with biodissolution experiments using bacterial consortia

Subtask 1.3. Investigation of Electrical Geophysical Response to Microbial Activity in the Saturated and Unsaturated Environments

- Complete U(VI) analysis of porewater samples collected during the fall of 2016.
- Prepare samples and conduct SEM/EDS analysis for columns 1 and 2 (Spring samples)
- Prepare samples and conduct SEM/EDS analysis for columns5 and 6
- Conduct speciation modeling to predict the formation of solid phases

Subtask 1.4: Contaminant Fate and Transport under Reducing Conditions

- Conclude experiments for the choice of the reducing agents in the aqueous phase
- Initiate experiments with pure minerals relevant to the Hanford Site in bicarbonate-free conditions and monitor Tc behavior
- Initiate experiments with pure minerals in the presence of bicarbonates

Task 2: Remediation Research and Technical Support for Savannah River Site

Subtask 2.1. FIU's Support for Groundwater Remediation at SRS F/H –Area

- Calculate sorption of acidified soil and plume soil in terms of specific surface area

- Perform speciation calculations for the different pH values studied
- Initiate kinetic experiments with plume soil at circumneutral conditions

Subtask 2.2 – The Synergistic Effect of Humic Acid and Colloidal Silica on the Removal of Uranium (VI)

- Prepare samples for batches 1, 4 and 7 in the pH range of 5-8 containing 30 ppm of uranium similar to previous batch samples
- Analyze batch samples for pH 3-8 via KPA for uranium and process the data and calculate uranium removal

Subtask 2.3. Humic Acid Batch Sorption and Column Experiments with SRS Soil

- Finalize kinetic experiment of uranium sorption on SRS sediment amended with Huma-K (20 ppm)
- Conduct kinetic experiment of uranium sorption on SRS sediment amended with Huma-K (100 ppm)
- Conduct batch experiments of uranium sorption (different concentrations) on SRS sediment with and without amended Huma-K at pH 4
- Complete analysis of samples collected during modified humate experiment
- Perform a column experiment to estimate uranium removal due to sorption onto the soil; this experiment will act as a control column test

Task 3: Surface Water Modeling of Tims Branch

Subtask.3.1. Modeling of surface water and sediment transport in the Tims Branch ecosystem

- Complete and submit the technical report deliverable on the surface water modeling of Tims Branch (Task 3) by August 17, 2017

Subtask 3.2. Application of GIS technologies for hydrological modeling support

- Complete the integration of the sampling location and water quality data collected during FIU ARC's visit to SRS in June 2017 into the existing geodatabase and generate shapefiles that can be used in the MIKE SHE and MIKE 11 models
- Import the cross section profile measurements using ArcGIS and MIKE HYDRO tools for implementation in the MIKE 11 model of the main Tims Branch stream which will be developed during FIU Performance Year 8
- Use GIS for cross section delineation and for preparing maps and charts of the study area that depict model results

Subtask 3.3. Biota, biofilm, water and sediment sampling in Tims Branch

- DOE Fellow Ron Hariprashad will work in collaboration with SREL and SRNL researchers to deploy the ISCO sampler and HOBO remote monitoring units once permit approval has been granted by SRS, after which water quality and flow measurements will be remotely collected

- Continue water and biofilm sampling at marked locations along Tims Branch, particularly after storm events. These samples will be analyzed in SREL labs under the supervision of SREL personnel for major contaminants of concern
- Maintain communication with SREL and SRNL regarding data retrieved by the ISCO and HOBO systems. Periodic support of the DOE labs for collecting water samples for analysis, particularly after storm events, will be based on budget and availability of personnel

Task 5: Remediation Research and Technical Support for WIPP

- Finalize column breakthrough, sequential batch and batch kinetics experiments
- Characterize solid phase of 0.1 and 5.0 M sequential batch and column experiments to observe sorption and incorporation processes in the absence and presence of flow, respectively
- Finalize and submit a publication on sorption and incorporation of Nd at variable ionic strengths
- Conduct mini column experiments investigating transport of Nd complexed with *Chromohalobacter* and other relevant ligands (as part of Zengotita's summer internship)
- Initiate a publication of Frances Zengotita's summer internship results

Project 3
Waste and D&D Engineering & Technology Development

Project Manager: Dr. Leonel E. Lagos

Project Description

This project focuses on delivering solutions under the decontamination and decommissioning (D&D) and waste areas in support of DOE EM. This work is also relevant to D&D activities being carried out at other DOE sites such as Oak Ridge, Savannah River, Hanford, Idaho and Portsmouth. The following tasks are included in FIU Performance Year 7:

Task No	Task
Task 1: Waste Information Management System (WIMS)	
Subtask 1.1	Maintain WIMS – database management, application maintenance, and performance tuning
Subtask 1. 2	Incorporate new data files with existing sites into WIMS
Task 2: D&D Support to DOE EM for Technology Innovation, Development, Evaluation and Deployment	
Subtask 2.1	D&D Technology Demonstration & Development and Technical Support to SRS's 235-F Facility Decommissioning
Subtask 2.2	Technology Demonstration and Evaluation
Subtask 2.3	Support to DOE EM-4.11 and the D&D Community
Task 3: D&D Knowledge Management Information Tool	
Subtask 3.1	Outreach and Training (D&D Community Support)
Subtask 3.2	Mobile Native Applications Development
Subtask 3.3	Data Mining and Visualization
Subtask 3.4	Social Media Integration
Subtask 3.5	IT Administration and Support

Task 1: Waste Information Management System (WIMS)

Task 1 Overview

This task provides direct support to DOE EM for the management, development, and maintenance of a Waste Information Management System (WIMS). WIMS was developed to receive and organize the DOE waste forecast data from across the DOE complex and to automatically generate waste forecast data tables, disposition maps, GIS maps, transportation details, and other custom reports. WIMS is successfully deployed and can be accessed from the web address http://www.emwims.org. The waste forecast information is updated at least annually. WIMS has been designed to be extremely flexible for future additions and is being enhanced on a regular basis.

Task 1 Quarterly Progress

The Waste Information Management System (WIMS) was developed to receive and organize the DOE waste forecast data from across the DOE complex and to automatically generate waste forecast data tables, disposition maps, GIS maps, transportation details, and other custom reports. WIMS is successfully deployed and can be accessed from the web address http://www.emwims.org. During this reporting period, FIU performed database management, application maintenance, and performance tuning to the online WIMS in order to ensure a consistent high level of database and website performance.

FIU received a new set of waste stream forecast and transportation forecast data from DOE on March 18, 2017. The revised waste forecast data was received as formatted data files and, to incorporate these new files, FIU built a data interface to allow the files to be received by the WIMS application and import it into SQL Server. SQL server is the database server where the actual WIMS data is maintained.

FIU completed the data import and deployed onto the test server for DOE testing and review on April 27, 2017 (milestone 2016-P3-M1.1). Figure 3-1 shows screenshots of the new dataset in WIMS. FIU received approval from the DOE data review and deployed the new data on the public server on May 10, 2017. The 2017 waste data replaces the previous waste data from 2016 and is now fully viewable and operational in WIMS.

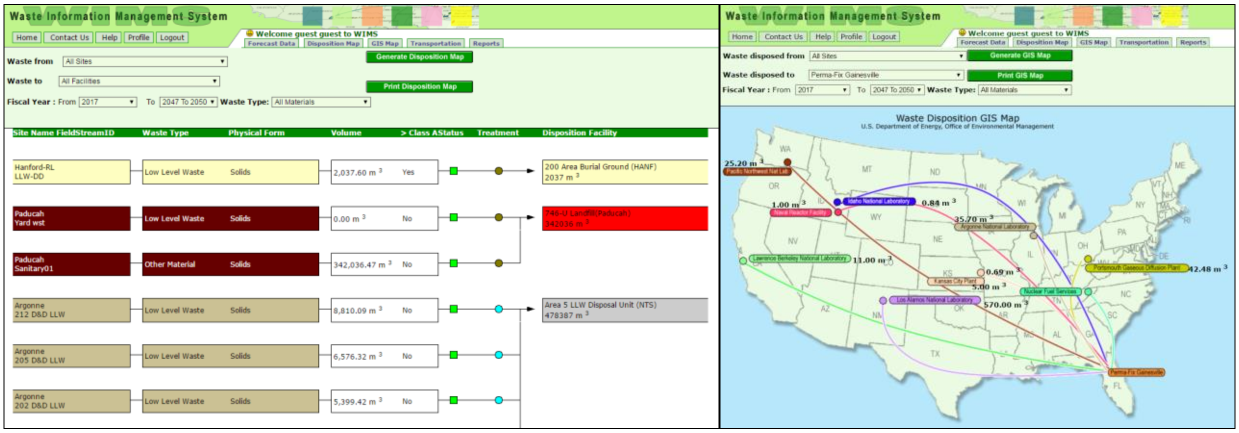

Waste from: All Sites
Waste to: All Facilities
Fiscal Year : From 2017 To 2047 To 2050 Waste Type: All Materials

Site Name FieldStreamID	Waste Type	Physical Form	Volume	> Class AStatus	Treatment	Disposition Facility
Hanford-RL LLW-DD	Low Level Waste	Solids	2,037.60 m 3	Yes		200 Area Burial Ground (HANF) 2037 m 3
Paducah Yard wst	Low Level Waste	Solids	0.00 m 3	No		746-U Landfill(Paducah) 342036 m 3
Paducah Sanitary01	Other Material	Solids	342,036.47 m 3	No		
Argonne 212 D&D LLW	Low Level Waste	Solids	8,810.09 m 3	No		Area 5 LLW Disposal Unit (NTS) 478387 m 3
Argonne 205 D&D LLW	Low Level Waste	Solids	6,576.32 m 3	No		
Argonne 202 D&D LLW	Low Level Waste	Solids	5,399.42 m 3	No		

Waste disposed from: All Sites
Waste disposed to: Perma-Fix Gainesville
Fiscal Year : From 2017 To 2047 To 2050 Waste Type: All Materials

Figure 3-1. WIMS screenshots with 2017 dataset: Disposition Map (left) and GIS Map (right).

Task 2: D&D Support to DOE EM for Technology Innovation, Development, Evaluation and Deployment

Task 2 Overview

This task provides direct support to DOE EM for D&D technology innovation, development, evaluation and deployment. For FIU Performance Year 7, FIU will assist DOE EM-4.11 in meeting the D&D needs and technical challenges around the DOE complex. FIU will expand the research in technology demonstration and evaluation by developing a phased approach for the demonstration, evaluation, and deployment of D&D technologies. One area of focus will be working with the Savannah River Site to identify and demonstrate innovative technologies in support of the SRS 235-F project. FIU will further support the EM's International Program and the EM-4.11 D&D program by participating in D&D workshops, conferences, and serving as subject matter experts.

Task 2 Quarterly Progress

Scientists from SRNL (Dr. Aaron Washington and Dr. Connor Nicholson) and the Project Engineer for the D&D of the hot cells at SRS 235-F (Jack Musall) visited FIU on May 17-19, 2017, to review progress on the efforts to adapt intumescent coatings as incombustible fixatives as well as the other D&D support subtasks. FIU received positive feedback on both the progress to date and the identified way ahead on the incombustible fixatives effort, and there was a clear expression of intent to employ the technology to address the problem set at the site. The themes centering on supporting standards development and DOE-HDBK-3010 updates were prevalent throughout the discussions and viewed as a viable model/approach to successfully transition the technology. The representatives also provided positive comments on the SRS 235-F Hot Cell Test Bed, and provided substantive guidance on how best to complete the final wall as well as objectives to incorporate into the test plan execution.

Subtask 2.1.1: Adaptation of Intumescent Coatings

The objective of this research task is to improve the operational performance of fixatives to mitigate the release of radioisotopes during fire and/or extreme heat conditions. FIU has performed a series of tests to subject test coupons of intumescent coatings (IC) to increasing temperatures using a muffle furnace along with adhesion and impact testing of these test coupons on various types of substrates, both before and after exposure to extreme heat conditions. FIU used the ASTM D3359 standard protocol during the adhesion testing in order to quantify the ability of two selected intumescent coatings (FX and FD) to adhere to stainless steel substrates under various conditions. The results will serve as the basis for future testing efforts designed to determine the impacts of fixatives/intumescent coatings on the airborne release fraction (ARF) and respirable fraction (RF) coefficients in the source term formula used to calculate a facility's safety basis.

FIU is also developing an article based on this research with the collaborators at SRNL for publication in an industry journal.

Subtask 2.1.3: Robotic Technologies for D&D Applications

As part of this subtask during FIU Performance Year 6, FIU performed research to identify robotic technology systems applicable to the challenges and needs of the SRS 235-F Facility. Research utilized the Robotic Database in D&D KM-IT to search and identify potential robotic technologies and compiled a spreadsheet of all of the available robotic technologies in the database. During FIU Performance Year 7, FIU is coordinating with SRNL to leverage the research already completed to assist in identifying cross-cutting applications of robotic technologies being developed at FIU in the high-level waste research area that could potentially be used in support of D&D activities.

During the May visit from the Project Engineer for the SRS 235-F facility as well as our research collaborators from SRNL, FIU conducted a detailed discussion concerning potential cross-cutting applications of ARC's robotic efforts for D&D activities in support of the SRS 235-F hot cell project. No specific requirements / applications were identified from this discussion.

Based on initial observations and finding from Phase II of the Incombustible Fixatives Test Plan, a potential requirement for a remote dry film thickness gauge capability has since been identified. Determining the precise thickness of fixatives applied in restricted spaces and confirming they are within specified parameters throughout the area has proven exceptionally challenging. It is possible that one of ARC's remote / robotic platforms could be modified and paired with a dry film thickness gauge to validate the thickness of the fixative application throughout the radioactive space. Further discussions on this potential requirement and application are being pursued with site stakeholders.

Task 2.2: Technology Demonstration and Evaluation

The primary objective of this task is to standardize and implement proven processes to refine and better synchronize DOE-EM technology needs, requirements, testing, evaluation, and acquisition by implementing a three-phased technology test and evaluation model. The development of uniformly accepted testing protocols and performance metrics is an essential component for testing and evaluating D&D technologies.

Subtask 2.2.1: Uniform Testing Protocols and Performance Metrics for D&D

The development of uniformly accepted testing protocols and performance metrics is an essential component for testing and evaluating D&D technologies. During FIU Performance Year 6, an FIU representative obtained official membership on ASTM International's E10 Committee on Nuclear Technologies and Applications and was selected to lead the ASTM International E10.03 Subcommittee. In this position, FIU oversaw the development of two new draft standard specifications for removable/strippable coatings and permanent coatings/fixatives.

The ASTM International E10.03 Subcommittee on Radiological Protection for Decontamination and Decommissioning for Nuclear Facilities and Components submitted two (2) draft standard specifications related to permanent and removable/strippable coatings and fixatives which were released for a formal Subcommittee ballot on February 23, 2017. The voting period for the E10.03 Subcommittee concluded on March 23, 2017. The 71% return rate surpassed the requirement to have at least 60% of the Subcommittee membership return a ballot. Both standards were unanimously approved by the Subcommittee members, with only minor editorial comments suggested for the revision.

The first full ASTM International E10 Committee balloting for the two (2) standard specifications on fixative technologies ended on May 1, 2017. Joe Sinicrope from FIU ARC attended the ASTM International Conference on June 19-22, and chaired the E10.03 Subcommittee during this same period. All comments received from the full ASTM International E10 Committee in May for the two (2) standard specifications on fixative technologies were successfully adjudicated and incorporated where deemed appropriate. The final revisions were further approved by the ASTM International Staff Manager and Editorial Board, and formal promulgation of the standards is expected during July 2017.

The two standard specifications include: 1) WK57873, Standard Specification for Permanent Coatings Used to Mitigate Spread of Radioactive Contamination; and 2) WK57872, Standard Specification for Strippable & Removable Coatings to Mitigate Spread of Radioactive Contamination. The "Standard Specification for Permanent Coatings Used to Mitigate Spread of Radioactive Contamination" is intended to provide an international basis for identification of non-removable permanent coatings and fixatives as a long term measure used to immobilize radioactive contamination, minimize worker exposure, and to protect uncontaminated areas against the spread of radioactive contamination. The “Standard Specification for Strippable & Removable Coatings to Mitigate Spread of Radioactive Contamination” is intended to provide an international basis for identification of strippable/removable materials used to immobilize radioactive contamination, minimize worker exposure, and facilitate subsequent decontamination or to protect uncontaminated areas against the spread of radioactive contamination.

FIU also drafted and supported subsequent revisions for an article based on this research for DOE to submit for publication to the EM Update newsletter.

Subtask 2.2.2: Technology Demonstration under Nonradioactive Conditions at FIU

Leveraging the research being performed on intumescent coatings as part of subtask 2.1.1 and including close coordination with DOE EM, SRNL, and SRS, FIU is conducting a cold demonstration / test and evaluation of applying intumescent coatings in a full-scale SRS 235-F hot cell mock-up at the FIU Hot Cell Test Bed during FIU Performance Year 7.

The test objectives outlined in the final test plan, *Adapting Intumescent Coatings as Fire Resilient Fixatives in Support of SRS 235-F D&D Activities Phase II: Construction of SRS 235-F Hot Cell Test Bed and Application Demonstration*, were developed through extensive coordination with SRS 235-F site personnel (i.e.; project managers, safety and fire representatives, etc.) and Savannah River National Laboratory (SRNL) research scientists, and are specifically designed to advance the testing, evaluation, and possible deployment of intumescent coating (IC) technologies as fire resilient fixatives to mitigate the potential release of radioisotopes during postulated fire scenarios highlighted in the basis for interim operations (BIO) and contingency planning documents in support of D&D activities at SRS 235-F, with a particular emphasis on the 235-F PuFF Facility Cells 6-9.

This test plan addresses Phase II of the overall research effort, with the first main objective centered on constructing a to-scale SRS 235-F Hot Cell Test Bed on site at ARC that mirrors the operating environment encountered in an adjoining corner and middle hot cell configuration at the SRS 235-F facility. The second main objective involves an evaluation on the mechanics and processes associated with applying the selected intumescent coatings in the hot cell configurations using: 1) the approved tools as identified in the 235-F Risk Reduction Tooling List, Rev 0, dated 26 January 2015; and 2) alternative application methods, such as airless sprayers, recommended by the IC manufacturer.

During this reporting period, FIU supported a visit from Rod Rimando (Director of EM’s Office of Technology Development) Mike Serrato (SRNL), and other representatives from across the DOE complex, who had the opportunity to tour the SRS 235-F Hot Cell Test Bed during the week of May 1, 2017. In addition, scientists from SRNL (Dr. Aaron Washington and Dr. Connor Nicholson) and the Project Engineer for the D&D of the hot cells at SRS 235-F (Jack Musall) visited FIU on May 17-19, 2017. During the SRS/SRNL visit to FIU, the following activities were conducted:

- Overview / presentation on FIU ARC support to DOE EM Cooperative Agreement, with a particular emphasis on D&D support to SRNL/SRS

- Review of incombustible fixatives (adapting intumescent coatings) efforts to date, and detailed discussion on proposed way ahead for FIU Performance Year 8
- Overview of significant D&D problem sets at SRS
- ARC facility tours (e.g., Robotics Lab and Radiation Lab)
- Detailed review and tour of completed SRS 235-F Hot Cell Test Bed
- Intumescent coating demonstrations
- Tour to highlight FIU's radiochemistry efforts

Strategic objectives for this visit included:

- Reinforce the tremendous collaborative relationship between SRNL D&D and ARC D&D research efforts, and emphasize FIU's long-term commitment to addressing problem sets the SRS 235-F project team may encounter during the D&D of the hot cells.
- Highlight the facilities / infrastructure available at ARC that compliments this mission set (e.g.: SRS 235-F Hot Cell Test Bed).
- The current effort demonstrates the potential use of intumescent coatings as a viable fixating material for the residual material at risk in the hot cells; it also helps to demonstrate the long-term, strategic viability of FIU's infrastructure/facilities to support research on a wide array of problem sets being faced in the out years in the EM complex.
- Engage the end-user and provide SRNL and ARC the opportunity to hear firsthand requirements from the SRS 235-F Project Engineer to facilitate his mission.

During April, FIU completed the construction of the middle cell, installed the Plexiglas window, installed glove ports, and installed gloves selected in consultation with SRNL and SRS personnel. The glove ports are 10" in diameter and exactly 15" from the inside floor of the hot cell to the center point of the glove port. The glove ports shown in the figure below are the lower ones, and the higher ones are stacked above it per the dimensions provided by SRS. Phase I of the test plan was completed on May 25, 2017 with the final construction of the SRS 235-F Hot Cell Test Bed.

Figure 3-2. Glove ports and installed gloves on the Hot Cell Test Bed at ARC.

During June, FIU developed an ARC Fact Sheet supporting Phase I of the test plan, highlighting the hot cell test bed's key components. This deliverable was reviewed by the SRNL collaborators and then submitted to DOE on June 28, 2017.

Figure 3-2. Completed construction of Hot Cell Test Bed at ARC.

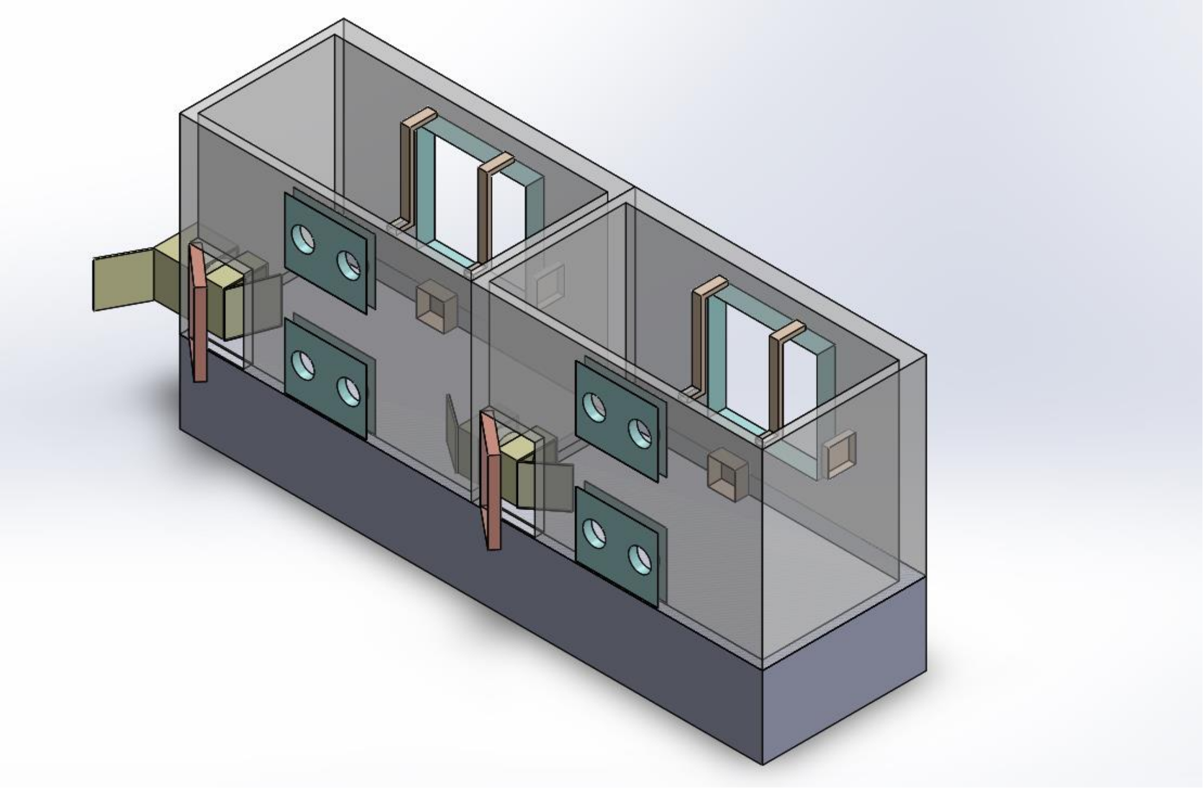

Figure 3-4. As-built design of the middle and corner hot cells with raised floor.

Figure 3-5. Testing ability of reaching all hot cell surfaces from lower glove ports using a manual long-reach tool outfitted with a roller for applying intumescent coatings.

Phase II of the test plan commenced on May 31, 2017 and is currently ongoing. Testing to date has included:

- Application of the intumescent coating using the site approved tools, specifically the extension pole and a roller brush. The previous figure shows photographs taken during the testing of the ability to reaching all hot cell surfaces from the lower glove ports using a manual long-reach tool outfitted with a roller for applying intumescent coatings.
- Monitoring of curing time.
- Observation and recording of ability of all required tools and materials to fit through the bag in/bag out port and pass-through port.
- Evaluation of volume/surface area of intumescent coating required to cover all surfaces to minimum thickness needed.

Subtask 2.2.3 Support to SRNL and SRS 235-F for Onsite Demonstration

FIU is coordinating with SRNL and SRS 235-F to support a possible onsite intumescent coating demonstration on a contaminated apparatus (i.e., hot demonstration). The objective of this subtask is to select and validate operational performance of fire resilient fixative coating material(s) for residual surface contamination after gross decontamination is completed.

Task 3: D&D Knowledge Management Information Tool (KM-IT)

Task 3 Overview

The D&D Knowledge Management Information Tool (KM-IT) is a web-based system developed to maintain and preserve the D&D knowledge base. The system was developed by Florida International University's Applied Research Center (FIU-ARC) with the support of the D&D community, including DOE-EM (EM-4.11 & EM-5.12), the former ALARA centers at Hanford and Savannah River, and with the active collaboration and support of the DOE's Energy Facility Contractors Group (EFCOG). The D&D KM-IT is a D&D community driven system tailored to serve the technical issues faced by the D&D workforce across the DOE Complex. D&D KM-IT can be accessed from web address http://www.dndkm.org.

Task 3 Quarterly Progress

DOE Fellows are supporting D&D KM-IT by reviewing the information in the vendor and technology modules and researching new vendors and technologies for adding to the system. As of July 7, 2017 the system included a total of 954 vendors and 1,337 technologies (including 521 robotic technologies). In addition, there were 982 registered users and 102 subject matter specialists.

FIU completed milestone 2016-P3-M3.3 on April 24 by deploying two pilot videos onto the YouTube platform, including "Robotic Climber H-1 Model" and "Remotely-Operated Advanced Segmentation Process (RASP)." These videos can be viewed by clicking on the "View Video" links next to the video titles with the Document Library module on KM-IT (https://www.dndkm.org/PictureLibrary/SearchVideo.aspx?Query=All). FIU will work with DOE EM, including the IT group, to determine the best path forward to stream all of the videos (legacy and non-legacy) from the YouTube platform. In support of this effort, FIU also compiled an inventory of the legacy videos provided to FIU on VHS format and subsequently digitized by FIU. Video titles, durations, and conversion information was provided to DOE.

D&D knowledge management through contributions in Wikipedia is a part of the outreach and training (D&D community support) subtask. The general D&D knowledge which has been gained through this project offers an opportunity to expand access to a broad audience via Wikipedia, which has a significant presence on the web, thereby offering greater opportunities for collaboration on D&D knowledge. During May, FIU researched and targeted D&D information on Wikipedia where FIU could provide additional relevant information. Four new Wikipedia articles and/or edits to existing articles were developed and submitted to Wikipedia, completing milestone 2016-P3-M3.2.

FIU maintains the KM-IT cyber security infrastructure on an ongoing basis based on the guidelines provided by DOE EM IT and NIST. The KM-IT system and infrastructure undergoes audits by internal and external auditors on a periodic basis. During June, FIU continued to implement solutions to the application, servers, and infrastructure based on two separate security audits performed in May. Once completed, FIU will then prepare report on the status and findings of the audits for DOE.

FIU also continued work on the development of a pilot native application using the D&D Fixatives Module for the Android platform. A native application is an app that is developed for use on a specific platform and which is downloaded onto a mobile device in order to be accessed. As such, the native app does not need an internet connection to be used. A web app, in contrast, is an internet-enabled app that is accessible via the mobile device's web browser; an internet connection is required to use a web app. The mobile apps developed for D&D KM-IT in prior years have all been web apps, requiring the user to access the mobile app module using their mobile device's web browser.

FIU sent the Google Web Analytic report for D&D KM-IT for the fourth quarter of 2016 (October to December) to DOE on April 4, 2017. This report includes information from Google Analytics (GA) and Google Web Master Tools (GWT) and a narrative to explain the results. Highlights from this report include:

- The fourth quarter outperformed the third quarter for the first time since the analytics have been tracked. The metrics with double digit improvements over the previous quarter included Pageviews, Avg. Session Duration, and Pages per Session. Sessions and Users also had significant increases.
- During 2016 Q4, the D&D KM-IT website served 285 unique documents.
- There was a total of 5,677 total combined visits (GA + GWT).
- Combined sessions improved by 18.9% over the same quarter last year.
- Safari took the third spot for the most used browser, passing Firefox for the first time.
- Six out of the top ten documents were Innovative Technology Summary Reports (ITSRs).
- The term "Mobile System" is back on top with the most impressions.
- The top 3 performing modules this quarter were Technology, Vendors and Global Search.
- The Technology module continues to capture the interest of the visitors with over 42% of the visits going to this module.
- There was an increase in direct and referral traffic and a decrease in search traffic.
- A significant increase in visitors from the state of Texas was noted, following the New Mexico surge during the last period.

FIU also completed the development of an annual Google Web Analytic report for D&D KM-IT for calendar year 2016 (January to December) and submitted it to DOE on June 30, 2017. During 2016, D&D KM-IT was visited from 122 countries with the top five being the United States, United Kingdom, India, Canada, and South Korea, with a combined 8,371 visits. The top five states that visited D&D KM-IT were Florida, California, Texas, Massachusetts, and the District of Columbia.

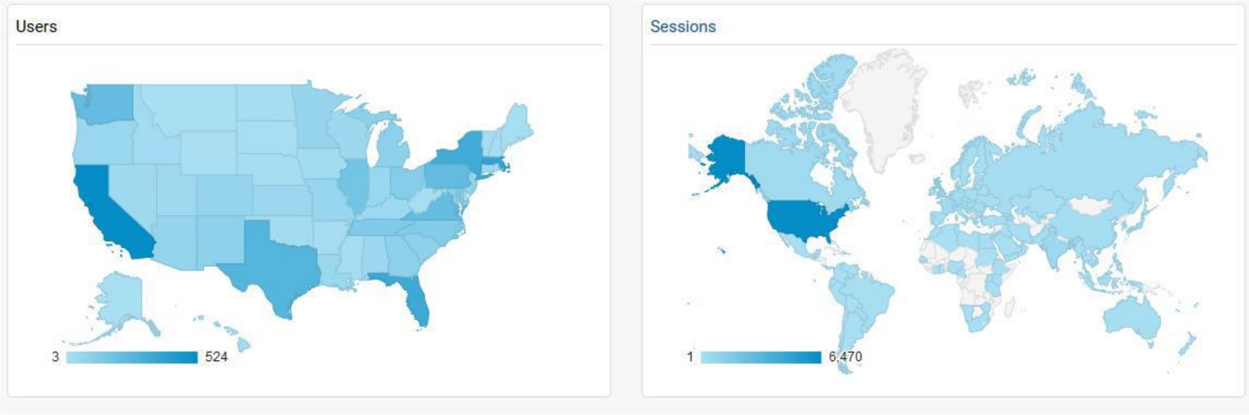

Figure 3-6. Users by state in the U.S. and by country.

Other highlights from the 2016 annual web analytics include:

- The double digit increase in Sessions and Users vs. the double digit decrease in pageviews, pages per session and average session duration show a new flow of traffic that spent less time on the site and which resulted in fewer pages per session and, ultimately, fewer pageviews.
- Half of the top 10 documents from 2016 come from the Innovative Technology Summary Reports (ITSRs) category. The site currently hosts 223 ITSR documents.
- Vendors increased by 40% since 2012 to 948 vendors at the end of 2016.
- Technologies increased by 57.8% since 2012 to 1310 technologies by 2016.
- In 2016, user registration grew by 9.9%. In 2015, the growth in user registrations was 22.84%.
- Subject matter specialist (SMS) membership increased by 8.8% during 2016 (a slowdown from 25.8% in 2015).
- Since 2012, user registration grew by 63.2% and SMS membership increased by 52%.

The data for this report comes from Google Analytics and Google Webmaster Tools (GWT) and makes significant use of graphics, designed to be consumed quickly to gain a high-level understanding of the web activity on the site during 2017. An infographic was developed to provide a visual representation of key information in the report.

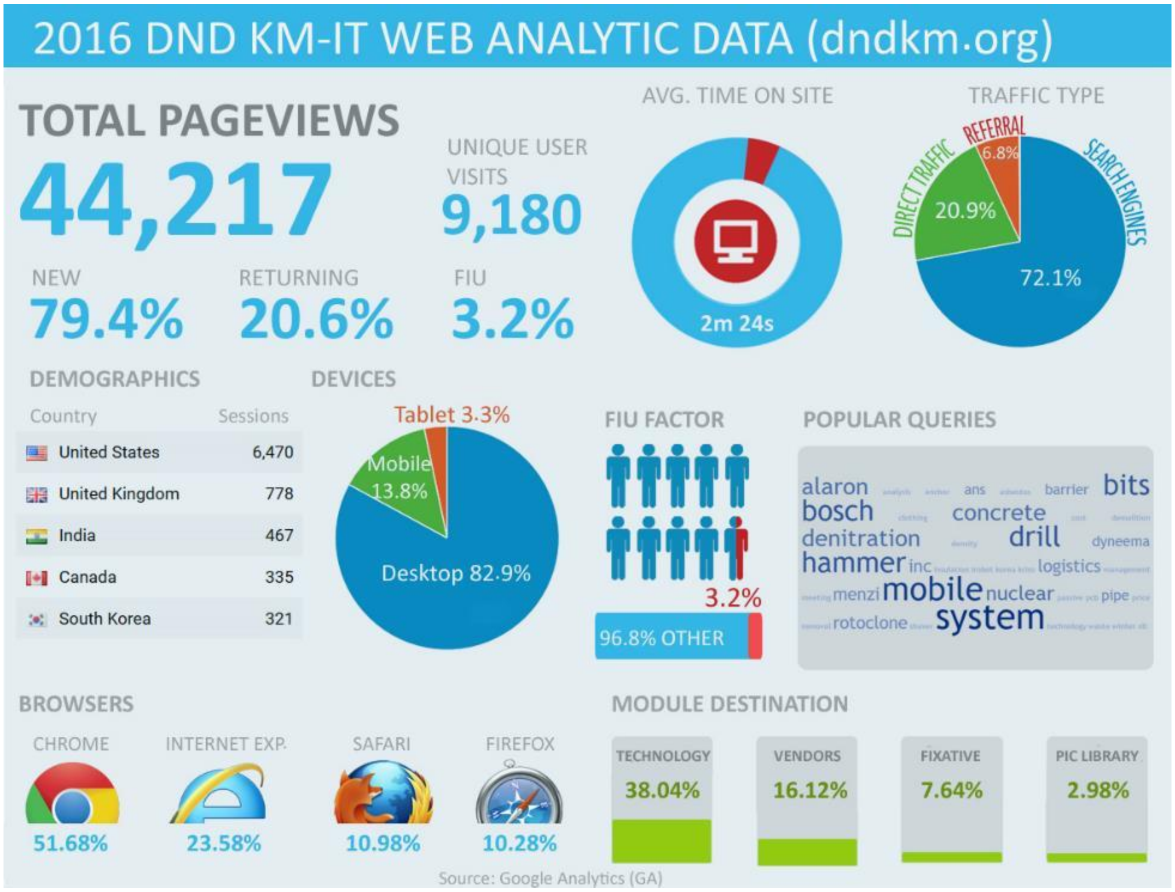

Source: Google Analytics (GA)

Figure 3-7. Web analytics infographic for calendar year 2016.

In addition, FIU completed the development of a Google Web Analytic report for D&D KM-IT for the first quarter of 2017 (January to March) and submitted the report to DOE on June 22. This report includes information from Google Analytics (GA) and Google Web Master Tools (GWT) and a narrative to explain the results. Highlights from this report include:

- The D&D KM-IT analytics opened the first quarter of 2017 with lower than expected engagement when compared to the previous quarter. This is due to the higher number of sessions and user visits but a lower amount of time spent on the site, which resulted in fewer pages per session.
- The metrics with double digit improvements over the previous quarter include Sessions, which increased 26.18%, followed by Users, which increased 33.69%. Metrics with double digit drops were Pages/Session with a 24.08% decrease and Avg. Session Duration with a 35.56% decrease.
- The system served 285 unique documents with a total of 3,041 direct visits (GWT).
- There was a total of 6,825 total combined visits (GA + GWT); that’s an increase of 22.1% over 2016 Q1.
- More than half of the users come from the U.S.
- Combining both the mobile and tablet categories, we see that mobile as a whole makes up 22.3% of the traffic to the system.
- The most dominant OS are Apple’s iOS and Google’s Android, with 49.58% and 47.92% of the entire mobile traffic, respectively.

- Seven from the top 10 documents belong to the Innovative Technology Summary Reports (ITSRs).
- The term “bosh hammer drill bits” resulted in the most impressions.
- New terms top the Impressions and Avg. Position list. Among the top 3 impressions is “Kriso,” which is a vendor from the robotics database.
- The top 3 performing modules this quarter were Technology, Vendors and Picture Library.
- The Technology module continues to capture the interest of the visitors with over 48.62% of the visits going to this module, representing almost half of the entire traffic to D&D KM-IT.
- Returning visitors decreased by 4.8% and visitors from the U.S. increased by 3.2% to 57.5%.
- There was an increase in search engine traffic to 79.4% from new visitors.
- 210 different types of mobile devices visited D&D KM-IT, but the iPhone dominated with 39.26% of the total mobile traffic.
- A significant increase in visitors from the state of Texas was noted, following the New Mexico surge during the last period.
- The system has had a 7.4% growth in users over the same period last year and 2% growth in SMS.

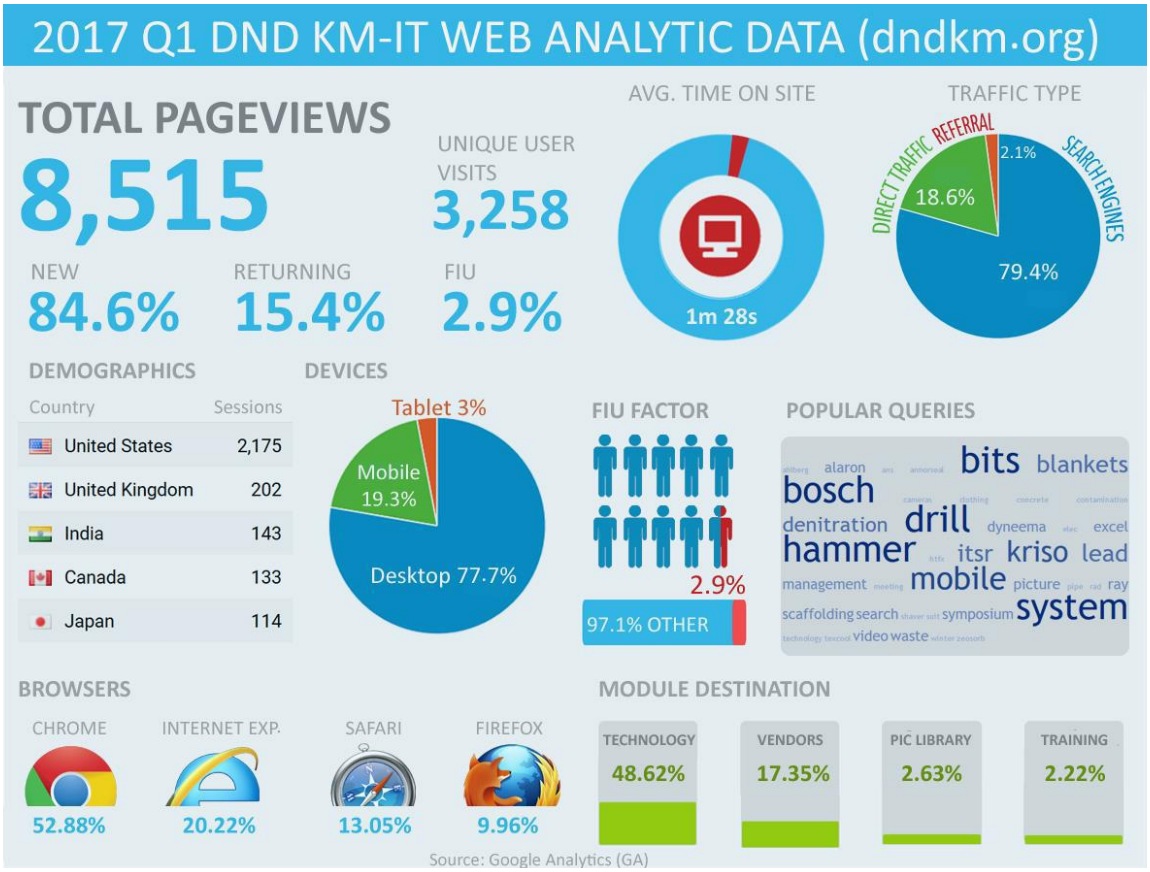

Source: Google Analytics (GA)

Figure 3-8. Infographic for 2017 Q1 Based on Web Analytic Data

Milestones and Deliverables

The milestones and deliverables for Project 3 for FIU Performance Year 7 are shown in the following table. FIU completed milestone 2016-P3-M3.3 by deploying two pilot technology videos from D&D KM-IT onto the YouTube platform on April 24, 2017. FIU also briefed DOE HQ officials visiting FIU during the week of May 1 on the current project accomplishments and planned scope of work for FIU Performance Year 8, which included the recommended D&D technologies to test using the 3-phased model, completing a deliverable under Task 2. FIU completed milestone 2016-P3-M1.1 on April 27, 2017 by importing the WIMS 2017 data set for waste forecast and transportation data; the new data set went live on the WIMS website on May 10, 2017. In addition, the security audit reports for D&D KM-IT were submitted to DOE on May 30, 2017.Milestone 2016-P3-M2.3, participation in the ASTM E10 committee meeting to coordinate developing standardized testing protocols and performance metrics for D&D technologies (subtask 2.2.1), was completed during the ASTM International Conference on June 19-21, 2017. In addition, milestone 2016-P3-M3.2, the integration of D&D knowledge/information into four Wikipedia edits/articles, was completed and a summary report was submitted to DOE on June 28, 2017.

FIU Performance Year 7 Milestones and Deliverables for Project 3

Task	Milestone/ Deliverable	Description	Due Date	Status	OSTI
Task 1: WIMS	2016-P3-M1.1	Import 2017 data set for waste forecast and transportation data	Within 60 days after receipt of data from DOE	Complete	
	2016-P3-M1.2	Draft paper submitted to WM17 conference	11/04/16	Complete	
Task 2: D&D	Deliverable	Draft Test Plan for IC Demo / Test & Evaluation at FIU (subtask 2.2.2)	1/6/17	Complete	OSTI
	2016-P3-M2.1	Participate in ASTM E10 committee meeting to coordinate developing standardized testing protocols and performance metrics for D&D technologies (subtask 2.2.1)	2/28/17	Complete	
	2016-P3-M2.2	Complete demonstration / test and evaluation of IC on FIU hot cell test bed (subtask 2.2.2)	4/28/17 Reforecasted to 7/31/17	Reforecast	
	Deliverable	Decision brief to DOE EM on recommended D&D technologies to test for FIU Performance Year 8 using the 3-phased model	4/28/17**	Complete	
	Deliverable	Draft summary report of robotic technologies for D&D (subtask 2.1.3)	5/31/17 Reforecasted	Reforecast – to be included in YER	OSTI
	Deliverable	Draft progress report on the adaptation of IC to enhance fire resiliency (subtask 2.1.1)	6/30/17 Reforecasted	Reforecast - to be included in technical report for IC test/ evaluation	OSTI
	2016-P3-M2.3	Participate in ASTM E10 committee meeting to	7/31/17	Complete	

		coordinate developing standardized testing protocols and performance metrics for D&D technologies (subtask 2.2.1)			
	Deliverable	Draft progress report on the identification of IC applications to other DOE EM problem sets (subtask 2.1.2)	7/31/17	Reforecast to FIU Performance Year 8	OSTI
	Deliverable	Draft technical reports for demonstrated technologies	30-days after evaluation/ demo	On Target	OSTI
	Deliverable	Draft Tech Fact Sheet for technology evaluations/ demonstrations	30-days after evaluation/ demo	On Target	
Task 3: D&D KM-IT	2016-P3-M3.1	Waste Management Symposium Draft Paper	11/4/16	Complete	
	Deliverable	D&D KM-IT Workshop to DOE EM staff at HQ	2/28/17** Reforecast TBD	Reforecast	
	Deliverable	Preliminary Metrics Progress Report on Outreach and Training Activities	3/10/17	Complete	
	Deliverable	Unclassified summary report on the status and findings of the KM-IT audits	3/24/17 Reforecast 5/31/17	Complete	
	2016-P3-M3.2	Four Wikipedia integration edits/articles	3/31/17 Reforecast to 6/30/17	Complete	
	Deliverable	First D&D KM-IT Workshop to D&D community /DOE Site	3/31/17	Complete	
	Deliverable	First infographic to DOE for review	3/31/17	Complete	
	2016-P3-M3.3	Deploy pilot video onto YouTube platform	4/28/17	Complete	
	2016-P3-M3.4	Deployment of pilot native mobile application for D&D Fixatives Module	5/31/17 Reforecast to 8/4/17	Reforecast	
	Deliverable	Second infographic to DOE for review	7/31/17	On Target	
	Deliverable	Metrics Progress Report on Outreach and Training Activities	8/18/17	On Target	
	Deliverable	Unclassified summary report on the status and findings of the KM-IT audits	8/25/17	On Target	
	Deliverable	Second D&D KM-IT Workshop to D&D community / DOE Site	8/25/17	On Target	
	Deliverable	D&D KM-IT Web Analysis Report	Quarterly	On Target	
	Deliverable	Draft Tech Fact Sheet for new modules or capabilities of D&D KM-IT	30-days after deployment of new module or capability	On Target	

***Completion of this deliverable depends on scheduling and availability of DOE EM staff*

Work Plan for Next Quarter

Project-wide:

- Draft the Year End Report (YER) for FIU Performance Year 7.
- Draft the Project Technical Plan (PTP) for FIU Performance Year 8.

Task 1: Waste Information Management System

- Perform database management, application maintenance, and performance tuning to WIMS.

Task 2: D&D Support

- Complete execution of the test plan for the cold demonstration / test & evaluation of intumescent coatings at FIU and develop technical report.
- Continue leading the working group in for ASTM International's E10 Committee on Nuclear Technologies and Applications and Subcommittee E10.03 - Radiological Protection for Decontamination and Decommissioning of Nuclear Facilities and Components to support the initiative of developing and promulgating uniform testing protocols and performance metrics for D&D technologies across the stakeholder community.

Task 3: D&D Knowledge Management Information Tool

- Complete development of a pilot native mobile application for D&D Fixatives Module.
- Develop quarterly website analytics report and submit to DOE for review.
- Complete metrics progress report on outreach and training activities.
- Perform outreach and training, community support, data mining and content management, and administration and support for the D&D KM-IT system, database, and network.
- Perform outreach and training, community support, data mining and content management, and administration and support for the D&D KM-IT system, database, and network.

Project 4
DOE-FIU Science & Technology Workforce Development Initiative

---

Project Manager: Dr. Leonel E. Lagos

Project Description

The DOE-FIU Science and Technology Workforce Development Initiative has been designed to build upon the existing DOE/FIU relationship by creating a "pipeline" of minority engineers specifically trained and mentored to enter the Department of Energy workforce in technical areas of need. This innovative program was designed to help address DOE's future workforce needs by partnering with academic, government and DOE contractor organizations to mentor future minority scientists and engineers in the research, development, and deployment of new technologies, addressing DOE's environmental cleanup challenges.

Project Overview

The main objective of the program is to provide interested students with a unique opportunity to integrate course work, Department of Energy (DOE) field work, and applied research work at ARC into a well-structured academic program. Students completing this research program would complete the M.S. or Ph.D. degree and immediately be available for transitioning into the DOE EM's workforce via federal programs such as the Pathways Program or by getting directly hired by DOE contractors, other federal agencies, and/or STEM private industry.

Project Quarterly Progress

FIU STEM (science, technology, engineering, and math) students are actively supporting the research efforts under the DOE-FIU Cooperative Agreement during FIU Performance Year 7. The following DOE Fellows are supporting the research under Projects 1-3:

Project 1: Max Edrei (graduate, M.S., mechanical engineering), Sebastian Zanlongo (graduate, Ph.D., computer science), Clarice Davila (undergraduate, mechanical engineering) Michael DiBono (undergraduate, mechanical engineering), Manuel Losada (undergraduate, electrical engineering), Anibal Morales (undergraduate, electrical engineering), and Joseph Coverston (graduate, M.S., mechanical engineering).

Project 2: Alejandro Garcia (graduate, M.S. geoscience), Alejandro Hernandez (undergraduate, chemistry), Alexis Smoot (undergraduate, environmental engineering), Awmna Kalsoom Rana (undergraduate, chemistry), Christine Wipfli (undergraduate, environmental engineering), Hansell Gonzalez (graduate, Ph.D., chemistry), Silvina Di Pietro (graduate, Ph.D., chemistry), Sarah Solomon (undergraduate, environmental engineering), Mohammed Albassam (undergraduate, environmental engineering), Frances Zengotita (undergraduate, chemistry and health), Juan Morales (graduate, M.S., public health), Ripley Raubenolt (undergraduate, environmental engineering), Ron Hariprashad (undergraduate, environmental engineering).

Project 3: Jesse Viera (undergraduate, mechanical engineering), Alexander Piedra (undergraduate, mechanical engineering), and Andres Cremisini (undergraduate, computer science).

Fellows continue their support to the DOE-FIU Cooperative Agreement by actively engaging in EM applied research and supporting ARC staff in the development and completion of the various tasks. The program director continues to work with DOE sites and HQ to fully engage DOE Fellows with research outside ARC where Fellows provide direct support to mentors at DOE sites, DOE-HQ, and DOE contractors. All Fellows also participated in a weekly meeting conducted by the program director, a conference line has been established to enable DOE Fellows conducting internship to join to weekly meeting and update program director on their internship. During each of these meetings, one DOE Fellow presents the work they performed during their summer internship and/or EM research work they are performing at ARC.

ARC researchers and DOE Fellows had the opportunity to participate in the first ever TechNeeds seminar which brought together robotic experts from federal agencies, national research laboratories, industry and academia to address the integration of robotic systems into hazardous work environments and how they can be used to assist and support the workforce to accomplish high priority/high risk tasks. Titled, “Robots, Sensors & Humans – Benefits & Challenges of the Implementation of Robotic Systems in Hazardous Environments,” the seminar was held at the Modesto A. Maidique campus of Florida International University (FIU) in Miami, FL, on May 3 and 4, 2017.

During the seminar, representatives from a variety of agencies discussed important key issues related to robotics and how they can be used to support their respective missions. Integration of robotic systems into hazardous work environments and how they can be used to assist and support the workforce to accomplish tasks are among a number of topics presented. Specific problems/needs were identified and the associated challenges and constraints with developing and integrating the systems were discussed. Rod Rimando, director of EM's Office of Technology Development, opened the event with a discussion of robotics needs and opportunities within EM.

On the afternoon of the first day, seminar participants had the opportunity to tour the FIU Applied Research Center facilities and view live technology demonstrations of commercially available robotics and robotic technologies under development. DOE Fellows attributed to the success of the event by participating as student assistants throughout the seminar.

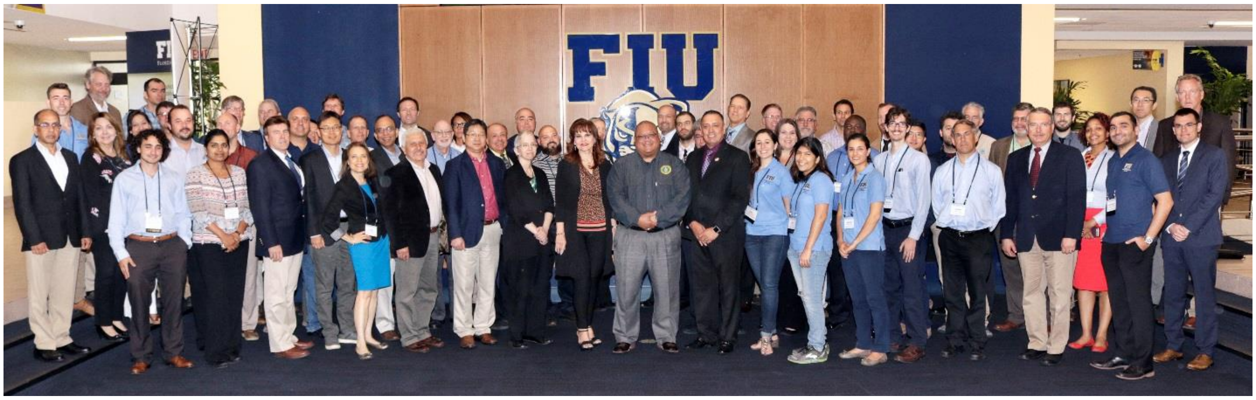

Figure 4-1. Robotics seminar participants.

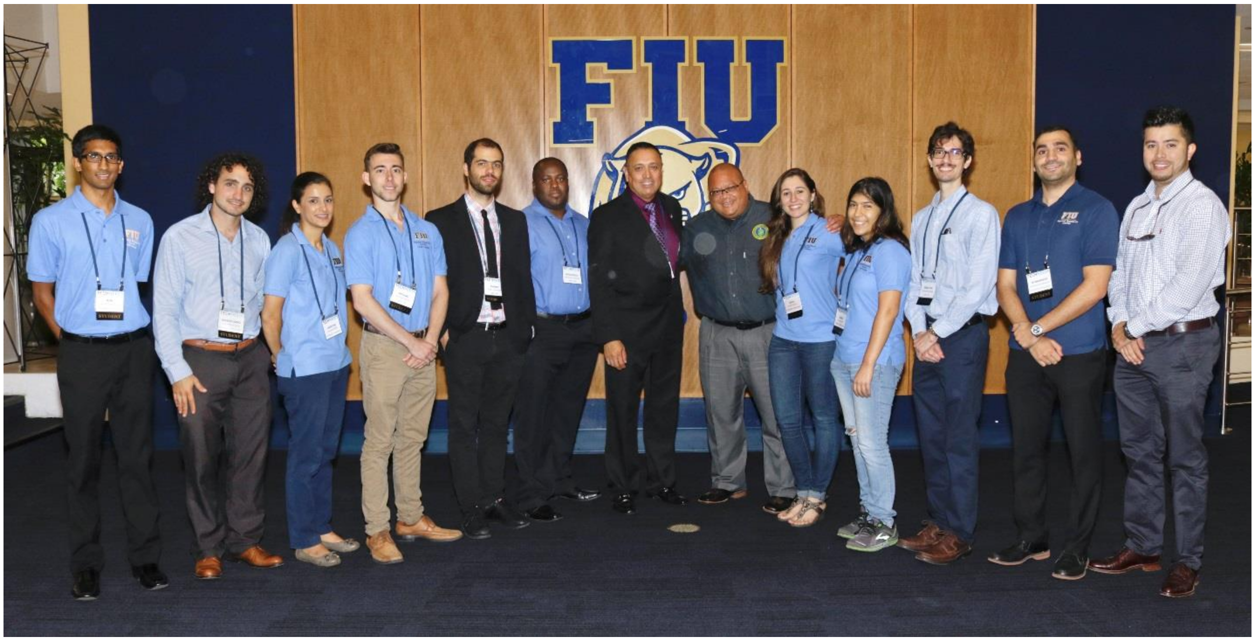

Figure 4-2. Leo Lagos (Director of Research, FIU ARC) and FIU's DOE Fellows with Rod Rimando (DOE EM).

DOE Fellows spring recruitment efforts were initiated on March 29 and ran through April 14. Recruitment campaigns were conducted by placing recruitment tables at the College of Engineering and at the main FIU campus in the physics & chemistry and computer science buildings. A signup sheet was used to collect contact information from interested students and emails were sent out with information on requirements and components of the program along with application instructions and a checklist. The deadline for FIU students to submit applications for DOE Fellowship was April 14, 2017, and a total of 18 applications were received. The DOE Fellows selection committee, comprised of ARC researchers and staff, reviewed the applications and recommended ten (10) FIU students for formal interviews which were conducted from May 9 through May 10, 2017. Dr. Leonel Lagos (Program Director) subsequently asked for the committees input and recommendations to make the final selections and complete the recruitment process. Three (3) students were selected to join the program as DOE Fellows Class of 2017 and assigned an ARC mentor based on their field of study:

Table 4-1. New DOE Fellows and ARC Mentors

First Name	Last name	Major	Degree	ARC Mentor
Anibal	Morales	Electrical Engineering	BS	Mr. Anthony Abrahao
Joseph	Coverston	Mechanical Engineering	MS	Dr. Reza Abassi Baharanchi
Manuel	Losada	Electrical Engineering	BS	Dr. Aparna Aravelli

Dr. Leo Lagos and Dr. Ravi Gudavalli conducted orientation sessions for Joseph Coverston on June 23, 2016, and discussed the expectations of the program, including program components such as hands-on research on DOE related challenges, summer internships, and potential future employment with DOE EM, national laboratories and DOE contractors. Joseph also completed the required environmental health and safety trainings prior to engaging in laboratory work.

DOE Fellows Anibal Morales and Manuel Losada will receive orientation and training when they begin working at ARC this fall.

Four DOE Fellows graduated from FIU and participated in FIU's spring 2017 graduation ceremonies held from April 29 to May 3.

- Alexandro Hernandez - B.S., Chemistry
- John Conley - B.S., Mechanical Eng
- Sarah Bird - B.S., Environmental Eng
- Christopher Strand - B.S., Environmental Eng

The DOE Fellows program director completed coordination for placement of DOE Fellows for summer internships. This summer, twelve (12) DOE Fellows are participating in 10-week internships across the DOE Complex and at two universities. The DOE Fellows are engaging in research projects at DOE Headquarters in Maryland, DOE national laboratories (Savannah River Nat. Lab and Sandia Nat. Lab), Savannah River Ecology Lab, the Waste Isolation Pilot Plant, University of Texas-Austin Nuclear and Applied Robotics Group, and San Jose State University. Table 4-2 shows the internships for summer 2017.

Figure 4-3. Summer 2017 Interns (DOE Fellows) with Program Director Dr. Leo Lagos.

Table 4-2. Summer 2017 Internships

Site	Mentor(s)	DOE Fellow(s)
DOE-HQ	Skip Chamberlain Kurt Gerdes	Juan Morales Mohammed Albassam
DOE HQ	Robert Seifert	Christine Wipfli
Sandia National Lab	Jake Deuel Phil Heermann	Sebastian Zanlongo
Sandia National Lab	Kristopher Klingler	Andres Cremisini
SRNL	Dan Kaplan	Sarah Solomon Ripley Raubenolt
SRNL	Aaron Washington Connor Nicholson	Alexander Piedra
SRNL/SREL	John Seaman (SREL) Brian Looney (SRNL)	Ron Hariprashad
University of Texas-Austin	Mitch Pryor	Michael Di Bono
WIPP	Don Reed Tim Dittrich	Frances Zengotita
San Jose State University	David Robertson Annalise Van Wyngarden	Alejandro Hernandez*

*This internship is separate from and not funded by the DOE-FIU Cooperative Agreement.

Highlights from the internship assignments are included below.

DOE FELLOWS: Mohammed Albassam and Juan Morales
LOCATION: DOE EM Headquarters, Maryland
MENTORS: Skip Chamberlain and Kurt Gerdes

Mr. Mohammed Albassam and Mr. Juan Morales (DOE Fellow Class of 2016) are conducting their summer internship at DOE- EM Headquarters in Maryland. Since their arrival, they have been assigned to conduct research involving surface/groundwater interface mechanisms, radionuclide contaminant plume migration applications, and an ecological risk assessment for the F-Area Seepage Basins located at the Savannah River Site. Their efforts are mentored by Mr. Skip Chamberlain, (Physical Scientist, EM-4.12) at the Office of Environmental Management. Their research will support former investigations contributing to the ecological effects of the SRS F-Area.

Figure 4-4. Mohammed Albassam, Kurt Gerdes, & Juan Morales (left) and Juan Morales, Skip Chamberlain, Mohammed Albassam (right).

Figure 4-5. DOE Fellow Juan Morales enjoying after hours recreational activities while on internship.

DOE FELLOWS: Ripley Raubenolt and Sarah Solomon
LOCATION: Savannah River National Laboratory
MENTORS: Dr. Paller, Dr. Looney, and Dr. Jackson

Ms. Ripley Raubenolt and Ms. Sarah Solomon (DOE Fellow Class of 2016) are conducting their summer internship at the Savannah River National Laboratory. Ripley and Sarah are investigating the ability of different types of diffusive gradients in thin film (DGT) probes to measure organic mercury in water, conduct mercury analyses on a mercury analyzer, perform computations, and write a project report. Development of a suitable method will facilitate risk reduction in contaminated soil, water, groundwater and sediment and help to improve and modernize environmental monitoring within the DOE complex.

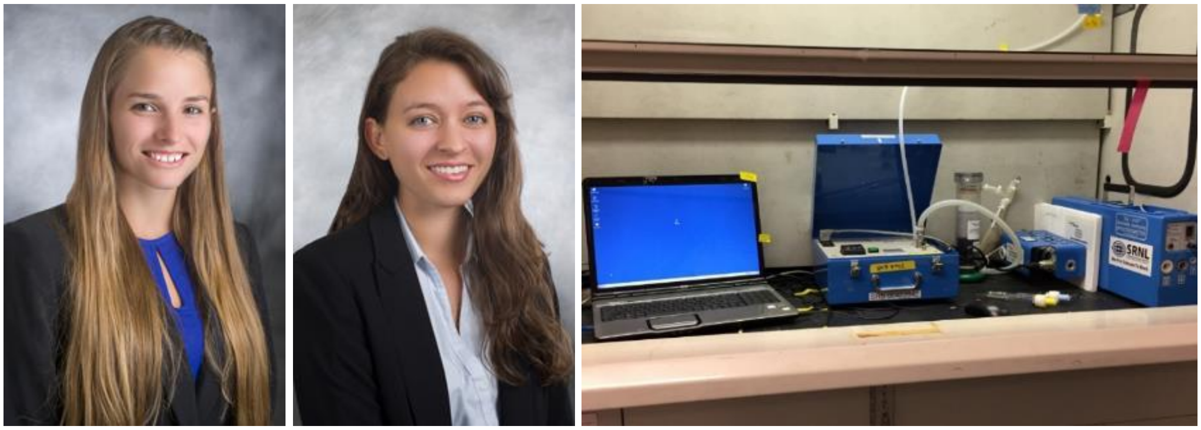

Figure 4-6. DOE Fellows Ripley Raubenolt, Sarah Solomon, and SRNL equipment for analysis.

Two DOE Fellows, including Sarah Solomon and Ron Hariprashad, were in the team of FIU STEM students who were awarded 2nd Place in the 2016-2017 Environmental Engineering and Science Foundation (EESF)/Association of Environmental Engineering and Science Professors (AEESP) Student Video Competition for their video production entitled "Take Action on Climate Change." This video is intended to motivate and teach young adults how they can impact climate change through their own day to day activities. The team traveled to Washington, DC to receive their award on April 13, 2017 at the 2017 Excellence in Environmental Engineering and Science Awards Luncheon and Conference. The video can be viewed on YouTube via the following link: [*https://www.youtube.com/watch?v=dOyhrCQKobc*](https://www.youtube.com/watch?v=dOyhrCQKobc)

Figure 4-7. AAEES National President Robert Williams awards FIU Students.

DOE Fellows have been participating in numerous opportunities for sharing the research that they have performed in support of DOE EM at FIU-ARC and during their past summer internships at DOE sites, DOE Headquarters, and national research laboratories. A brief description of the recent presentations that were given by the DOE Fellows follows.

- Silvina Di Pietro presented the effects of ammonia and variable redox conditions on mineral dissolution to the 253rd American Chemical Society National Meeting & Exposition in San Francisco, CA, on April 2-6, 2017. Silvina is studying the use of an innovative remediation technique that would inject ammonia gas into the subsurface at the Hanford Site to decrease the movement of uranium contamination below ground. The results can help to predict the long-term effectiveness of the remediation technique.

Figure 4-8. DOE Fellow Silvina Di Pietro presenting at 253rd American Chemical Society National Meeting & Exposition in San Francisco, CA

- Frances Zengotita presented the role of ionic strength on the sorption of neodymium on dolomite at the 5th Annual Life Sciences South Florida Undergraduate Research Symposium at Palm Beach State College, FL on April 1, 2017. This research will lead to a better understanding of the long-term behavior of contaminants in the subsurface at the Waste Isolation Pilot Plant (WIPP) and will be used to update the long-term risk assessment models for the site.

- Alexander Piedra presented the baseline adhesion testing of intumescent coatings at the 5th Annual Life Sciences South Florida Undergraduate Research Symposium at Palm Beach State College, FL on April 1, 2017. Alexander is researching the effectiveness of commercially available intumescent coatings to enhance the fire resiliency of fixatives and facilities in support of D&D projects facing potential fire and/or extreme heat conditions.

- Gene Yllanes presented on the T-Rex, multipurpose all-terrain robotic platform, at the 5th Annual Life Sciences South Florida Undergraduate Research Symposium at Palm Beach State College, FL on April 1, 2017. Gene's research is investigating how to integrate robotic systems into hazardous work environments to accomplish high priority/high risk tasks, thereby reducing the risks to the workforce.

Figure 4-9. DOE Fellows and ARC staff at 5th Annual Life Sciences South Florida Undergraduate Research Symposium: Vasileios Anagnastoplous, Gene Yllanes, Alexander Piedra, Frances Zengotita, Ripley Raubenolt and Leonel Lagos.

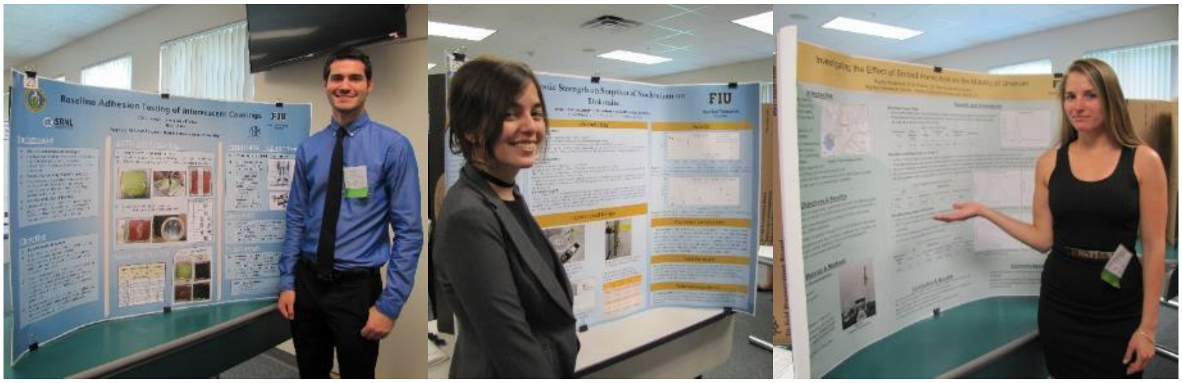

Figure 4-10. DOE Fellows Alexander Piedra (left) Frances Zengotita (middle) and Ripley Raubenolt (right) at the Annual Life Sciences South Florida Undergraduate Research Symposium

- Ripley Raubenolt presented the effect of sorbed humic acid on the mobility of uranium at the 2nd Annual FIU Undergraduate Research Conference on March 31, 2017 as well as at the 5th Annual Life Sciences South Florida Undergraduate Research Symposium at Palm Beach State College, FL on April 1, 2017. Ripley's research will help determine if the use of a low cost unrefined material containing humic acid can be used to facilitate the adsorption of uranium in order to control its movement in the groundwater at the Savannah River Site (SRS).
- Awmna Rana presented the investigation of the properties of acid-contaminated sediments and its effect on contaminant mobility and Alexis Smooth presented the synergetic interactions between uranium, humic acid, silica colloids and SRS sediments at variable pH at the 2nd Annual FIU Undergraduate Research Conference on March 31, 2017. Alexis's research is investigating the potential effects of the presence of colloidal silica and humic acid on the removal of uranium from contaminated groundwater at SRS.

Figure 4-11. DOE Fellows Ripley Raubenolt (Top Left), Alexis Smoot (Bottom Left) and Awmna Rana (Right) presenting their research posters at the FIU undergraduate research conference.

- Juan Carlos Morales presented the accumulated metalloestrogens analysis for health risk assessment and watershed toxicology management in Tims Branch, Savannah River Site (SRS) at the 2017 Society of Toxicology Expo in Baltimore, MD, on March 12-17, 2017. Juan's research will be used for modeling contaminant transport in the groundwater at SRS and an assessment of environmental health risks from human exposure.

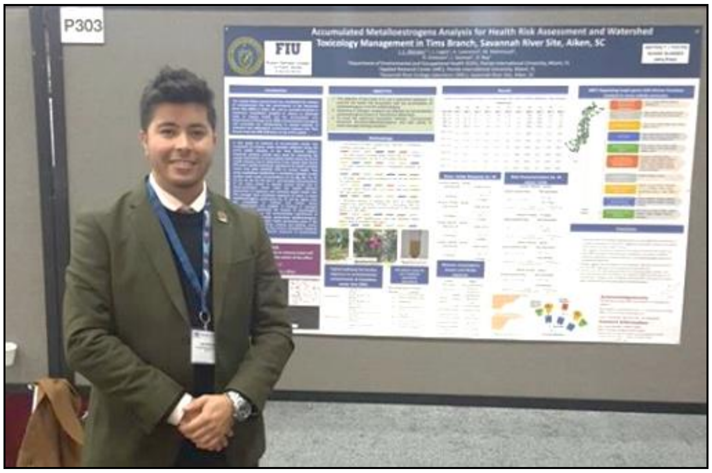

Figure 4-12. DOE Fellow Juan Morales presenting his research poster at the Society of Toxicology Expo.

- DOE Fellow Alexis Smoot leveraged her experience from her summer 2016 internship at DOE-EM Headquarters in Washington, D.C., to present her research on the development of a sustainability index at the FIU Undergraduate Research Presentation event for FIU's Foundation Board of Directors on January 27, 2017, as well as at the 2017 National Conference on Undergraduate Research on April 6-8, 2017, in Memphis, TN. The sustainability index attempts to quantify the relative sustainability of active and passive remediation strategies by examining a variety of metrics and perspectives from those involved in the decision-making process.

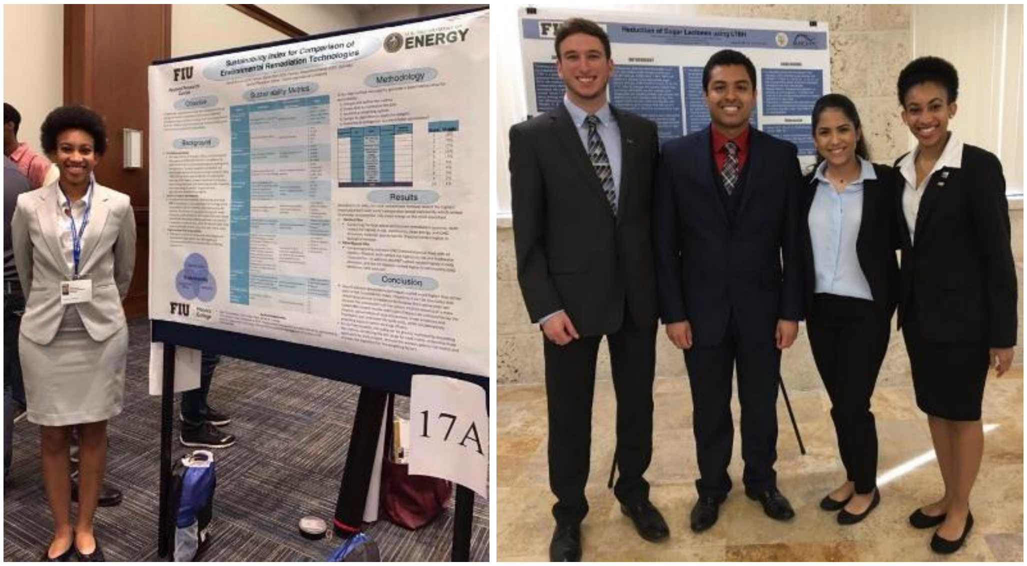

Figure 4-13. DOE Fellow Alexis Smoot presenting at the 2017 National Conference on Undergraduate Research in Memphis, TN (left) and the our FIU students who presented at the FIU Honors College Board of Directors Research Event (right).

- Silvina Di Pietro, spoke at FIU's Panther Alumni Week (PAW) 1st year Honors College interdisciplinary course. She talked about her undergraduate experience within FIU and the FIU's Honors College and advised students on leadership. She stressed the importance of participating in an internship before graduating and shared her internship experience at Pacific Northwest National Lab last summer as part of the DOE Fellows Program at FIU.

Figure 4-14. Silvina Di Pietro introducing FIU students to DOE Fellows program at Panther Alumni Week (PAW).

FIU continued working with DOE Fellows interested in federal jobs. FIU supports our Fellows with identifying federal entry-level career opportunities within DOE and other federal agencies on USA Jobs and forward those vacancy announcements to the DOE Fellows. FIU also continues to identify those DOE Fellows who are preparing to transition from academia to the workforce within the next year for conducting focused mentoring sessions with those Fellows on resume preparation and the USA Jobs application process.

During this month, the Fellows continued their research in the DOE EM applied research projects under the cooperative agreement and research topics identified as part of their summer internships at DOE sites, national labs, and/or DOE HQ. Each DOE Fellow is assigned to DOE EM research projects as well as ARC mentors. A list of the current Fellows, their classification, areas of study, ARC mentor, and assigned project task is provided below.

Table 4-3. Project Support by DOE Fellows

Name	Classification	Major	ARC Mentor	Project Support
Alejandro Garcia	Graduate - B.S.	Geoscience	Dr. Yelena Katsenovich	Influence of microbial activity on corresponding electrical geophysical response after ammonia injections in the vadose zone
Alejandro Hernandez	Undergrad - M.S.	Chemistry	Dr. Vasileios Anagnostopoulos	Contaminant Fate & Transport Under Reducing Conditions
Alexander Piedra	Undergrad - B.S.	Mechanical Engr.	Mr. Joseph Sinicrope	Database of Robotic Technologies for D&D
Alexis Smoot	Undergrad - B.S.	Environmental Engr.	Dr. Ravi Gudavalli	Synergistic Effects of Silica & Humic Acid on U(VI) Removal
Andres Cremisini	Undergrad - B.S.	Computer Science	Dr. Himanshu Upadhyay	D&D KM-IT
Anibal Morales	Undergrad - B.S.	Electrical Engr.	Mr. Anthony Abrahao	Development of Inspection Tools for DST Primary Tanks
Awmna Kalsoom Rana	Undergrad - B.S.	Chemistry	Dr. Vasileios Anagnostopoulos	Investigation on the Properties of Acid-Contaminated Sediment and its Effect on Contaminant Mobility
Christine Wipfli	Undergrad - B.S.	Environmental Engr.	Dr. Vasileios Anagnostopoulos	Groundwater Remediation at SRS F/H Area
Clarice Davila	Undergrad - B.S	Mechanical Engr.	Dr. Aparna Aravalli	Investigation Using an Infrared Temperature Sensor to Determine the Inside Wall Temperature of DSTs
Frances Zengotita	Undergrad - B.S.	Chemistry & Health	Dr. Hilary Emerson	Absorption of Neodymium into the Dolomite Mineral
Hansell Gonzalez	Graduate - Ph.D.	Chemistry	Dr. Yelena Katsenovich	Sorption Properties of Humate Injected into the Subsurface System
Jesse Viera	Undergrad - B.S.	Mechanical Engr.	Mr. Joseph Sinicrope	Incombustible Fixatives

Name	Classification	Major	ARC Mentor	Project Support
Joseph Coverston	Graduate – M.S.	Mechanical Engr.	Dr. Reza Abassi Baharanchi	Computational Fluid Dynamics Modeling of HLW Processes in Waste Tanks
Juan Morales	Graduate – M.S.	Public Health	Ms. Angelique Lawrence	Development of Flow and Contaminant Transport Models for SRS
Manuel Losada	Undergrad - B.S.	Electrical Engr.	Dr. Aparna Aravalli	Investigation Using an Infrared Temperature Sensor to Determine the Inside Wall Temperature of DSTs
Maximiliano Edrei	Graduate – M.S.	Mechanical Engr.	Dr. Dwayne McDaniel	Computational Fluid Dynamics Modeling of a Non-Newtonian Fluid Undergoing Sparging for Estimating PJM Mixing Times
Michael DiBono	Undergrad - B.S.	Mechanical Engr.	Mr. Anthony Abrahao	Development of Inspection Tools for DST Primary Tanks
Mohammed Albassam	Graduate – M.S.	Environmental Engr.	Dr. Noosha Mahmoudi	Environmental Remediation and Surface Water Modeling of Tims Branch Watershed at SRS
Ripley Raubenolt	Undergrad - B.S.	Environmental Engr.	Dr. Ravi Gudavalli	Modeling of the Migration and Distribution of Natural Organic Matter Injected into Subsurface Systems
Ron Hariprashad	Undergrad - B.S.	Environmental Engr.	Dr. Noosha Mahmoudi	Surface Water Modeling of Tims Branch
Sarah Solomon	Undergrad - B.S.	Environmental Engr.	Dr. Yelena Katsenovich	Investigation on Microbial-Meta-Autunite Interactions - Effect of Bicarbonate and Calcium Ions
Sebastian Zanlongo	Graduate - Ph.D.	Computer Science	Dr. Dwayne McDaniel	Cooperative Controls for Robotic Systems
Silvina Di Pietro	Graduate - Ph.D.	Chemistry	Dr. Hilary Emerson	Evaluation of Ammonia for Uranium Treatment

Milestones and Deliverables

The milestones and deliverables for Project 4 for FIU Performance Year 7 are shown in the following table. No milestones or deliverables were due in April, May, or June 2017.

FIU Performance Year 7 Milestones and Deliverables for Project 4

Milestone/ Deliverable	Description	Due Date	Status	OSTI
2016-P4-M1	Draft Summer Internships Reports	10/14/16	Complete	
Deliverable	Deliver Summer 2016 interns reports to DOE	10/31/16	Complete	OSTI
Deliverable	List of identified/recruited DOE Fellow (Class of 2016)	10/31/16	Complete	
2016-P4-M2	Selection of new DOE Fellows – Fall 2016	10/31/16	Complete	
2016-P4-M3	Conduct Induction Ceremony – Class of 2016	11/04/16	Complete	
2016-P4-M4	Submit student poster abstracts to WM17 Symposium	1/16/17	Complete	
Deliverable	Update Technical Fact Sheet	30 days after end of project	On Target	

Work Plan for Next Quarter

- Draft the Year End Report (YER) for FIU Performance Year 7.
- Draft the Project Technical Plan (PTP) for FIU Performance Year 8.
- Continue research by DOE Fellows in the four DOE-EM applied research projects under the cooperative agreement and research topics identified as part of their summer internships.
- Complete DOE Fellow internships for summer 2017 and begin preparation of summer internship technical reports.
- Coordinate fall recruitment period and complete review submitted application packages.
- Begin preparation and coordination for the DOE Fellows Poster Exhibition & Competition (October 2017).
- Begin preparation and coordination for the DOE Fellows Induction Ceremony for the Class of 2017 (November 2017).